Subcellular localization and molecular interactions of phosphoinositide 5'-phosphatases of the yeast synaptojanin-like protein family

Von der Fakultät Geo- und Biowissenschaften der Universität Stuttgart
zur Erlangung der Würde eines Doktors der
Naturwissenschaften (Dr. rer. nat.) genehmigte Abhandlung

vorgelegt von
Claudia Böttcher-Sehlmeyer
aus Halle (Saale)

Hauptberichter: PD Dr. Birgit Singer-Krüger
Mitberichter: Prof. Dr. Dieter H. Wolf
Tag der mündlichen Prüfung: 19.12.2006

Institut für Biochemie der Universität Stuttgart
2006

Hiermit versichere ich, dass ich diese Arbeit selbst verfasst und dabei keine anderen als die angegebenen Quellen und Hilfsmittel verwendet habe.
Stuttgart, den 12.11.2006

Claudia Böttcher-Sehlmeyer

Table of contents

Abbreviations

Amp	ampicilin
AMPA	α-amino-3-hydroxy-5-methyl-4-isoxazolepropionic acid
AP	clathrin heterotetrameric adaptor protein
APS	ammonium persulfate
3AT	3-amino-1,2,4-triazole
ATP	adenosine 5`-triphosphate
β-ME	β-mercaptoethanol
BAR	Bin/Amphiphysin/Rvs
BSA	bovine serum albumine
CCV	clathrin-coated vesicle
CLAP	chymostatin, leupeptin, antipain, pepstatin
kDa	kilo Dalton
DMSO	dimethylsulfoxide
DNA	desoxyribonucleic acid
DTT	D,L Dithiothreitol
EE	early endosome
ENTH	epsin N-terminal homology domain
ER	endoplasmic reticulum
ERAD	ER-dependent degradation
FM4-64	*N*-(3-triethylammoniumpropyl)-4-(*p*-diethylaminophenyl-hexatrienyl) pyridinium dibromide
5-FOA	5-fluoro orotic acid
FYVE	(Fab1, YOTB, Vac1, and early endosomal antigen 1) domain
GGA	Golgi-associated, γ-adaptin homologous, Arf-interacting protein
GFP	green fluorescent protein
GST	glutathione S-transferase
HA	hemagglutinin
IP	immunoprecipitation
IPTG	isopropyl-beta-D-thiogalactopyranoside
MVB/LE	multivesicular body/late endosome
NEB	New England Biolabs
NEM	N-ethtylmaleimide
NP-40	nonidet P-40
OD_{600}	optical density at 600 nm
PM	plasma membrane
PBS	phosphate saline buffer
PCR	polymerase chain reaction
PI	phosphoinositide
PMSF	phenylmethylsulfonyl fluoride
PPIP	polyphosphoinositide phosphatase
PRD	prolin-rich domain
PtdIns	phosphatidylinositol
PtdIns(3)P	phosphatidylinositol-3-phosphate
PtdIns(3,5)P_2	phosphatidyl-inositol-3,5-bisphosphate
PtdIns(4)P	phosphatidylinositol-4-phosphate
PtdIns(4,5)P_2	phosphatidyl-inositol-4,5-bisphosphate
RNase	Ribonuclease
SD	synthetic growth medium
SDS-PAGE	sodium dodecyl sulfate-polyacrylamide gel electrophoresis

TCA	trichloroacetic acid
TEMED	Tetramethylethyldiamine
TGN	*trans*-Golgi network
ts	temperature sensitive
Triton X-100	alkylpehnylpolyethylengycol
Tween 20	polyoxyethylensorbitolmonolaurate
Ub	ubiquitin
UIM	ubiquitin interacting motif
v/v	volume/volume
WASP	Wiscott-Aldrich syndrome protein
w/v	weight/volume
YPD	yeast complete medium

Abstract

Phosphorylated derivates of phosphatidylinositol, collectively called phosphoinositides (PIs), are a minor class of short-lived lipids that control numerous cellular processes including cell signaling, growth, vesicular traffic, and actin cytoskeletal arrangements. Different PI isoforms, which are caused by the reversible phosphorylation at distinct positions of the inositol ring, are concentrated in distinct subcellular compartments, with for example phosphatidylinositol 4,5-bisphosphate [PtdIns(4,5)P_2] at the plasma membrane, PtdIns(3)P on early endosomes and PtdIns(4)P on Golgi membranes. The spatial distribution of the various PIs establishes and maintains organelle identities by increasing the affinity of membranes for specific peripheral membrane proteins. PIs also play a role in the mechanism by which the direction of membrane traffic is controlled. Membrane traffic is the process by which endocytic pathway controls the protein and lipid composition of the plasma membrane, regulates the signaling pathways, membrane recycling, and the uptake of fluid and receptor-bound extracellular nutrients. The major fraction of the material internalized at the plasma membrane is transported through the endosomal compartments to the vacuole. The endosomal compartments also exchange material with the *trans*-Golgi network (TGN) and the vacuole via vesicular transport by several routes. Thus, the correct formation of vesicles is essential to maintain the dynamic exchanges between these different compartments. To guarantee the proper vesicle formation and targeting to the acceptor compartment, the differential distribution of PIs is mediated by specific PI kinases, which localize to specified subcellular compartments. Conversely, a set of phosphatases and lipases regulates the PI turnover, thereby controlling the distribution and duration of signalling events mediated by the PI second messengers. Previous studies implicated de-phosphorylation of PtdIns(4,5)P_2 by the mammalian polyphosphoinositide phosphatase synaptojanin 1 as an important step in endocytosis. Since then, indirect evidence exists in different model organism for a role of the synaptojanin proteins in the un-coating of clathrin-coated endocytic vesicles.

Members of the highly conserved synaptojanin family are defined by a three-domain structure. The N-terminal domain, homologous to yeast Sac1p, exhibits in some family members polyphosphoinositide phosphatase (PPIP) activity that can hydrolyse the phosphate at the 3´, 4´, or 5´ position of the inositol ring. The central PI 5´phosphatase (5-Pase) domain specifically hydrolyses the phosphate at the 5´ position of PtdIns(4,5)P_2. In contrast to the highly conserved catalytic domains, the C-terminal proline-rich domain is more variable among the different family members.

The yeast *Saccharomyces cerevisiae* contains three synaptojanin-like (Sjl) proteins, Sjl1p, Sjl2p, and Sjl3p (also named Inp51p, Inp52p, and Inp53p). All three family members exhibit 5-Pase activity, while only Sjl2p and Sjl3p possess the PPIP activity. The proline-rich domains of the three family members also share minor identity.

While previously Sjl1p has not been assigned to vesicular transport, Sjl3p has been implicated in clathrin-mediated membrane traffic between the TGN and endosomes. Pair-wise deletions of the yeast synaptojanin genes have discovered that Sjl2p likely functions in endocytosis. Since less data existed about the function of Sjl2p, the work of this thesis focused on further evidence for a specific role of Sjl2p in clathrin-mediated endocytosis.

Initially, in this PhD thesis evidence is provided for an association of each family member with filamentous actin assembled *in vitro*. However, Sjl1p seems to be associated with F-actin more tightly than Sjl2p and Sjl3p, because Sjl1p withstands high salt treatment. Binding partners of Sjl1p with the non-catalytic Sac1-homologoues domain, the NPF motif in the proline-rich domain, or the proline-rich domain itself may explain this biochemical behaviour.

As already described above, earlier studies provided evidence for a localization and function of the three yeast synaptojanin family members at distinct subcellular compartments. Since the catalytic domains are highly conserved, distinct interaction partners of the proline-rich domains maybe mediate the individual recruitments. Notably, also the PPIP domains seem to specify the subcellular localization by interacting with specific protein. Sjl2p and Sjl3p, but not the non-catalytic Sac1-domain of Sjl1p, specifically bind to the cortical actin patch component Bsp1p (B. Singer-Krüger's laboratory). Therefore, although yeast synaptojanins display similar enzymatic activities *in vitro*, each member may be recruited and/or activated at a unique subcellular site by distinct signalling cascades. To identify specific Sjl2p-binding partners, GST-pulldown assays and co-immunoprecipitation experiments were performed. GST-pulldown assays using the proline-rich domain of Sjl2p revealed the association of the following proteins: the putative endocytic vesicle scission factor Rvs167p, the early endocytic protein End3p, and, most importantly, clathrin heavy chain (Chc1p), the major component of clathrin-coated vesicles. Co-immunoprecipitation experiments revealed Sla1p as an Sjl2p-specific binding partner, because Sla1p did not interact with Sjl3p or Sjl1p. The interaction of Sjl2p with Sla1p appears to occur independent of Sla1p phosphoregulation, required for coat disassembly. Although most likely transiently, Sjl2p seems to be part of the Sla1p/Pan1p complex. Sla1p and Pan1p are multivalent proteins, which bind to a variety of endocytic proteins and thereby regulate the progress of early steps of endocytosis. For example, the

Sla1p/Pan1p/End3p complex has a key role in actin polymerization during the endocytic process.

Since Sla1p binds to the proline-rich domain of Sjl2p, but not Sjl3p and Sjl1p, the hypothesis was supported that distinct binding partners of the proline-rich domains are implicated in the subcellular localization of the Sjl-proteins. For a further examination of this suggestion, the proline-rich domain of Sjl3p was fused to the PPIP and 5-Pase domains of Sjl2p. The chimeric protein Sjl2/3p was stable in the cell and did not interact with Sla1p. Since Sjl2/3p was not able to rescue the lethality of *Δsjl1Δsjl2Δsjl3* mutants and the growth phenotype of *Δgga1Δgga2Δsjl3* cells, it can be assumed that Sjl2/3p is non-functional. It is possible that the catalytic domains and the proline-rich domain need to be linked by intermolecular components to provide functionality.

In yeast, the question was still unresolved whether the synaptojanin-like proteins are associated with clathrin-coated vesicles (CCVs). To address that, an established protocol was used to isolate clathrin-coated vesicles from *S. cerevisiae*. Indeed, Sephacryl S-1000 gel filtration chromatography resulted in co-fractionation of Sjl2p and Sjl3p with clathrin-coated vesicles, while Sjl1p eluted with the main peak of the cytoplasmic phosphoglycerate kinase and actin, well separated from vesicles. Most likely, the putative vesicle scission factor Rvs167p is also found in CCV-positive fractions. Although the immunodetection of Sjl2p with CCVs was unsuccessful by electron microscopy, several lines of evidence from this thesis and recently published work support the idea that Sjl2p resides on endocytic clathrin-coated vesicles. Sjl3p, which co-fractionates with CCVs, is likely associated with vesicles derived from the TGN. In contrast to lately published data, Sjl2p and Abp1p were not found to bind to each other. Moreover, Sjl2p still co-migrated with clathrin-coated vesicles isolated from *Δabp1* cells. Experiments performed to identify the putative recruiting factor of Sjl2p to CCVs demonstrated that neither the deletion of the proline-rich domain of Sjl2p nor decreased levels of PtdIns(4,5)P_2 or the deletion of identified interaction partners, in particular Sla1p and Bsp1p, were sufficient to abolish the co-elution of Sjl2p with CCVs. These results raise the idea that multiple factors act together to establish a correct subcellular localization of Sjl2p to endocytic sites. This assumption is also supported by the finding that mutation of the first two conserved amino acids in the clathrin-binding box, present in Sjl2p, was not sufficient to reduce the binding to Chc1p.

An emerging body of evidence indicates that posttranslational modifications play a key role in the most, if not all, cellular processes in eukaryotes. The activity of a variety of plasma membrane transporters, channels, and receptors is regulated by internalization via the

endocytic machinery. The internalization is initiated by phosphorylation and/or the attachment of an ubiquitin moiety to specific amino acid residues. In *S. cerevisiae*, phosphorylation of *trans*-acting proteins is one of the key factors in the actin dynamics at an endocytic vesicle. Furthermore, recent studies have shown that some *trans*-acting proteins of the endocytic machinery are also mono-ubiquitinated, such as Rvs167p. In this PhD thesis it was found that Sjl2p and Sjl3p are modified by tyrosine phosphorylation as well as by ubiquitination, while Sjl1p was not. For mammalian synaptojanin 1, the tyrosine- and serine phosphorylations in its proline-rich domain are described in detail as regulatory mechanisms by inhibiting the binding to endophilin. Thus, it is tempting to speculate that the tyrosine phosphorylation also regulates the phosphatase activities of Sjl2p and Sjl3p. Whether this regulation mechanism is conserved among eukaryotes remains to be elucidated. The impact of ubiquitination on *trans*-acting proteins is yet unclear.

In summary, Sjl3p likely associates with clathrin-coated vesicles, while the proposition is supported that Sjl1p is not involved in clathrin-mediated transport. Apparently, Sjl2p and Sjl3p are modified by tyrosine phosphorylation and ubiquitination, which might regulate the interaction with binding partners and thereby their enzymatic activities. Results of this PhD thesis provide further evidence for a role of Sjl2p during clathrin/actin-mediated endocytosis. These results include not only its possible association with clathrin-coated vesicles, but also interactions with different proteins of the endocytic machinery, such as Sla1p and Pan1p *in vivo*, and Rvs167p, End3p, and Chc1p *in vitro*.

Zusammenfassung

Phosphorylierte Derivate von Phosphatidylinositol, auch als Phosphoinositide bezeichnet (PIs), sind eine Klasse von kurzlebigen Glycerophospholipiden, die zu einem geringen Anteil in der Zelle vertreten sind. Sie regeln verschiedene zelluläre Prozesse, wie beispielsweise Signalprozesse, das Wachstum, den vesikulären Transport und die Organisation des Aktinzytoskelettes. Die verschiedenen PI-Isoformen, welche durch Phosphorylierung von bestimmten Hydroxylgruppen am Inositolring gebildet werden, sind innerhalb der Zelle unterschiedlich verteilt. Phosphatidylinositol-4,5-bisphosphat [PtdIns(4,5)P_2] befindet sich zum Beispiel vorwiegend an der Plasmamembran, PtdIns(3)P an den frühen Endosomen und PtdIns(4)P an Membranen des Golgi-Apparates. Die räumliche Verteilung der verschiedenen PIs etabliert und hält die Identität der jeweiligen Organellen aufrecht, da die Isoformen mit verschiedenen peripheren Membranproteinen wechselwirken. Sie übernehmen auch regulatorische Aufgaben in Prozessen, die den spezifischen Vesikeltransport vermitteln. Eine entscheidende Rolle spielt der Vesikeltransport in der Clathrin und Aktin-vermittelten Endozytose, da diese die Protein- und Lipidzusammensetzung der Plasmamembran, die Regulation von Signalwegen und vor allem die Aufnahme von extrazellularen Nährstoffen kontrolliert. Ein großer Anteil der endozytotierten Substanzen wird über Endosomen zur Vakuole transportiert. Die endosomalen Kompartimente stehen über Transportvesikel auch im Austausch mit dem trans-Golgi-Netzwerk (TGN) und der Vakuole. Dabei werden sehr unterschiedliche Routen verwendet. Da der Transportvesikel das korrekte Ziel nur erreichen kann, wenn alle molekularen Komponenten richtig zusammenwirken, nimmt die Bildung von spezifischen Vesikeln eine zentrale Rolle ein. Um die korrekte Vesikelformation zu gewährleisten, wird die exakte Verteilung der PIs zum einen durch die an der Biosynthese beteiligten, spezifischen PI Kinasen kontrolliert, welche an den entsprechenden Organellen lokalisieren. Umgekehrt regulieren Phosphatasen und Lipasen die Dephosphorylierung und den Abbau von PIs. Alle drei Enzyme zusammen beeinflussen somit die Verteilung und Dauer der PI „Second-Messenger“-Signale. Frühere Studien beschrieben, dass die Dephosphorylation von PtdIns(4,5)P_2 durch die Polyphosphoinositid-Phosphatase Synaptojanin 1 vermutlich ein wichtiger Schritt in der Clathrin- und Aktin-vermittelte Endozytose in Säugetierzellen ist. Seither bekräftigen weitere Hinweise aus verschiedenen Modellorganismen die Annahme, dass die Synaptojanin-Proteine bei der Abdissoziation von Komponenten der Clathrin-umhüllten Transportvesikeln eine Rolle spielen.

Mitglieder der hochkonservierten Familie der Synaptojanin Proteine bestehen aus drei Domänen. Die N-terminale Domäne ist homolog zum Sac1-Protein der Hefe. Diese Domäne

hydrolysiert in einigen Familienmitgliedern PI-Isoformen an der 3´, 4´ und 5´ Position des Inositolrings (PPIP-Aktivität). Die zentrale Domäne, die PI 5´Phosphatase (5-Pase), hydrolysiert spezifisch die Phosphatgruppe an der Position 5´ des Inositolringes von PtdIns(4,5)P_2. Im Gegensatz zu diesen beiden hochkonservierten katalytischen Domänen, ist die C-terminal gelegene, prolinreiche Domäne (PRD) innerhalb der verschiedenen Familienmitglieder variabel.

Die Hefe *Saccharomyces cerevisiae* exprimiert drei Synaptojanin-ähnliche (Sjl) Proteine, Sjl1p, Sjl2p und Sjl3p. Diese werden auch als Inp51p, Inp52p und Inp53p bezeichnet. Alle drei Familienmitglieder besitzen 5-Pase-Aktivität, die katalytische PPIP- Aktivität besitzen jedoch nur Sjl2p und Sjl3p. Die prolinreichen Domänen der Sjl-Proteine zeigen ebenfalls geringe Übereinstimmung in ihren Aminosäuresequenzen.

Während Sjl1p bisher nicht dem Vesikeltransport zugeordnet werden konnte, existierten bereits Hinweise dafür, dass Sjl3p am Clathrin-vermittelten Membranentransport zwischen dem TGN und Endosomen beteiligt ist. Aufgrund des Auftretens von Endozytosedefekten in verschiedenen Sjl-Doppelmutanten wurde vermutet, dass Sjl2p hauptsächlich an der Endozytose beteiligt ist. Da aber keine weiteren Daten für die genaue Funktion von Sjl2p in der Endozytose vorlagen, fokussierte sich diese Doktorarbeit auf die Frage welche Rolle die Sjl2p-Phosphatase in der Clathrin und Aktin-vermittelten Endozytose spielt.

Zu Beginn dieser Arbeit wurden Beweise erbracht, dass jedes Hefe-Synaptojanin Familienmitglied mit *in vitro* polymerisierten Aktinfilamenten assoziiert. Jedoch scheint Sjl1p fester an Aktinfilamente zu binden als Sjl2p und Sjl3p, da es durch einen Puffer mit hoher Salzkonzentration nicht abgelöst werden konnte. Die katalytisch nicht aktive Sac1p-Domäne, das NPF-Motiv in der prolinreichen Domäne oder die Domäne selbst könnten für die biochemischen Eigenschaften verantwortlich sein.

Wie bereits beschrieben, gab es aufgrund früherer Studien bereits Indizien für eine Lokalisierung und Funktion der drei Synaptojanin-ähnlichen Proteine aus der Hefe an unterschiedlichen subzellularen Organellen. Die jeweilige Rekrutierung könnte durch spezifische Interaktionspartner gewährleistet werden, die zum Beispiel an die variablen prolinreichen Domänen binden. Dass aber auch die PPIP Domänen spezifische Interaktionspartner rekrutieren, zeigt die Bindung von Bsp1p mit Sjl2p und Sjl3p. Bsp1p, welches an kortikalen Aktinflecken lokalisiert, wechselwirkt nicht mit der katalytisch-inaktiven Sac1-Domäne von Sjl1p (B. Singer-Krüger Labor). Verschiedene Signalkaskaden könnten somit dafür verantwortlich sein, dass die Sjls zu ihren individuellen Funktionsorten rekrutiert und/oder an ihnen aktiviert werden.

Um spezifische Bindungspartner von Sjl2p zu identifizieren, wurden GST-Pulldown Experimente und Co-Immunopräzipitationen durchgeführt. In den GST-Pulldown Versuchen wurde eine Fusion aus der prolinreichen Domäne von Sjl2p mit dem GST-Epitop verwendet. Dabei konnte Rvs167p als Bindungspartner identifiziert werden. Rvs167p ist wahrscheinlich an der Abschnürung endozytotischer Transportvesikel von der Plasmamembran beteiligt. Außerdem wurde End3p nachgewiesen, welches sich bereits zu einem frühen Zeitpunkt am Ort der Endozytose befindet. Ein wichtiger Beweis für eine Beteiligung von Sjl2p an Clathrin-vermittelten Transportprozessen war der Nachweis der schweren Clathrinkette (Chc1p) als Bindungspartner der prolinreichen Domäne von Sjl2p. Chc1p stellt die Hauptkomponente des Hüllkomplexes von Clathrin-umhüllten Vesikeln dar. Die Co-Immunopräzipitationen identifizierten Sla1p als spezifischen Interaktionspartner der prolinreichen Domäne von Sjl2p, da es weder an Sjl3p noch an Sjl1p bindet. Die Interaktion von Sjl2p und Sla1p findet vermutlich unabhängig vom Phosphorylierungsstatus von Sla1p statt. Am endozytotischen Transportvesikel dient die Phosphorylierung von Sla1p als Signal zur Dissoziation einiger Hüllkomponenten. Sjl2p scheint außerdem mit Sla1p und Pan1p einen Komplex zu bilden, der jedoch vermutlich nur transient existiert. Sla1p und Pan1p gehen wiederum multivalente Bindungen mit anderen endozytotischen Proteinen ein und sind im Komplex mit End3p Schlüsselfaktoren für die Aktinpolymerisierung im endozytotischen Prozess.

Da Sla1p spezifisch an die prolinreiche Domäne von Sjl2p bindet, wird die Hypothese unterstützt, dass definierte Interaktionspartner durch diese Domäne rekrutiert werden. Um diese Vermutung genauer zu untersuchen, wurde ein chimäres Protein erzeugt, welches aus der prolinreichen Domäne von Sjl3p und beiden katalytischen Domänen von Sjl2p besteht. Das Fusionsprotein Sjl2/3p liegt in der Zelle stabil vor und zeigt keine Interaktion mit Sla1p. Es scheint aber in bezug auf seine Phosphataseaktivitäten nicht funktionell zu sein, da es sowohl die Lethalität der *Δsjl1Δsjl2Δsjl3* Mutante, als auch den Wachstumsphänotyp von *Δgga1Δgga2Δsjl3* Zellen nicht heilen konnte. Diese Beobachtungen deuten darauf hin, dass die katalytischen Domänen vermutlich mit der prolinreichen Domäne intramolekular in Verbindung gebracht werden müssen, um funktionell zu sein.

In *S. cerevisiae* war die Frage noch offen, ob die Sjl-Proteine mit Clathrin-umhüllten Vesikeln (CCV) assoziieren. Um diese Fragestellung zu beantworten, wurde ein etabliertes Protokoll zur Isolation von CCVs verwendet. Tatsächlich zeigte die Sephacryl S-1000 Gelfiltrations-Chromatographie, dass Sjl2p und Sjl3p mit CCVs co-fraktionierten, wohingegen Sjl1p zusammen mit den Peaks der zytosolischen Phosphoglyceratkinase und Aktin co-eluierte,

welche klar von den CCV-Fraktionen getrennt waren. Vermutlich befindet sich Rvs167p ebenfalls in CCV-positiven Fraktionen. Obwohl die elektronenmikroskopische Immunodetektion von Sjl2p an CCVs bisher nicht erfolgreich war, weisen die Ergebnisse der Co-Immunopräzipitationen und der GST-Pulldowns dieser Doktorarbeit, sowie neuere veröffentlichte Studien darauf hin, dass Sjl2p an endozytotischen Clathrin-umhüllten Vesikeln zu finden ist. Sjl3p assoziiert vermutlich ebenfalls mit Clathrin-umhüllten Vesikeln, die aber am TGN gebildet werden. Im Gegensatz zu einer kürzlich veröffentlichten Arbeit, konnte eine Wechselwirkung zwischen Sjl2p und Abp1p nicht nachgewiesen werden. Außerdem cofraktionierte Sjl2p mit CCVs, die aus *Δabp1* Zellen isoliert worden waren. Experimente, die mögliche Rekrutierungsfaktor von Sjl2p an CCVs aufzeigen sollten, wiesen nach, dass weder eine Deletion der prolinreichen Domäne von Sjl2p, noch verringerte Mengen an PtdIns(4,5)P_2 oder Deletionen der bekannten Interaktionspartner Sla1p und Bsp1p ausreichend sind, um die Co-Fraktionierung von Sjl2p mit CCV-Fraktionen zu inhibieren. Somit liegt die Vermutung nahe, dass verschiedene Komponenten der Endozytosemaschine zusammenarbeiten, um eine korrekte, subzelluläre Lokalisierung von Sjl2p an seinen Wirkungsort zu gewährleisten. Diese Theorie wird auch dadurch gestützt, dass die Mutation der ersten beiden Aminosäuren im Clathrin-bindenden Motiv in der prolinreichen Domäne von Sjl2p die Bindung an Chc1p nicht beeinflusst.

Immer mehr Daten sprechen dafür, dass posttranslationale Modifikationen eine Schlüsselrolle in vielen, wenn nicht sogar allen, zellulären Prozessen in Eukaryonten einnehmen. Die Aktivität von vielen Transportern, Kanälen und Rezeptoren an der Plasmamembran wird durch deren Internalisierung mittels Endozytose reguliert. Dies wird durch Anhängen eines Phosphatrestes und/oder von Ubiquitin an spezielle Aminosäurereste festgelegt. In *S. cerevisiae* spielt die Modifikation von Proteinen der Endozytosemaschine, sogenannter *trans*-agierender Proteine, mittels Phosphorylierung zum Beispiel eine Rolle bei der Aktindynamik am endozytotischen Vesikel. Neueste Ergebnisse zeigen, dass einige *trans*-agierende Proteine auch mono-ubiquitiniert werden, wie zum Beispiel Rvs167p. Während dieser Doktorarbeit konnte gezeigt werden, dass Sjl2p und Sjl3p, aber nicht Sjl1p, sowohl durch Tyrosin-phosphorylierung als auch Ubiquitinierung posttranslational modifiziert werden. Für Synaptojanin 1 in Säugetierzellen wurde bereits gezeigt, dass die Tyrosin- und auch die Serinphosphorylierung in dessen prolinreicher Domäne Regulationsmechanismen für die Interaktion mit einem seiner Bindungspartner darstellen und dadurch die 5-Pase-Aktivität reguliert wird. Aufgrund dieses Ergebnisses kann spekuliert werden, dass die PI Phosphatase-Aktivitäten von Sjl2p und Sjl3p zumindest durch die Tyrosinphosphorylierung reguliert

werden. Aber ob dieser Regulationsmechanismus tatsächlich innerhalb der Eukaryonten konserviert ist, müssen weitere Analysen klären. Die Bedeutung der Ubiquitinierung von *trans*-agierenden Proteinen ist momentan noch unklar.

Zusammenfassend kann geschlossen werden, dass Sjl3p wahrscheinlich mit Clathrin-umhüllten Vesikeln assoziiert. Für Sjl1p wurde die Annahme bekräftigt, dass es nicht an Clathrin-vermittelten Transportprozessen beteiligt ist. Sjl2p und Sjl3p werden durch Tyrosinphosphorylierung und Ubiquitinierung modifiziert. Dies könnte deren Interaktion mit anderen Proteinen und dadurch die Phosphataseaktivitäten beeinflussen. Im Rahmen dieser Doktorarbeit konnten verschiedene Beweise für eine Rolle von Sjl2p in der Clathrin- und Aktin-basierten Endozytose erbracht werden. Diese beinhalten nicht nur die mögliche Assoziierung mit CCVs, sondern auch die Interaktion mit unterschiedlichen Proteinen der Endozytosemaschine, wie Sla1p und Pan1p *in vivo* sowie End3p, Rvs167p und Chc1p *in vitro*.

1 Introduction

1.1 Membrane traffic in the budding yeast *Saccharomyces cerevisiae*

1.1.1 Yeast as a model for studying membrane traffic

Saccharomyces cerevisiae is a convenient organism to study endocytic internalization and trafficking events, because the organellar composition and physiology of unicellular yeast and higher eukaryotes are remarkably similar. The ease of combining biochemical analyses with genetic studies has made it a central model system of modern biological research.

In particular, genes that are not essential for viability can be easily deleted from the haploid yeast genome, resulting in phenotypes pointing to the function of the genes. The recent determination of the complete nucleotide sequence of the *S. cerevisiae* genome (Goffeau *et al.*, 1996) greatly facilitated the identification of homologous of yeast genes implicated in membrane traffic in other eukaryotic species. This had lead to the understanding that genes and mechanisms involved in many cellular processes are highly conserved across eukaryotic organisms (Mell and Burgess, 2002).

Yeast strain collections in which every non-essential open reading frame has been individually disrupted are powerful tools in discovering cellular pathways, conferrable to processes in mammalian cells. Using this advantage, genes involved in a wide range of cellular processes are identified, including those that result in defects in endocytosis and intracellular traffic (D'Hondt *et al.*, 2000). Furthermore, life cell imaging in yeast has become an emerging method in shedding `light´ into the process of endocytic internalization by the use of GFP spectral variants to visualize single protein movements at the plasma membrane.

1.1.2 The endocytic compartments

In all eukaryotic cells, intracellular compartments are maintained via an organized system of transport pathways that traffic lipids and proteins via vesicular organelles in a specific and regulated manner (Ferro-Novick and Jahn, 1994). These processes are time-, temperature- and energy-dependent.

Particularly, the endocytic pathway is required for the control of the protein and lipid composition of the plasma membrane, regulation of signaling pathways, control of cell surface area, e.g. down-regulation of receptors, membrane recycling, and uptake of nutrients. In *S. cerevisiae*, endocytosis was first demonstrated using the fluid-phase internalization marker Lucifer yellow (LY), which is internalized independently of receptors, and hence unsaturable (Riezman, 1985). Later studies have used the mating pheromone α-factor, which

is expressed in *MAT***a** cells, to demonstrate receptor-mediated internalization by binding to the Ste2p receptor (Chvatchko *et al.*, 1986). These approaches revealed that endocytic mutants, which are defective in receptor-mediated endocytosis are also defective in fluid-phase endocytosis, suggesting that these pathways share most of their machinery (D'Hondt *et al.*, 2000).

Clathrin-mediated endocytosis appears to be the major pathway for internalization of proteins and lipids from the plasma membrane in yeast (Fig. 1) (Payne *et al.*, 1988), although in clathrin heavy chain temperature sensitive mutants there is only a 50 % reduction in endocytosis (Tan *et al.*, 1993). Internalization of plasma membrane components and extracellular material occurs in specific transport vesicles, so called clathrin-coated vesicles (CCV). Consequent studies allowed the separation of compartments responsible for the process by which internalized material finally is delivered to the vacuole (Singer and Riezman, 1990; Vida *et al.*, 1993). Recent advanced techniques revealed that endocytosis depends on an extensive network of interacting proteins that assemble in a spacial and temporal order. It has been suggested that the internalization process can be subdivided in

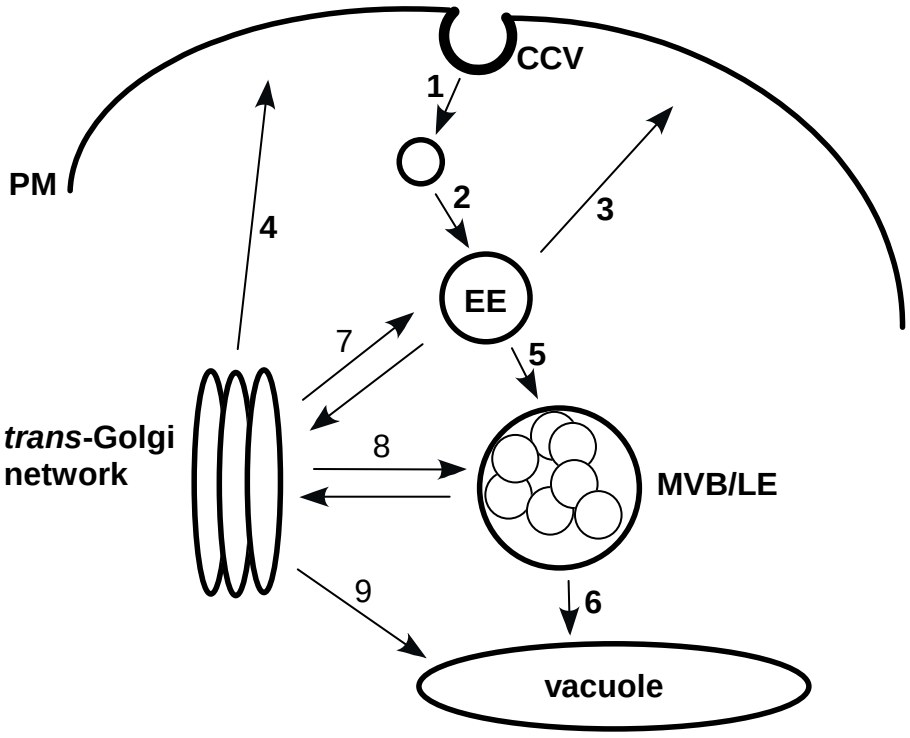

Fig. 1. Schematic drawing of the transport pathways in the endomembrane system in yeast
Newly internalised material (1) is transported to the early endosomes (2). At this compartment, proteins destined for recycling are sorted back to the plasma membrane (3 and 4), whereas proteins destined for degradation are transported to the late endosomal compartment/MVB (5) and subsequently to the lysosome/vacuole (6). Conversely, in the biosynthetic pathway newly synthesized proteins are sorted through the Golgi apparatus to their final destination (7, 8) or to the vacuole (9). The cellular compartments are indicated: plasma membrane (PM), clathrin-coated vesicles (CCV), early endosome (EE), late endosome (MVB/LE), vacuole, and *trans*-Golgi network.

four subprocesses, which subsequently mediate cargo sorting, membrane invagination, vesicle scission, and vesicle targeting. The first step in endocytosis is the binding of extracellular cargo molecules to specific cell-surface receptors. Intracellular adaptor proteins (APs) then sequester these receptors and other membrane proteins destined for endocytosis at endocytic sites. But the relative importance of adaptor proteins seems less in yeast than in mammalian cells. The adaptors, together with clathrin and other accessory proteins, form an endocytic coat at the plasma membrane, which then bends to form an invagination that subsequently pinches off to form a cargo-filled vesicle (Kaksonen *et al.*, 2006; Robinson, 2004). After disassembly of the protein coat and movement of the endocytic vesicle into the cytoplasm, the internalized material moves through at least three different endosomal subcompartments, two kinds of endosomes and the vacuole. Endosomes have been identified chemically and defined kinetically by distinct densities in a density gradient (Singer-Krüger *et al.*, 1993). Internalized material moves first through a compartment of higher density, the early endosomes. Recently, significantly advanced techniques have visualized that free endocytic vesicles (Fig. 1; arrow 1) are captured efficiently by early endosomes, because of moving along actin cables (arrow 2) (Toshima *et al.*, 2006). At this compartment proteins destined for recycling are sorted back to the plasma membrane (arrow 3 and 4) (Chen and Davis, 2000; Lafourcade *et al.*, 2004). Proteins destined for degradation are transported through the late endosomal compartment/ multivesicular body (MVB) (arrow 5), which is the compartment of lower density, and subsequently fuses with the lysosome/vacuole (arrow 6) (Prescianotto-Baschong and Riezman, 2002; Singer-Krüger *et al.*, 1993).

1.1.3 Membrane traffic at the *trans*-Golgi network

The vacuole receives membrane and lumenal content not only from the cell surface via the endocytic pathway, but also from the biosynthetic pathway (Abb. 1) (Klionsky *et al.*, 1990), including the endoplasmic reticulum (ER), Golgi cisternae, and the *trans*-Golgi network (TGN).

The TGN functions as a central compartment that sorts newly synthesized proteins. Once proteins reach the TGN they face several possible destinations: secretory vesicles, endosomes (arrows 7 and 8), or the lysosome/vacuole (arrow 9). The TGN sorts proteins to each of these destinations by segregating them into specific sets of membrane-enclosed carriers. Between the different identified types of vesicles, clathrin-coated vesicles are proposed to be involved in the pathways between the TGN and early/late endosomes (arrows 6 and 7) (Black and Pelham, 2000; Costaguta *et al.*, 2001; Ha *et al.*, 2003).

1.2 Role of lipids in endocytosis

The plasma membrane has the highest concentration of sphingolipids and free ergosterol among all the membranes in yeast cells. Screenings for new mutants defective in endocytosis (*end* mutants) have revealed that lipids are important determinants in endocytic traffic events. For example, End3p/Lcb1p and End11p/Erg2p are involved in the biosynthesis of sphingolipids and ergosterol, respectively (Heese-Peck *et al.*, 2002; Munn *et al.*, 1999). Ergosterols and sphingolipids can interact with each other leading to the formation of special membrane domains, referred to as `rafts´ (Simons and Ikonen, 1997). It was shown that lipid rafts are preferred platforms for membrane-linked actin polymerization. Rafts seem to withstand treatment with detergent at low temperature. It is becoming more and more evident that different types of rafts can exist in one and the same membrane (Opekarova *et al.*, 2005; Pichler and Riezman, 2004). Beside other functions, these specialized plasma membrane domains are supposed to be platforms where internalization step of endocytosis occurs. In yeast, at least the plasma membrane proteins Ste2p seems to be embedded in these rafts (Opekarova *et al.*, 2005). Although the deletion of not all proteins that are involved in ergosterol synthesis result in defects in internalization steps of endocytosis, the formation of distinct plasma membrane domains containing defined ergosterols is most likely important for endocytosis. In contrast, α-factor internalization is impaired at very early stages of endocytosis when sphingolipids synthesis is blocked. Sphingolipids have at least two functions in the cell. One is a structural function in formation of membranes and specific membrane domains, like rafts. The other function is its capability to generate second messengers. Furthermore, membrane phosphoinositides are implicated in endocytosis and maybe rafts, in particular PtdIns(4,5)P_2, by regulating actin cytoskeleton remodelling and recruiting endocytic proteins to the plasma membrane. Thus, the requirement of raft-type lipids in endocytosis points to their role in controlling vesicle formation and release. It is assumed that the tension of lipid raft domains supports the membrane invagination that finally results in the release of an endocytic vesicle (reviewed in Liu *et al.*, 2006; Souza and Pichler, 2006).

1.3 Clathrin/actin-mediated vesicle transport

1.3.1 Clathrin

Coated vesicles were firstly described in mammalian cells by Roth and Porter suggesting that coated pits at the plasma membrane form invaginations and vesicles, which eventually pinch off, loose the coat, and fuse with other organelles (Roth and Porter, 1964).

Further studies revealed the basic coat architecture – a lattice of pentagons and hexagons that curves around to enclose a bilayer vesicle. The main proteins of these coated vesicles were later isolated and named clathrin-heavy chain (Chc1p) (Pearse, 1975) and clathrin-light chain (Clc1p) (Kirchhausen and Harrison, 1981; Ungewickell and Branton, 1981), according to their molecular mass in a SDS-gel. Clathrin-coated vesicles are formed in all eukaryotic cells, from yeast to human. Three clathrin-heavy chains form a trimer that appears as a triskelion, each leg extending radially. The legs are joined at a central trimerization domain and each leg is associated with a light chain. The globular N-terminal domain of the heavy chain protrudes to form an inner layer, thereby binding to various mono- and hetero-tetrameric adaptor proteins and other clathrin-binding-box containing proteins (Kirchhausen, 2000; Maldonado-Baez and Wendland, 2006). The clathrin coat is either recruited onto the plasma membrane to mediate endocytosis or onto the TGN for protein transport to the endosomal compartment.

In *S. cerevisiae*, cortical actin patches have been defined as sites of endocytic internalization (Kaksonen *et al.*, 2003), but the exact role of clathrin in this process was unclear (Payne *et al.*, 1988; Payne *et al.*, 1987; Tan *et al.*, 1993). It was believed that, although cells lacking clathrin function are compromised for growth and mislocalize TGN resident membrane proteins to the cell surface, the role of clathrin is not absolutely essential in membrane traffic (Lemmon and Jones, 1987; Payne *et al.*, 1987; Seeger and Payne, 1992; Tan *et al.*, 1993). Recent studies propose that cortical clathrin is associated with and behaves like other cortical actin patch components, that are believed to be present in endocytic structures (Newpher *et al.*, 2005). Moreover, clathrin seems to be important for actin patch organisation and dynamics during the different steps of endocytosis (Newpher and Lemmon, 2006). Although clathrin may not be critically required for invagination and vesicle formation it is a determining factor for the efficiency of endocytic- (Kaksonen *et al.*, 2005) and maybe TGN-site assembly.

1.3.2 The requirement of the actin in clathrin-coated vesicle formation

Several lines of evidence supported the requirement of the actin in endocytosis. First, the treatment of yeast cells with the actin polymerization inhibitor latrunculin A, which binds to actin monomers and prevents their assembly into filaments, dramatically blocks internalization (Ayscough *et al.*, 1997; Lappalainen and Drubin, 1997). In turn, jasplakinolide, which stabilizes actin filaments and prevents their de-polymerization, blocks endocytosis completely (Ayscough, 2000; Ayscough *et al.*, 1997). Second, mutations in most genes affecting both fluid-phase and receptor-mediated internalization, such as the major coat component Chc1p (Payne *et al.*, 1987) or Sla1p (Kaksonen *et al.*, 2005; Warren *et al.*, 2002),

also disrupt the distribution of the cortical actin cytoskeleton and vice versa, for example like actin (Kübler and Riezman, 1993) or the actin-dependent motor proteins Myo3p and Myo5p (Geli and Riezman, 1996). Third, punctuate cortical actin patches were shown to co-localize at least partially with many endocytic proteins (reviewed in Engqvist-Goldstein and Drubin, 2003; Kaksonen *et al.*, 2005) and a study using immunoelectron-microscopy revealed the localization of actin patches to membrane invaginations likely intermediates of endocytic vesicle formation (Mulholland *et al.*, 1994). Forth, several protein-protein interactions indicate links between the endocytic machinery and the actin cytoskeleton (Engqvist-Goldstein and Drubin, 2003).

In sum, these results provide evidence that cortical actin patches at the plasma membrane mark to endocytic sites (Huckaba *et al.*, 2004; Kaksonen *et al.*, 2003; Kaksonen *et al.*, 2005; Newpher *et al.*, 2005). In fact, the endocytic cortical actin patch assembly is a hierarchical process in which assembly factors initially associate with the plasma membrane, followed by the recruitment of actin-nucleating factors, incorporation of actin filaments (F-actin), and finally actin-dependent proteins resulting in the formation of an endocytic vesicle (see below) (Kaksonen *et al.*, 2005; Kaksonen *et al.*, 2006). Although proteins recruited early to endocytic sites seem to localize to the plasma membrane independently of F-actin, the following steps including invagination of the plasma membrane, vesicle formation and transport highly depend on actin nucleation. In sum, actin polymerization is coincident with the formation of the invaginated membrane and is followed by the release of a newly formed vesicle, which moves rapidly toward the interior of the cell.

The dynamic process of actin assembly in conjunction with vesicle formation at the TGN is not yet analysed in the same detail as during endocytosis. So far, some hints exist that actin polymerization may play a similar role during the formation of clathrin-coated vesicle at the TGN and/or subsequent movements of the clathrin-coated vesicles (Carreno *et al.*, 2004).

1.3.3 Vesicle formation and fission at the plasma membrane

The formation and budding of transport vesicles involve the recruitment of cytosolic coat proteins to the donor membrane. Four different types of vesicle coats have been identified, COP-I, COP-II, retromers and clathrin, which are implicated in distinct transport steps between organelles (Bonifacino and Rojas, 2006). Proteinaceous coats have two principal functions - they provide a scaffold that participates to deform a membrane to generate small (≈ 60-100 nm diameter) vesicles, and they select the cargo to be transported by the vesicle (Marsh, 2001). In the case of clathrin-coated vesicles derived from the plasma membrane, the cell surface cargo includes for example channels or receptor-bound ligands,

like the pheromone α-factor receptor in yeast (Toshima *et al.*, 2006) or the epidermal growth factor receptor in mammalian cell (Maudsley *et al.*, 2000).

Using life cell microscopy of fluorescently labelled endocytic/cortical actin patch proteins in wildtype or mutant cells in yeast, several laboratories revealed the spatiotemporal localization of single proteins at endocytic sites (Huckaba *et al.*, 2004; Kaksonen *et al.*, 2003; Kaksonen *et al.*, 2005; Toshima *et al.*, 2006).

Clathrin-coated vesicles (CCVs) are formed by the coordinated assembly of clathrin triskelia. The early recruitment and polymerization of the clathrin layer at endocytic sites is assisted by adaptor proteins, which simultaneously bind to clathrin, membrane lipids, and in many cases to transmembrane cargo proteins (Kirchhausen, 1999; Robinson, 2004). The sequestration of specific cargo in forming endocytic vesicles is mediated by several specific `sorting signals´ (Robinson, 2004; Traub, 2003). Proteins of the so called WASP/Myo module, like the Arp2/3p activators Las17p (Winter *et al.*, 1999) and Myo5p (Geli and Riezman, 1996), which is also an actin-dependent motor protein, arrive at endocytic sites after clathrin (Kaksonen *et al.*, 2005). Activation of the Arp2/3p complex by both proteins results in actin-filament nucleation at the plasma membrane. Myo5p may also anchor the actin filaments to the plasma membrane. Therefore, Las17p and Myp5p participate in the control of the actin network growth. Furthermore, Las17p interacts with several endocytic proteins, such as the coat protein Sla1p (Warren *et al.*, 2002). Beside other proteins, the coat proteins Sla1p and Pan1p arrive at endocytic sites after Las17p, independent of F-actin (Kaksonen *et al.*, 2003). While Sla1p is rather involved in actin dynamics (Holtzman *et al.*, 1993), Pan1p directly further triggers actin-filament nucleation as the second Arp2/3p complex activator (Duncan *et al.*, 2001). But both proteins perform several other functions besides regulating actin dynamics. Pan1p is a multivalent protein that binds to a variety of endocytic proteins and potentially links the actin filaments to the coat (Kaksonen *et al.*, 2006). Another function of Sla1p is the role as an adaptor in receptor-mediated endocytic uptake (Holtzman *et al.*, 1993). Since Sla1p participates in actin dynamics and has a role as an adaptor, it is suggested that actin polymerization is co-ordinated with cargo loading to maximize endocytic uptake efficiency (Kaksonen *et al.*, 2005). As already described above, actin polymerization is required for vesicles internalization (reviewed in Kaksonen *et al.*, 2006). In fact, actin, actin-related and actin-associated proteins, such as the actin-filament-crosslinking protein Sac6p (Karpova *et al.*, 1995) and the third Arp2/3p complex activator Abp1p (Goode *et al.*, 2001) arrive at the membrane invagination after the coat proteins. Abp1p seems not have a significant role in initiating actin polymerization, but seems to have an inhibitory function,

because it turns off actin polymerization. This function may represent a regulatory factor in actin dynamics at the evolving endocytic membrane invagination. Sac6p cross-links the actin filaments, which is essential for endocytic internalization (Kaksonen *et al.*, 2005). A recent model proposes that polymerization of actin filaments provides the force for the deformation of the membrane at endocytic sites into a tubular invagination, pushing and/or pulling the invaginated membrane inward (Kaksonen *et al.*, 2003; Kaksonen *et al.*, 2006). But not only actin participates in this process, the membrane invagination is likely facilitated by different membrane lipids, that are also differentially localized along the tube thereby causing a substantial interfacial tension (Liu *et al.*, 2006; Souza and Pichler, 2006). While Las17p remains at the neck of the evolving membrane invagination/tube, the coat proteins clathrin, Sla1p, and Pan1p move away from the cell cortex together with the tip of the membrane invagination. During the later steps of actin polymerization the amphiphysin-like protein Rvs167p briefly localizes along the tubular neck of the invagination (Kaksonen *et al.*, 2005). Rvs167p and its homologue Rvs161p contain N-BAR domains that are supposed to sense and mediate the curvature of membranes. Moreover, this domain is able to bind and tubulate membranes *in vitro*, as demonstrated in mammalian cells (Peter *et al.*, 2004). Rvs167p is proposed to participate in the final fission event, because of its timing and behaviour at endocytic sites (Kaksonen *et al.*, 2005), which are similar to the observations of its mammalian homologue amphiphysin (Merrifield *et al.*, 2005).

Overall, a synergy of membrane bending effector proteins and lipids, that are distributed at specific membrane subdomains, `neck´, `tub sides´, or `tube tip´, likely affect the curvature at specific regions resulting in the formation and finally fission of an endocytic vesicle (reviewed in Liu *et al.*, 2006).

It was shown that the released vesicle moves then rapidly away from the plasma membrane toward the interior of the cell, which coincides with a short burst of actin polymerization (reviewed in Kaksonen *et al.*, 2006; Toshima *et al.*, 2006). But, during this movement, actin filaments and other endocytic components already start to disassemble to allow fusion of the vesicle with the acceptor membrane (Huckaba *et al.*, 2004; Kaksonen *et al.*, 2003; Kaksonen *et al.*, 2005; Young *et al.*, 2004). The turn off of F-actin polymerization is probably initiated by negative-regulation of the Arp2/3p complex-mediated actin filament nucleation (Welch and Mullins, 2002). This regulation is achieved by interacting proteins of the Arp2/3p complex activators Pan1p (Zeng *et al.*, 2001), Las17p (Naqvi *et al.*, 1998), and Abp1p (Fazi *et al.*, 2002). For example, the interaction of Las17p with Sla1p leads to an inhibition of the activating effect of Las17p on the Arp2/3p complex (Rodal *et al.*, 2003).

Protein phosphorylation also has a role in regulating the actin polymerization at endocytic sites, mainly the inhibition of actin polymerization. For example, phosphorylation of Pan1p and Sla1p by the actin-regulating kinases Ark1p and Prk1p inhibits the functions of both proteins on actin (Toshima *et al.*, 2005; Zeng *et al.*, 2001). But not only phosphorylation of endocytic proteins results in coat disassembly. The turnover of certain lipids and phosphoinositides at the plasma membrane is believed to be critical for the un-coating step of the endocytic vesicle (see below), similar to their supposed impact in internalization (Souza and Pichler, 2006).

1.3.4 Clathrin-coated vesicle formation at the TGN

Vesicle formation at the TGN in yeast is not yet studied in the same extend as at the plasma membrane. On the basis of results from the mammalian system, it is suggested that both machineries share similar structures but also shows differences. For example adaptor proteins (APs) exhibit a similar structural organization, but display differences in the cellular localization patterns. In particular, AP-2 functions at the plasma membrane and AP-1 at the TGN and at endosomes. A second family of adaptors, the GGAs [Golgi-localized, γ-ear-containing, adenosine diphosphate ribosylation factor (ARF)-binding protein] appear to mediate membrane traffic between the TGN and endosomes (Bonifacino, 2004). Furthermore, it seems that different lipids and phosphoinositides found to be enriched either at the TGN or plasma membrane provide a further distinction between the two sites (McNiven and Thompson, 2006). These different lipids and phosphoinositides may recruit distinct proteins, which in turn exhibit similar function to fulfil the clathrin-based vesiculation at both sites.

1.4 Posttranslational modifications as molecular `switches´

1.4.1 The role of protein phosphorylation in membrane traffic

In eukaryotic cells, it is becoming more and more clear that posttranslational modifications are a major regulatory mechanism that controls many basic cellular processes, like cell proliferation, development, and membrane traffic (Ficarro *et al.*, 2002; Hunter, 2000; Ohno *et al.*, 1995). Although it might not be universally required, phosphorylation is a signal that often precedes ubiquitination of proteins, which indicates that the two modifications are in tight cooperation (Hicke, 2001b; Seet *et al.*, 2006). Phosphorylation and de-phosphorylation cycles of nerve terminal proteins by various kinases and phosphatases has been proposed to regulate synaptic vesicle recycling (Turner *et al.*, 1999). Particularly, dynamin 1, synaptojanin 1 and the amphiphysins undergo stimulation-dependent de-

phosphorylation (Cousin *et al.*, 2001; Slepnev *et al.*, 1998). Prevention of de-phosphorylation events by ATP-depletion results in an increased number of clathrin cages and clathrin-coated pits (Schmid and Carter, 1990; Slepnev *et al.*, 1998).

The dynamics of mammalian synaptojanin 1 phosphoregulation have been recently demonstrated in detail by Irie *et al*. (2005). Upon ephrinB2-ligand binding, EphB2p receptor tyrosine kinase (RTK) signaling results in the phosphorylation of synaptojanin 1 at three tyrosine residues (Tyr^{1018}, Tyr^{1059}, and Tyr^{1172}) in its proline-rich domain. The phosphorylation of the two most distal tyrosines (Tyr^{1059} and Tyr^{1172}) in the proline-rich domain leads to a selective inhibition of the interaction with endophilin. Since this interaction normally stimulates the 5-Pase activity (Lee *et al.*, 2004), converting PtdIns(4,5)P_2 to PtdIns(4)P, upon synaptojanin phosphorylation its phosphatase activity is decreased. After treatment of cells with ephrinB2, increased levels of PtdIns(4,5)P_2, indicate the inactivity of the 5-Pase activity of synaptojanin 1, pointing to that the EphB2p activity is responsible for the regulation of endophilin-synaptojanin 1 binding. The tyrosine phosphorylation of synaptojanin 1 likely stimulates the progress of early endocytosis, because a phosphorylation-deficient synaptojanin 1 mutant (Y1059F and Y1172F) prevented the internalization of the GluR1 subunit of the AMPA-type glutamate receptors, whose internalization depends on clathrin-mediated mechanisms. In the later phase of endocytosis, the de-phosphorylation of synaptojanin 1 is required for the clathrin-coated vesicle un-coating process, because subsequent ephrinB2- and transferrin-treatment likely resulted in a block of the transport of transferrin to endosomes and the accumulation of clathrin-positive vesicles along the plasma membrane. The de-phosphorylation of synaptojanin 1 at a later stage facilitates the vesicle un-coating process by promoting the interaction of synaptojanin 1 with endophilin (Hopper and O'Connor, 2005; Irie *et al.*, 2005). In contrast to the stimulus-induced tyrosine phosphorylation within the PRD of synaptojanin 1 by EphB2p, serine phosphorylation (Ser^{1144}) in the PRD of synaptojanin 1 by the proline-directed serine/threonine protein kinase Cdk5p (Dhavan and Tsai, 2001) represents re-phosphorylation after Ca^{2+}-dependent de-phosphorylation of this serine residue (Lee *et al.*, 2004). Also in this case, Cdk5p-mediated serine phosphorylation within the proline-rich domain of synaptojanin 1 negatively regulates the synaptojanin-endophilin interaction (Lee *et al.*, 2004). Notably, amphiphysin and dynamin 1, which are interaction partners of synaptojanin 1, were also found to be physiological substrates for Cdk5p, but not of EphB2p (Irie *et al.*, 2005). It is currently unclear if these different types of phosphorylation influence each other or represent independent steps in a complex regulation mechanism. However, this example demonstrates the complexity of not

yet well understood regulation mechanisms of protein activities by posttranslational modifications.

In *S. cerevisiae* phosphorylation is estimated to affect 30 % of the proteome (Ptacek *et al.*, 2005). Whereas tyrosine phosphorylation is less characterized (Castellanos and Mazon, 1985), attachment of phosphate groups to serine and threonin residues is described in membrane traffic. In particular, a family of conserved serine/threonine kinases is known to be implicated in endocytosis, Ark1p and Prk1p (Cope *et al.*, 1999; Sekiya-Kawasaki *et al.*, 2003). They are essential kinases, which phosphorylate the endocytic proteins Sla1p and Pan1p, thus resulting in a stop of polymerization of actin filaments (Zeng *et al.*, 2001). Therefore, Ark1p and Prk1p might be important for the termination of vesicle movement and coat protein disassembly. Prk1p was further shown to phosphorylate Ent1p and Ent2p, which bind to clathrin and EH (Eps15-homology) domain-containing proteins, like Pan1p (Aguilar *et al.*, 2003). Their modification by threonine phosphorylation result in a negative regulation of endocytosis, likely by regulating Pan1p activity (Watson *et al.*, 2001). Until now it is suggested that phosphorylation of yeast endocytic proteins by the Ark1p/Prk1p kinases inhibits endocytic functions (Sekiya-Kawasaki *et al.*, 2003).

In the mammalian system, phosphorylation of membrane proteins, that cycle within the TGN/endosomal system is known to influence their trafficking (Bonifacino and Traub, 2003). In some cases, phosphorylation of a serine or threonine residue influences the activity of a nearby sorting signal, whereas in other cases phosphorylation generates a new sorting signal that functions by binding to an accessory protein (Bonifacino and Traub, 2003). In yeast, the role of phosphorylation in sorting of cargo that cycles between the Golgi and endosomes is largely unclear. A recent study indicates that in the case of the pheromone processing enzyme Ste13p the phosphorylation regulates its transport between the Golgi complex and endosomes (Johnston *et al.*, 2005).

1.4.2 The implication of ubiquitin in cellular membrane transport

The modification of proteins by ubiquitination, the covalent attachment of the polypeptide ubiquitin onto lysine residues, is induced by a vast variety of external stimuli or other signaling events in cells, like ligand binding or phosphorylation. A major difference between ubiquitination and phosphorylation is that Ub is a chemically more complex molecule, since it has a larger surface to interact with other proteins and has the ability to form chains (Haglund and Dikic, 2005). Ubiquitination was originally described as a signal that could target cellular proteins to rapid degradation by the proteasome. But ubiquitination turned out to be a highly regulated system that is important for many cellular functions,

including protein trafficking. As believed in the beginning of research in this field, not only membrane proteins themselves become modified by ubiquitin and thereby targeted to their destination, but also the proteins of the trafficking machinery are often ubiquitinated (Staub and Rotin, 2006).

Ubiquitin ligases (E3) carry out the important task of the spacial and temporal selection of substrates (Gao and Karin, 2005). The fact that there are hundreds of E3 enzymes in eukaryotic cells (54 in yeast and ≅ 1000 in humans) indicates that ubiquitination is a key regulator in cellular function. There are two major types of E3 ligases: the RING finger E3s and the HECT E3s distinguished by the mode of the transfer of the ubiquitin moiety to the substrate. The ubiquitin moieties are usually ligated onto lysine residues of the substrate or of ubiquitin itself. Hence, proteins can either be mono-ubiquitinated (one ubiquitin polypeptide on a single lysine), multi-ubiquitinated (several lysines modified with just one ubiquitin), or poly-ubiquitinated (poly-ubiquitin chain) (Staub and Rotin, 2006). In particular, during membrane traffic, membrane proteins and proteins of the trafficking machinery are generally mono- or multi-ubiquitinated. Mono- and multi-ubiquitination of a substrate influences the ability to interact with other proteins, possibly by changing its conformation, stability, activity, and subcellular distribution (Hicke, 2001b; Seet *et al.*, 2006). Conversely, ubiquitin (Ub) can be rapidly removed by de-ubiquitinating enzymes making this system to a powerful molecular `switch´ within cells.

In *S. cerevisiae* mono-ubiquitination is the principal signal for internalization of several plasma membrane proteins, like the pheromone receptor Ste2p (Hicke and Riezman, 1996), the ABC-transporter Ste6p (Kölling and Hollenberg, 1994), the uracil permease Fur4p (Galan *et al.*, 1996) into primary endocytic vesicles. In the cases of Ste2p and Fur4p phosphorylation precedes ubiquitination and their inactivation is Rsp5p-dependent. In yeast, the E3 ligase Rsp5p is the unique member of the conserved Rsp5/Nedd4 HECT-family. Rsp5p contains motifs responsible for driving interactions with both proteins and lipids (Wang *et al.*, 1999). It is involved in the (mono-)ubiquitination of receptors, channels and transporters as a signal for internalization from the plasma membrane (Rotin *et al.*, 2000) and intracellular sorting into the MVB (Katzmann *et al.*, 2002). Additionally, it is becoming clear that *trans*-acting proteins of the endocytic machinery, like Sla2p, which links the early endocytic coated vesicle to the actin polymerization machinery (Kaminska *et al.*, 2002; Newpher and Lemmon, 2006), and the amphyphysin homologue Rvs167p (Stamenova *et al.*, 2004) are targets of the ubiquitin ligase Rsp5p. However, the requirement of ubiquitination for the early steps of receptor endocytosis is still controversial based on the fact that, although Ub facilitates the

removal of receptors from the cell membrane, it is also dispensable for the constitutive internalization of many transmembrane receptors (Holler and Dikic, 2004).

Nevertheless, in recent years it has become evident that ubiquitin may also play a role in the sorting of proteins from the TGN. In particular, ubiquitination of cargo proteins, such as the general amino acid permease Gap1p, at the TGN is implicated in the sorting to different cellular destinations, like the vacuole or plasma membrane (Polo *et al.*, 2003; Staub and Rotin, 2006). Gap1p becomes either mono-ubiquitinated and hence targeted to the plasma membrane or poly-ubiquitinated and transported into the vacuole. Both types of modification depend on Rsp5p (Helliwell *et al.*, 2001). Although not ubiquitinated themselves, the coat components Gga1p and Gga2p of the TGN sorting pathway bind directly to ubiquitin (Scott *et al.*, 2004). Gga1p and Gga2p are monomeric adaptors, which promote the incorporation of proteins into clathrin-coated vesicles destined for transport to endosomes (Bonifacino, 2004). The interaction of the GAT domain of Gga2 with ubiquitinated Gap1p is required for the ubiquitin-dependent sorting of the Gap1p amino acid transporter from the TGN to endosomes (Scott *et al.*, 2004).

The real impact of multi/mono-ubiquitination on protein function and sorting is only starting to be appreciated.

1.5 The role of phosphoinositides in membrane traffic and their turnover by phosphatases of the synaptojanin family

1.5.1 Phosphoinositide isoforms and their subcellular distribution

The organelles of the endocytic and biosynthetic pathways have distinct functions, molecular compositions, and environments. To achieve this diversity of structure and composition, the membranes of the distinct organelles must keep separate for the most part to prevent fusion. The minor class of phosphoinositides (PIs) is thought to contribute to this diversity, because distinct isoforms localize to different compartments. The isoforms are caused by the reversible phosphorylation of the inositol headgroup of phosphatidylinositol (PtdIns) at one or a combination of the hydroxy groups at the 3′, 4′, and 5′ position of the inositol ring (Roth, 2004). The different PIs bind with variable affinities and specificities to a variety of protein motifs (Lemmon, 2003). As second messengers, phosphoinositides additionally control several cellular processes including cell signaling, cell growth, vesicular trafficking, transcription, and actin cytoskeletal arrangement (Hurley and Meyer, 2001; Martin, 2001; Roth, 2004; Simonsen *et al.*, 2001). The synthesis and turnover of PIs are

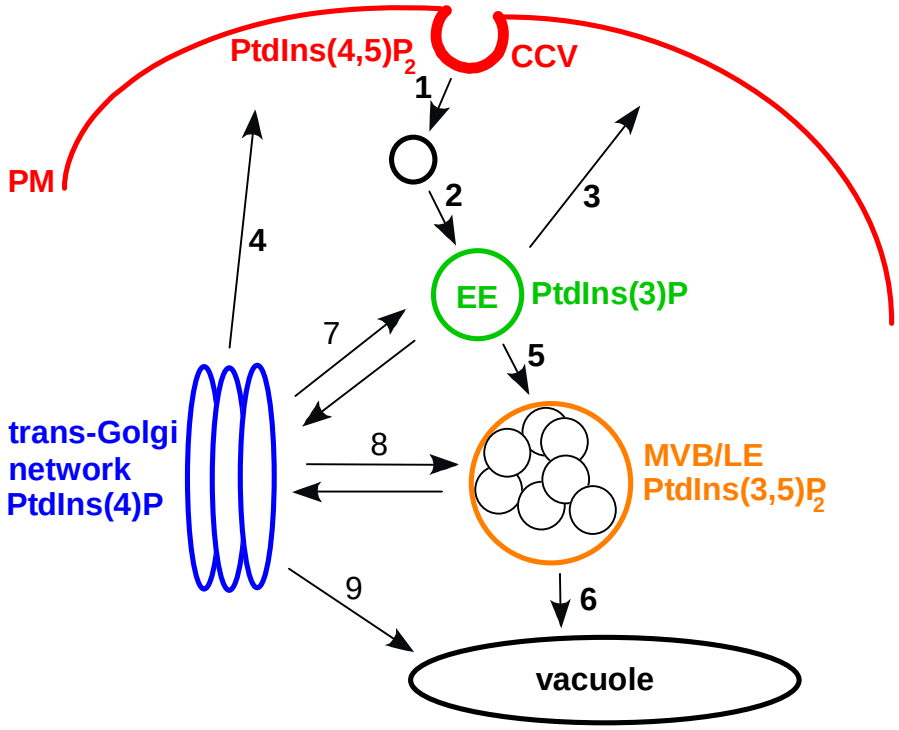

Fig. 2. Subcellular distribution of the major phosphoinositide isoformes
The major concentration of phosphatidylinositol-4,5-bisphosphate [PtdIns(4,5)P_2] (red) is within the plasma membrane. PtdIns(3)P (green) is concentrated in early endosomes, while the majority of PtdIns(3,5)P_2 (orange) is in the late endosomes. PtdIns(4)P (blue) is the main phosphatidylinositol within membranes of the Golgi complex.

regulated by a set of kinases, phosphatases, and lipases localized to discrete membrane sites (Fig. 2) (Odorizzi *et al.*, 2000). Overexpression of kinases or deletion of phosphatases that consume phosphoinositides causes changes in the specific distribution of the different phosphoinositides, possibly resulting in dramatic alterations of the cell morphology. Therefore, it is crucial that local concentrations of phosphoinositides are controlled dynamically through a balanced synthesis by kinases and phosphatases that hydrolyse them.

Along the endocytic pathway, phosphatidylinositol 4,5-bisphosphate (PtdIns(4,5)P_2) is the major PI found at the plasma membrane, where it participates in the recruitment of proteins involved in endocytosis and the actin cytoskeleton via binding of e.g. ENTH domain (Martin, 2001; Yin and Janmey, 2003). Binding of PtdIns(4,5)P_2 by the ENTH (epsin 1 NH_2-terminal homology) domain causes the NH_2-terminal helix of the domain to penetrate into the lipid bilayer, which induces membrane curvature (Roth, 2004). PtdIns(4,5)P_2 interacting partners are e.g. Sla2p, epsins En1p and Ent2p, which contain ENTH domains (Aguilar *et al.*, 2003; Engqvist-Goldstein *et al.*, 1999), and the Arp2/3p complex activator protein Las17p. In turn, Sla2p and epsins bind to clathrin and other proteins with multiple interacting domains like Pan1p (Henry *et al.*, 2002; Wendland *et al.*, 1999). The multivalent adaptor protein Pan1p is able to associate both with proteins required for endocytosis and actin cytoskeleton

organization, like for example to the adaptor yAP180p and the cortical actin patch component Sla1p (Wendland and Emr, 1998). Epsins also associate with receptors destined for internalization (Shih *et al.*, 2002). Thus, the interaction of epsins and Sla2p with PtdIns(4,5)P_2 may tether the clathrin lattice to the plasma membrane. In fact, PtdIns(4,5)P_2 plays a crucial role in enhancing clathrin coat formation at the plasma membrane (Cremona and De Camilli, 2001).

PtdIns(3)P is found within early endosomal membranes and participates in sorting steps from early endosomes (Odorizzi *et al.*, 2000). Human EEA1, a protein that specifically binds to PtdIns(3)P, has been shown to participate in the docking of clathrin-coated vesicles to early endosomes (Rubino *et al.*, 2000). During endosome biogenesis, PtdIns(3)P is required for the sorting of some endocytic cargo molecules into multivesicular bodies by recruiting components of the sorting machinery (Katzmann *et al.*, 2003).

PtdIns(3,5)P_2 is synthesized on late endosomal membranes by the yeast PtdIns(3)P-5 kinase Fab1p, which is recruited to the membrane by PtdIns(3)P. Fab1p activity has been shown to be required for the maintenance of the vacuolar size and some of its effectors may play a role in the recycling of membranes from the vacuole to the MVB (Gary *et al.*, 1998).

The major pool of PtdIns(4)P is found at the Golgi complex. Interestingly, in mammalian cells it has been found that a ninefold lower than at the plasma membrane, but considerable amount of PtdIns(4,5)P_2 is also present within Golgi membranes (Terui *et al.*, 1994). Several studies propose that the Golgi-localized PtdIns(4,5)P_2 is required to maintain its structure (Sweeney *et al.*, 2002). Nevertheless, PtdIns(4)P regulates the targeting of the clathrin adaptor AP-1 complexes to the Golgi (Wang *et al.*, 2003). In yeast, membrane traffic through the Golgi requires PtdIns(4)P (Audhya *et al.*, 2000). In *Saccharomyces cerevisiae*, synthesis of PtdIns(4)P is mediated by two PtdIns 4-kinases, Pik1p and Stt4p. Pik1p has been demonstrated to play a direct role in late events of the secretory pathway, secretory vesicle budding at the late Golgi, integrity of Golgi structure, and cytokinesis (Flanagan and Thorner, 1992; Walch-Solimena and Novick, 1999). Stt4p is required for actin cytoskeleton organization, cell wall integrity, and maintenance of vacuole morphology (Audhya *et al.*, 2000). Interestingly, the PI-phosphatase Sac1p preferentially acts on a pool of PtdIns(4)P synthesized by the Stt4p kinase (Foti *et al.*, 2001).

1.5.2 The synaptojanin family

Synaptojanin family members are highly conserved phosphoinositide 5-phosphatases that are conserved from yeast to human. Three domains define them (McPherson *et al.*, 1996): a N-terminal Sac1-like domain that resembles the polyphospho-inositide phosphatase domain

of the yeast Sac1p, a central phosphoinositide 5´phosphatase (5-Pase) domain, and a C-terminal proline-rich domain (Fig. 3A). While the 5´phosphatase activity specifically hydrolyses the phosphate at the 5' position of the inositol ring of PtdIns(4,5)P_2, the Sac1-like domain of some synaptojanin members possesses a polyphosphoinositide phosphatase (PPIP) activity that results in the de-phosphorylation of PtdIns(3)P, PtdIns(4)P, and PtdIns(3,5)P_2 to PtdIns (Fig. 3B) (Guo *et al.*, 1999). The C-terminal proline-rich domain of the synaptojanin family members is the most variable region and may provide specialized function as an interaction platform for a large number of proteins. Synaptojanin 1 in mice is one of the best-characterized members of the synaptojanin family. Synaptojanin 1-knockout mice accumulated an increased number of clathrin-coated vesicles and PtdIns(4,5)P_2 in the nerve terminals. Therefore, synaptojanin 1 is proposed to be implicated in the de-phosphorylation of PtdIns(4,5)P_2 to PtdIns(4)P. This de-phosphorylation is suggested to reduce the affinity of

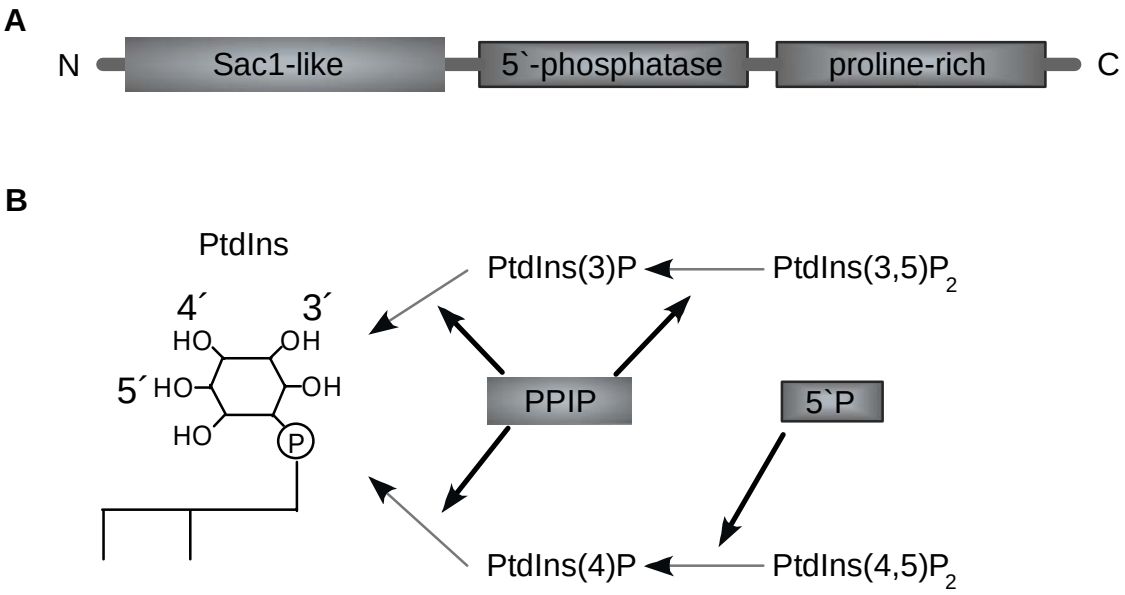

Fig. 3. Domain structure and phosphatase activities of synaptojanin proteins
(**A**) The conserved three domain structure of synaptojanin proteins (**B**) Schematic structure of PtdIns, which is made up of glycerol, fatty acid and the base is replaced by a hexahydric alcohol namely inositol. The Sac1-like domain of some synaptojanin proteins possesses a polyphosphoinositide phosphatase (PPIP) activity resulting in the turnover of phosphatidylinositolphosphates: PtdIns(3)P, PtdIns(4)P, and PtdIns(3,5)P_2. The 5-Pase domain de-phosphorylates specifically PtdIns(4,5)P_2.

endocytic coat components to the vesicle membrane (Cremona *et al.*, 1999). Further evidence for this idea came from observations of a clathrin-coated vesicle accumulation after deletion of members of the synaptojanin 1 orthologues in the model organisms *Caenorhabditis elegans* and *Drosophila melanogaster*. Mutants in *unc-26*, the unique synaptojanin-like protein in *C. elegans*, exhibit a pleiotropic phenotype. Defects were observed at different stages of

endocytosis: the recruitment of the endocytic machinery, the fission of vesicles from the plasma membrane, and the un-coating of vesicles after fission from the membrane (Harris *et al.*, 2000). Similarly, *D. melanogaster* Synj mutants are dramatically impaired in the process of endocytosis. In these mutants densely coated, reminiscent of clathrin-coated, vesicles were observed at the synaptic membrane (Verstreken *et al.*, 2003). A similar phenotype was also described for lamprey giant synapses after disruption of synaptojanin function (Gad *et al.*, 2000).

Since endocytosis and actin dynamics are tightly coupled processes (see section 1.3.2), it is not surprising that defects in the interaction of synaptic vesicles with the actin cytoskeleton were observed in the synaptojanin mutants of mice as well as of flies and worms (Dickman *et al.*, 2006; Harris *et al.*, 2000; Kim *et al.*, 2002; Verstreken *et al.*, 2003).

1.5.3 The synaptojanin-like family in *Saccharomyces cerevisiae*

The yeast *Saccharomyces cerevisiae* contains three synaptojanin-like (Sjl) proteins, Sjl1p, Sjl2p, and Sjl3p (also named Inp51p, Inp52p, and Inp53p). Single *sjl1*, *sjl2*, *sjl3* null mutants are viable and produce little changes in the phenotype when compared to wildtype cells. Cells deficient for all three synaptojanin genes are inviable (Srinivasan *et al.*, 1997; Stolz *et al.*, 1998). Since Sjl2p and Sjl3p distribute to cortical actin patches under osmotic stress conditions it was suggested that a defective cell wall structure is a critical factor for the lethality of the triple knockout (Ooms *et al.*, 2000). Pair-wise deletions of the synaptojanin genes have discovered differences among the three double deletion mutants. It was found that receptor-mediated and fluid-phase endocytosis were impaired in Δ*sjl2*Δ*sjl3* cells, but more severely in Δ*sjl1*Δ*sjl2* mutants (Singer-Krüger *et al.*, 1998). This impairment based likely on folded plasma membrane invaginations visible in Δ*sjl1*Δ*sjl2* mutants, demonstrating a selective impairment of endocytosis in these cells (Singer-Krüger *et al.*, 1998; Stolz *et al.*, 1998). In Δ*sjl2*Δ*sjl3* cells, an overall pronounced thickening of the cell wall might explain the defects in endocytosis (Stolz *et al.*, 1998). *Δsjl1Δsjl2* and *Δsjl2Δsjl3* mutants exhibited alterations in the organization of the actin cytoskeleton and in the cell surface morphology (Singer-Krüger *et al.*, 1998; Srinivasan *et al.*, 1997; Stolz *et al.*, 1998). Surprisingly, the Δ*sjl1*Δ*sjl3* mutant in which Sjl2p is present appeared similar to wildtype (Singer-Krüger *et al.*, 1998; Srinivasan *et al.*, 1997; Stolz *et al.*, 1998). Subsequent genetic and functional analysis of *SJL1*, *SJL2*, and *SJL3* supported the view that the corresponding enzymes are, despite some redundant function, not simply redundant isozymes.

All described physiological consequences of inactivating the yeast synaptojanins are thought to be specifically due to an increase in PtdIns(4,5)P_2 levels on internal membranes as

well as the plasma membrane, because the lethality of *Δsjl1Δsjl2Δsjl3* cells can be rescued by a Sac1 domain-defective form of Sjl2p (Stefan *et al.*, 2002). Thus, the three synaptojanin-like proteins play a key role in the control of the turnover and hence the localization of PtdIns(4,5)P_2 in *S. cerevisiae*. Concluding, by the regulation of PtdIns(4,5)P_2 levels the yeast synaptojanins probably control two pathways, endocytosis and sorting between the TGN and endosomes likely in conjunction with clathrin (Ha *et al.*, 2003; Stefan *et al.*, 2002). Indeed, convincing evidence existed that Sjl3p exhibit a specific role in clathrin-mediated protein sorting at the TGN (Bensen *et al.*, 2000; Ha *et al.*, 2001; Ha *et al.*, 2003). In contrast, Sjl2p may represent the major player in early steps of endocytosis based on the analysis of the endocytic defects in the three yeast synaptojanin-like double mutants (Singer-Krüger *et al.*, 1998). Sjl1p seems to play a general role in regulating actin cytoskeletal organization, endocytosis, and delivery of endocytic vesicles to the vacuole, apparently via control of PtdIns(4,5)P_2 levels (Singer-Krüger *et al.*, 1998; Stefan *et al.*, 2002).

To summarize, like their homologs in mammals, flies, and worms, the yeast synaptojanins seem to control vesicle trafficking by regulating phosphoinositide turnover. Since the yeast synaptojanins all possess a similar catalytic activity, it is possible that their distinct localization, specific regulation mechanisms, and different interacting partners determine specific functions.

1.6 Goal of this project

The goal of this PhD work was to gain new insights into the functional differences between the three yeast synaptojanin-like family members Sjl1p, Sjl2p, and Sjl3p, also designated as Inp51p, Inp52p, and Inp53p, respectively. All three synaptojanin proteins possess a highly conserved 5-Pase activity, but only Sjl2p and Sjl3p possess PPIPase activities. The C-terminal proline-rich domains of the synaptojanin-like family members share minor identity. The enzymatic activities of these phosphoinositide phosphatases are critical for the turnover of PtdIns(4,5)P_2 and hence membrane traffic. In particular, the synaptojanin-like proteins were assumed to participate in clathrin-mediated vesicle transport.

Previous studies have tentatively implicated Sjl3p in the clathrin-mediated transport between the TGN and endosomes, but the explicit subcellular localization of Sjl1p and Sjl2p remained to be elucidated. Sjl2p was suggested to be the key player during endocytosis in yeast, but clear evidence for a function in this pathway was still lacking. To support the idea of a specific function of Sjl2p in endocytosis, new interaction partners were identified *in vivo* by co-immunoprecipitations and *in vitro* GST-pulldown experiments. To determine the possible association with clathrin-coated vesicles, they were isolated and the co-fractionation

of all three synaptojanins was investigated. Next, it was addressed which domains or interaction partners of Sjl2p may recruit this phosphatase to clathrin-coated vesicles. The proline-rich domains of the synaptojanin proteins are highly variable and are supposed to provide an interaction platform for proteins, which may target the yeast family members to distinct subcellular sides. To reveal whether this domain mediates the interaction with specific binding partners, the subcellular localization and physical interaction partners of a chimeric protein were investigated, in which the C-terminal proline-rich domain of Sjl3p was fused to the catalytic domains of Sjl2p. Since recent work has shown that posttranslational modifications play an important regulatory role in endocytosis as well as the sorting from the TGN, Sjl1p, Sjl2p, and Sjl3p were analysed for modification by phosphorylation and ubiquitination.

2 Materials and Methods

2.1 Materials

2.1.1 Saccharomyces cerevisiae strains

The *Saccharomyces cerevisiae* strains used in this study are listed below.

Yeast strains	Genotype	Source
BS64	*MAT*a *his4 ura3 leu2 lys2 bar1-1*	Singer-Krüger et al., 1994
BS620	*MAT*^{1} *his4 ura3 leu2 lys2 bar1-1*	B. Singer-Krüger
BS1175	*MAT*α *ura3 leu2 SJL2::3-HA-HIS5 (S. pombe) sec7 bar1-1*	B. Singer-Krüger
BS1198	*MAT*α *ura3 leu2 lys2 SLA1::3-HA-HIS5 (S. pombe) bar1-1*	B. Singer-Krüger
BS1248	*MAT*a *his4 ura3 leu2 lys2 SJL2::13-Myc-kan^{r} bar1-1*	B. Singer-Krüger
BS1678	*Δrvs167*	H. Riezman
CB1	*MAT*α *ura3 leu2 lys2 SJL2::13-Myc-kan^{r} SLA1::3-HA-HIS5 (S. pombe) bar1-1*	this study
CB2	*MAT*α *ura3 leu2 lys2 SJL2-13-Myc-kan^{r} ABP1::3-HA-HIS5 (S. pombe) bar1-1*	this study
CB25	*MAT*α *his4 ura3 leu2 lys2 SJL3::3-HA- kan^{r} bar1-1*	this study
CB42	*MAT*α *ura3 leu2 lys2 SJL1::3-HA-HIS5 (S. pombe) SJL2-13-Myc-kan^{r} SJL3::3-HA-kan^{r} bar1-1*	this study
CB45	*MAT*a *ura3 leu2 lys2 SJL2::13-Myc-kan^{r} SLA1::3-HA-HIS5 (S. pombe) bar1-1*	this study
CB47	*MAT*α *ura3 leu2 lys2 SLA1::3-HA-HIS5 (S. pombe) BSP1::13-Myc-kan^{r} bar1-1*	this study
CB53	*MAT*a *his4 ura3 leu2 lys2 BSP1::13-Myc-kan^{r} bar1-1*	this study
CB58	*MAT*a *his4 ura3 leu2 lys2 PAN1::3-HA-kan^{r} bar1-1*	this study
CB71	*MAT*α *his4 ura3 leu2 lys2 SLA1::3- HA-HIS5 (S. pombe) PAN1::3-HA-kan^{r} bar1-1*	this study
CB72	*MAT*α *his4 ura3 leu2 lys2 SJL2::13-Myc-kan^{r} SLA1::3-HA-HIS5 (S. pombe) PAN1::3-HA-kan^{r} bar1-1*	this study
CB77	*MAT*α *his4 ura3 leu2 lys2 PAN1::3-HA-kan^{r} SLA1::13-Myc-HIS5 (S. pombe) bar1-1*	this study
CB84	*MAT*α *his4 ura3 leu2 lys2 3-HA::CLC1 -kan^{r} bar1-1*	this study
CB105	*MAT*a *ura3 leu2 lys2 SJL3::13-Myc-kan^{r} SLA1::3-HA-HIS5 (S. pombe) PAN1::3-HA-kan^{r} bar1-1*	this study
CB128	*MAT*α *ura3 leu2 lys2 abp1Δ::kan^{r} SJL2::13-Myc-kan^{r} SLA1::3-HA-HIS5 (S. pombe) bar1-1*	this study
CB131	*MAT*α *his4 ura3 leu2 lys2 abp1Δ::kan^{r} SJL2::13-Myc-kan^{r} bar1-1*	this study
CB136	*MAT*a *ura3 leu2 lys2 SJL1::3-HA-HIS5 SLA1::13-Myc-kan^{r} bar1-1*	this study
CB137	*MAT*a *his4 ura3 leu2 lys2 SLA1::13-Myc-kan^{r} bar1-1*	this study
CB140	*MAT*α *his4 ura3 leu2 lys2 SLA1::13-Myc-kan^{r} bar1-1*	this study

CB164	*MAT^{l} his4 ura3 leu2 lys2 sla1Δ::kan^{r} SJL2::13-Myc-kan^{r} bsp1Δ::kan^{r} bar1-1*	this study
CB175	*MAT*a *his4 ura3 leu2 SJL3::3-HA-kan^{r} sec7bar1-1*	this study
CB178	*MAT*a *his4 ura3 leu2 lys2 bar1-1* GFP-*ABP1* [pDD890 (D.Drubin)]	this study
CB181	*MAT*a *his4 ura3 leu2 lys2 SJL2::13-Myc-kan^{r} bar1-1* GFP-*ABP1* [pDD890 (D.Drubin)]	this study
CB185	*MAT^{l} his4 ura3 leu2 lys2 sjl2Δ::kan^{r} SLA1::13-Myc-kan^{r} bar1-1*	this study
CB195	*MAT^{l} ura3 leu2 SLA1::13-Myc-kan^{r} SJL2::3-HA-HIS5 (S.pombe) sec7 bar1-1*	this study
CB197	*MAT^{l} ura3 leu2 SLA1::13-Myc-kan^{r} sec7 bar1-1*	this study
CB207	*MATa ura3 leu2 SJL2::3-HA-HIS5 (S. pombe) SLA1::13-Myc-kan^{r} bar1-1*	this study
CB228	*MAT^{l} his4 ura3 leu2 lys2 pik1-83::TRP1 SJL2::13-Myc-kan^{r} bar1-1*	this study
CB233	*MAT^{l} his4 ura3 leu2 lys2 sjl2Δ::kan^{r} SLA1::13-Myc-kan^{r}* pRS315-SJL2/3-3-HA *bar1-1*	this study
CB240	*MATa ura3 leu2 SJL2::3-HA-HIS5 (S. pombe) SLA1::13-Myc-kan^{r} bar1-1* pRS415-RSP5-Flag	this study
CB246	*MATα his4 ura3 leu2 lys2 SLA1::13-Myc-kan^{r} bar1-1* pRS415-RSP5-Flag	this study
CB248	*MAT^{l} ura3 leu2 lys2 sjl1Δ::his5 (S. pombe) sjl2Δ::kan^{r} sjl3Δ::kan^{r}* pRS316-SJL2 pRS315-SJL2/3-3-HA	this study
CB260	*MAT*a *his4 ura3 leu2 lys2 ade2* pRS315	this study
CB263	*MAT^{l} his4 ura3 leu2 lys2 ade2 gga1Δ::kan^{r} gga2Δ::kan^{r} sjl3Δ::kan^{r}* pRS315-SJL2/3-3-HA	this study
CB266	*MAT^{l} his4 ura3 leu2 lys2 ade2 gga1Δ::kan^{r} gga2Δ::kan^{r} sjl3Δ::kan^{r}* pRS315-SJL2/3-3-HA	this study
CB270	*MAT^{l} his4 ura3 leu2 lys2 ade2 gga1Δ::kan^{r} gga2Δ::kan^{r} sjl3Δ::kan^{r}* pRS315	this study
CB272	*MAT^{l} his4 ura3 leu2 lys2 ade2 gga1Δ::kan^{r} gga2Δ::kan^{r} sjl3Δ::kan^{r}* pRS315	this study
CB276	*MAT^{l} his4 ura3 leu2 lys2 ade2 gga1Δ::kan^{r} gga2Δ::kan^{r} sjl3Δ::kan^{r}* pRS416-SJL3 (YOR109W)	this study
CB278	*MAT^{l} his4 ura3 leu2 lys2 ade2 gga1Δ::kan^{r} gga2Δ::kan^{r} sjl3Δ::kan^{r}* pRS416-SJL3 (YOR109W)	this study
SK3	*MAT^{l} his4 ura3 leu2 lys2 sjl2Δ::kan^{r} bar1-1* pRS315-SJL2-Δprd-3HA	Svenja Kaden
SK7	*MAT^{l} ura3 leu2 lys2 sjl1Δ::his5 (S. pombe) sjl2Δ::kan^{r} sjl3Δ::kan^{r} bar1-1* pRS316-SJL2 pRS315-SJL2	Svenja Kaden
SK9	*MAT^{l} ura3 leu2 lys2 sjl1Δ::his5(S. pombe) sjl2Δ::kan^{r} bar1-1* pRS316-SJL2 pRS315- SJL2-Δprd-3-HA	Svenja Kaden
SK22	*MAT^{l} his4 ura3 leu2 lys2 sjl2Δ::kan^{r} SLA1::13-Myc-kan^{r} bar1-1* pRS315- SJL2-Δprd-3-HA	Svenja Kaden
SK94	*MAT^{l} ura3 leu2 lys2 sjl1Δ::his3 (S. pombe) sjl2Δ::kan^{r} r*	Svenja Kaden

	sjl3Δ::kann bar1-1 pRS315-SJL2-3-HA	
Y190	*MAT*a *gal4 gal80 his3 trp1-901 ade2-101 ura3-52 leu2-3, -112 +URA3::GAL→lacZ, LYS2::GAL→HIS3 cyh^r*	S. Elledge, USA
Y190Δ*sla1*	*MAT*a *gal4 gal80 his3 trp1-901 ade2-101 ura3-52 leu2-3, -112 +URA3::GAL→lacZ, LYS2::GAL→HIS3 cyh^r sla1Δ::kan^r*	B. Singer-Krüger

[1] not determined

2.1.2 *Escherichia coli* strains

The DH5α strain was used for all plasmid amplifications and DNA ligations.

DH5α	F´/endA1 hsdR17($r_{k-}m_{k+}$) supE44 thi-1 recA1 gyrA (Nal_r)	Hanahan, 1983
BL21		(Novagene, Madinson, WI)

2.1.3 Plasmids

The plasmids used in this study are listed below.

Plasmid name	**Characteristics**	**Source**
pGEX5T-3-Chc1-369	contains *BamH*I/*Sal*I fragment of *CHC1* (encodes amino acids 1-369)	this study
pGEX5T-3-Chc1-483	contains *BamH*I/*Sal*I fragment of *CHC1* (encodes amino acids 1-483)	this study
pAS1-Sjl2-588	encodes the proline-rich domain of *SJL2*	B. Singer-Krüger
3´Sjl2#19	encodes the ORF of *ABP1*	B. Singer-Krüger
pRS315-HA-Sjl2-Δprd	encodes *SJL2* lacking the proline-rich domain	B. Singer-Krüger
pRS415Gal1-Flag-RSP5	encodes full-length *RSP5*	M.Tyres (Wolf group)
pRS315-SJL2	encodes full-length *SJL2*	B. Singer-Krüger
pRS315-HA-SJL2	encodes full-length SJL2 tagged with 3 HA epitopes	B. Singer-Krüger
pGEM-T-easy-PRD-SJL3-HA	contains *Sac*II/*SnaB*I fragment of *SJL3* (encodes amino acids 863-1108 of *SJL3*; the C-terminal 3 HA epitopes and the ADH terminator)	this study
pRS315-HA-Sjl2/3	contains *Sac*II/*SnaB*I fragment of *SJL3* (encodes amino acids 1-887 of *SJL2* followed by amino acids 863-1108 of *SJL3*)	this study
pRS316-Sjl2	encodes full-length *SJL2*	B. Singer-Krüger
pGEX5-3-SJL2-3`end	encodes the proline-rich domain of *SJL2*	B. Singer-Krüger
pGEX5-3-SJL2-3`end-LI>AA	encodes the proline-rich domain of *SJL2* with amino acids L_{944} and I_{945} mutated to alanines (mutagenesis of the plasmid pGEX5-3-SJL2-3`end)	this study

2.1.4 Antibodies

Antibodies used in this study are listed below and dilutions used for immunoblotting are specified.

2.1.4.1 Primary antibodies used for immunoblotting

Antibodies	Dilution	Source
Mouse monoclonal purified anti-HA, clone 16B12	1:2000	Covance
Mouse monoclonal anti-c-Myc	1:1000	Oncogene
Mouse monoclonal anti-Chc1p ascites fluid	1:250-500	S. Lemmon, USA
Rabbit polyclonal anti-Vps10p	1:500	B. Singer-Krüger
Mouse anti-actin (C4)	1:500	Boehringer
Mouse monoclonal anti-PGK (22C5-D8)	1:1000	Oncogene
Rabbit polyclonal anti-Sjl2p	1:100	B. Singer-Krüger
Mouse anti-Ubiquitin, clone P4G7	1:100	Covance
Rabbit polyclonal anti-Rvs167p	1:1000	H. Riezman
Mouse monoclonal anti-phosphotyrosin (PY-20)	1:1000	Sigma
Rabbit polyclonal anti-FAS	1:2000	Egner *et al.*, 1993 (Wolf group)
Rabbit polyclonal anti-Ape1p	1:1000	Klionsky *et al.*, 1992 (Wolf group)

2.1.4.2 Secondary antibodies used for immunoblotting

Antibodies	Dilution	Source
Goat anti-mouse IgG, alkaline phosphatase-conjugated	1:1000	Kirkegaard & Perry Laboratories
Goat anti-rabbit IgG, alkaline phosphatase-conjugated	1:1000	Kirkegaard & Perry Laboratories

2.1.4.3 Antibodies used for immunoprecipitations

Antibodies	Source
Mouse monoclonal purified anti-HA, clone 3F10	Roche
Mouse monoclonal anti-c-Myc, A-14 (789)	Santa Cruz Biotechnologies, Inc.
Rabbit polyclonal anti-Sjl2p	B. Singer-Krüger
Rabbit polyclonal anti-Rvs167p	H. Riezman

2.1.4.4 Antibodies used for quantitative immunoblotting

Primary antibodies were used as for immunoblotting (see section 2.1.4.1). If they were from mice, an unlabeled rabbit anti-mouse IgG antibody (dilution 1:1000, Sigma-Aldrich) was used as a secondary antibody. Dilutions for labeling of the IgGs with [^{125}I]protein A (Amersham Bioscience) were calculated depending on decay of Iodine-125 from the activity reference date.

2.1.5 Enzymes and kits used for molecular biology

Restriction endonucleases used in this study were provided either by Roche or New England Biolabs (NEB). The Vent DNA polymerase (NEB), the Taq DNA polymerase (Roche), and the Polymerase Mix of the Expand long template PCR system (Roche) were used for DNA amplifications by the polymerase chain reaction (PCR).

The QIAprep Spin Miniprep Kit (Qiagen) was used for DNA isolation from *Escherichia coli* cells, the QIAEX II Gel Extraction Kit (Qiagen) for DNA extraction from agarose gels. The QIAquick PCR Purification Kit (Qiagen) was used for PCR fragment purification.

2.1.6 Chemicals

Unless otherwise indicated, the companies Genaxxon, Merck, Roth, and Sigma provided chemicals used in this study.

2.1.7 Media

Yeast strains were propagated either in complete medium (YPD) (1 % (w/v) Bacto® yeast extract, 2 % (w/v) Bacto® peptone, 2 % (w/v) glucose, pH 5.5) or in synthetic growth medium (SD medium) (0.67 % (w/v) yeast nitrogen base, 2 % (w/v) glucose, pH 5.6) containing 0.3 mM adenine, 0.4 mM tryptophan, 1 mM lysine, 0.3 mM histidine, 1.7 mM leucine, and 0.2 mM uracil (final concentration) (complete SD medium). Cells were grown to early/mid logarithmic phase (0,1-0,8 OD_{600} units/ml) at 30 °C on a rotary shaker, unless otherwise indicated. Yeast transformants carrying a plasmid were grown in SD medium lacking either leucine or uracil depending on the selection marker (*LEU2* or *URA3*, respectively) present on the plasmid (selective SD medium).

Solid medium contained 2 % (w/v) Bacto® Agar in addition to the YPD or SD medium components. Plasmid shuffle in yeast transformants carrying one plasmid with the *URA3* marker and a second with the *LEU2* marker was induced by growth on SD plates lacking leucine and containing 1mg/ml fluoro-orotic acid (5-FOA) and 0,75 mM uracil, resulting in the loss of the plasmid carrying the *URA3* marker. Selective growth of yeast cells carrying a gene deletion or an epitope marked by the kan^r gene for geneticin resistance was performed by incubation on YPD plates containing 0,2 mg/ml geneticin (G-418 sulfate).

The sporulation of diploid cells was induced by incubation at 25 °C on presporulation plates (0.8 % (w/v) Bacto® yeast extract, 0.3 % (w/v) Bacto® peptone, 10 % (w/v) glucose, 2 % (w/v) Bacto® Agar) for 1 day and sporulation plates (1 % (w/v) potassium acetate, 0.1 %

(w/v) Bacto® yeast extract, 0.05 % (w/v) glucose, 2 % (w/v) Bacto® Agar, 0.075 mM adenine, 0.1 mM tryptophan, 0.25 mM lysine, 0.075 mM histidine, 0.42 mM leucine, 0.05 mM uracil) for 5 to 10 days at 25 °C.

Escherichia coli cells transformed with plasmids carrying the gene Amp^r for ampicillin resistance as selection marker were propagated in LB medium (0.5 % (w/v) yeast extract, 1% (w/v) Bacto® trypton, 0.5 % (w/v) NaCl, pH 7.5) containing 0,1 mg/ml ampicillin.

2.2 Methods

2.2.1 Generation of DNA constructs

All DNA manipulations were done by standard techniques (Sambrook *et al.*, 1989). Enzymes were used as suggested by the provider. *E. coli* cells were transformed by heat shock. All PCR-amplified DNA fragments subcloned in a vector were sequenced (MWG, Martinsried) to exclude the presence of PCR errors.

2.2.1.1 Mutagenesis of pGEX5-3-SJL2-3´end

In order to mutate the clathrin-binding box in the proline-rich domain Sjl2p site-directed mutagenesis was performed according to the technical manual of the GeneEditor™ (Promega). Approximately 2 µg from the plasmid pGEX5-3-SJL2-3´end (B. Singer-Krüger) that encodes the proline-rich domain of Sjl2p were denatured by alkaline denaturation. Subsequent annealing of the mutagenic oligonucleotide (see below) to this prepared single-stranded DNA template, synthesis of the mutant strand, and counterselection of the *E. coli* strains by antibiotic agents resulted finally in the replacement of the nucleotide sequence CTAATT (amino acids L_{944} and I_{945}) of Sjl2p by GCAGCT (two alanines). These nucleotide exchanges have introduced a new restriction site for *Pvu*II allowing the screening of positive clones, which were confirmed by sequencing (pGEX5-3-SJL2-3`end-LI>AA).

The primer for the mutagenesis is listed below.

Primer	**Sequence**
LI>AAPvuII,phos	TCAGCGGGCATAAAA***GCAGCT***GACCTAGATGATAC

2.2.1.2 Generation of the chimeric fragment pRS315-HA-Sjl2/3

To amplify a HA-tagged fragment of the proline-rich domain of Sjl3p by polymerase chain reaction (PCR), chromosomal DNA was isolated from the strain CB25, carrying HA-epitope-tagged Sjl3p. The PCR-fragment encoded the proline-rich domain of HA-Sjl3p from amino acid 863 to the ADH terminator after the three HA epitopes. Simultaneously, the PCR primers inserted the restriction sites *Sac*II and *Sna*BI. The PCR product was transformed in a

pGEM-T-easy vector (pGEM-T-easy-PRD-SJL3-HA) and prepared for ligation by digestion with *Sac*II and *Sna*BI. The vector pRS315-SJL2 carries *SJL2* including a *Sna*BI restriction sites N-terminal of the proline-rich domain at amino acid position 888 and a *Sac*II restriction site C-terminal of the PRD. After ligation of the PRD of *SJL3* to the catalytic domains of *SJL2*, the insert (pRS315-SJL2/3-HA) was verified by sequencing. Expression of the protein was checked by generation of cell extracts after transformation into yeast strains.

The primers are listed below.

Primer	**Source**
3`SpeBglII, ADH,Sjl3	B. Singer-Krüger
5`SnaBI, Sjl3	B. Singer-Krüger

2.2.2 Generation of strains

SJL1-HA, *SJL3-HA*, and *SJL3-13-Myc* specific fragments were generated by PCR using pFA6a-3HA-kanMX6 and pFA6a-13Myc-kanMX6 (Longtine *et al.*, 1998) as templates, with oligonucleotides described below, and were inserted downstream of, and in frame with the chromosomal *SJL1*, *SJL2*, and *SJL3* loci, respectively, by homologous recombination. Transformants were purified and correct integration was verified by PCR.

The primers were provided by MWG.

Primer	**Sequence**
5´myc_SJL3	AAGGCCAAACTAAACCATATGACTTTAGACTCATGGCAGCCATTG ACCCCAAAACGGATCCCCGGGTTAATT AAC
5´HA,SJL2	AACCCTGAACTAGAGAAGCTAAGCGTTCATCCATTGAAGCCTTGC GACCCCAATGGAGCAGGGGCGGGTGC
3´HA,SJL2	GAACAACGGTATTTTCATAACAGCCATAGTAATACAGATCATGGT TTGAAAGGTCGAGGTCGACGGTATCGA TAAG
5´HA_SJL1	AGAGATCCCAATCCATTCGTTGAGAACGAAGATGAGCCACTTTTT ATAGAAAGGGGAGCAGGGGCGGGTGC
3´HA-SJL1	TTCAGTTAGAAGATCTACACAGGGACAACAATGATTTGGCAAAAA GTTCCAGCCGAGGTCGACGGTATCGATAAG
5´HA_SJL3	AAGGCCAAACTAAACCATATGACTTTAGACTCATGGCAGCCATTG ACCCCAAAACCCGGGTTAATTAAATC
3´HA_SJL3	TTAATGTGTCCTATTTTTCAGCTTTAAACCCGGCGCGCCTTATTAA CGCACTCCCATCGATGAATTCGAGCTCG

Crossing of haploids, subsequent sporulation of diploids, selection of haploids, and expression analysis generated strains carrying multiple epitope-tagged genes.

2.2.3 Mating, sporulation, dissection, transformation of yeast cells, and two hybrid assays

To generate heterozygous strains, a particular strain of mating type a was mixed with a particular strain of mating type α on YPD plates. After an overnight incubation at 25 °C, the mixture was streaked out at 30 °C on YPD or on selective SD plates to obtain single colonies. After an additional overnight incubation the biggest colonies were marked and analysed under the light microscope for diploid cells at the next day. Colonies of such diploids were streaked out for overnight incubation on presporulation plates at 25 °C and then transferred to sporulation plates. After incubation at 25 °C for at least 5 days up to 10 days, cells were prepared for tetrad dissection in dissection buffer (1,2 M sorbitol, 50 mM Tris/HCl pH7.5) containing lyticase low (isolated by B. Singer-Krüger). Tetrads were separated under the light microscope using a needle for tetrad dissection (Singer Instruments) coupled to a micromanipulator.

Transformation of yeast cells was performed after the lithium acetate method (Ito *et al.*, 1983).

Two-hybrid assays were performed to determine whether the proline-rich domain of Sjl2p interacts with Abp1p in the yeast reporter strain Y190 lacking *SLA1* (Y190Δ*sla1*). The activation of the reporter lacZ gene was analysed using the β-galactosidase colony filter assay (Fields and Song, 1989). The activation of the reporter gene *HIS3* was tested by incubation of the Y190 and Y190Δ*sla1* transformants on selective SD plates lacking uracil, tryptophan and histidine and containing 25 mM 3-amino-1,2,4-triazole (3AT).

2.2.4 Biochemical methods

2.2.4.1 Generation of cell extracts

Total cell extracts were prepared by alkaline lysis as follows. One OD_{600} unit of cells, grown in YPD at 25 °C to early logarithmic phase (0,1-0,3 OD_{600} units/ml), was washed once with ice-cold ddH_2O and resuspended in 1 ml ddH_2O. One hundred µl of 2 N NaOH/5 % (v/v) β-ME were added and cells were lysed for 10 min on ice. Proteins were precipitated by the addition of 6 % (w/v) trichloroacetic acid (TCA) (final concentration) for 30 min on ice. After a 20 min centrifugation at 13.000 rpm, pellets were washed with 1 ml ice-cold acetone. After air-drying at 37 °C, pellets were resuspended in 100 µl of SDS-PAGE 1x Laemmli sample buffer containing 2,5 % β-mercaptoethanol (β-ME) (see below). Samples were vortexed for 20 min at 37 °C, incubated at 95 °C for 5 min, and centrifuged at 13.000 x *g* for 5 min.

A second method for preparing cell extracts is lysis by glass beads. 0,85 OD_{600} units of cells were harvested by spinning at 4.000 rpm for 5 min at room temperature and washed once with 500 µl ice-cold TEPI-buffer (50 mM Tris/HCl pH7.5; 5 mM EDTA/NaOH pH8.0). The cell pellet was resuspended in 100 µl ice-cold TEPI containing 1 x CLAP and 0,1 to 0,12 g glass beads were added. Cells were mechanically lysed by vortexing for 1 min and cooling on ice for 1 min for 5 rounds. 100 µl of 2 x Laemmli sample buffer samples containing 5 % β-ME were added, boiled at 95 °C for 5 min and centrifuged for 5 min at 13.000 x *g* at room temperature. 4 x Laemmli sample buffer is composed of 0,04 % [v/v] bromophenolblue; 10 mM EDTA/NaOH pH8.0; 20 % [w/v] glycerin; 8 % [w/v] SDS; 200 mM Tris/HCl pH6.8) (Laemmli, 1970).

2.2.4.2 SDS-PAGE and Western blotting

SDS-PAGE (sodium dodecyl sulfate – polyacrylamide gel electrophoresis) is a method used for the separation of proteins by molecular mass. Sodium dodecyl sulfate (SDS) is an anionic detergent which denatures secondary and non-disulfide-linked tertiary structures of proteins and applies a negative charge in proportion to the protein mass. Separation of proteins can therefore be conducted in an electrical field in a polyacrylamide gel. The narrow pores of this gel allow small proteins to migrate faster than protein with a higher molecular size. Separation of proteins can be varied by different pore size. Conventional polyacrylamid gels were 1,5 mm thick and consisted of a 4 % stacking gel with the loading pockets for protein samples on top and a 7,5 % resolving gel. Resolving and stacking gel were prepared freshly and filled between the glass plates of the gel pouring system (Biorad, Mini Protean III) after the addition of ammonium persulfate (APS) and TEMED. Around 8 ml of resolving gel were poured first and overlayed with ddH_2O till the polymerization was finished approximately after 45 min at room temperature. As soon as the resolving gel was polymerized the water was rinsed off with filter paper and the stacking gel was poured. Before polymerization of the stacking gel a 15-slot comb was put into the gel and removed after polymerization. For electrophoresis the gel together with the glass plates were transferred into the Biorad Mini Protean III electrophoresis chamber and overlayed with approximately 300 ml SDS running-buffer (25 mM Tris; 190 mM Glycin; 0,1 % SDS). After loading the slots with 5-30 µl of protein sample (mixed with 1 x Laemmli buffer containing 2,5 % β-ME and heated for 5 min at 95 °C) and 2,5 µl of protein molecular mass standard (High range or low range molecular weight marker, Biorad) proteins were separated at 23 mA per gel during running in the stacking gel and 37 mM per gel in the resolving gel for 1-2 h.

After electrophoresis proteins were either stained with Coomassie Brilliant Blue (0,25 % [w/v] Coomassie BB R-250; 7,5 % [v/v] acidic acid; 50 % [v/v] methanol) or transferred onto a nitrocellulose membrane by Western blotting.

Table. 1. Components and volumes for SDS gels

Components	7,5 %	10 %	Stacking gel
ddH_2O	4 ml	3,3 ml	2,6 ml
1,5 M Tris pH 8,8 + 0,4 % (m/v) SDS	2 ml	2 ml	
1,5 M Tris pH 6,8 + 0,4 % (w/v) SDS	-	-	1 ml
Acrylamide/ bisacrylamide solution (37,5 :1)	2 ml	2,7 ml	0,4 ml
10 % (w/v) APS	32 µl	32 µl	14 µl
TEMED	3,2 µl	3,2 µl	5 µl

During Western blotting proteins that were separated by SDS-PAGE (23/37 mA) are transferred from the SDS gel onto a nitrocellulose membranes on which it is possible to probe proteins with specific antibodies for their visualisation. This method was conducted as described by (Towbin *et al.*, 1979) using Mini-Trans-Blot cell system (Biorad). A `sandwich` consisted of one layer of Whatman paper (GB002), a sponge, three layers of Whatman paper, a nitrocellulose membrane, the SDS gel and again three layers of Whatman paper, a sponge and one Whatman paper and was prepared in tank blotting buffer (150 mM Glycin, 20 mM Tris, 20 % methanol). Before use the Whatman papers and the nitrocellulose membrane were rinsed in tank blotting buffer. The `sandwich` was transferred into the blotting apparatus with an orientation of black to black and white to red. Proteins were then transferred to the membrane for 4 h at 200 mA, using a 7,5 % SDS-PAGE gel, respectively. The whole assembly was placed in ice to prevent heating up. After transfer, the nitrocellulose membrane was incubated for 5 min in Ponceau S solution (5 % [v/v] acidic acid; 0,2 % [w/v] Ponceau S) and washed with H_2O to detect transfer of proteins, dried, and stored at room temperature.

2.2.4.2.1 General immunoblotting and detection of ubiquitin

All following incubation steps were performed at room temperature with agitation on a shaker, unless otherwise indicated. After the transfer of the proteins the nitrocellulose membrane was blocked in milk buffer [1 x phosphate saline buffer (2,7 mM KCl; 1,5 mM KH_2PO_4; 137 mM NaCl; 5,6 mM Na_2HPO_4; 1,1 mM NaH_2HPO_4) containing 2,5 % (w/v) low fat milk and 0,2 % (w/v) Tween 20] for one hour at room temperature. Then the membrane was incubated with the first antibody solution for 1 h (section 2.1.4.1), followed by a washing step to wash away unbound antibodies with changing 10 ml of milk buffer 4 times every 5

min. The second antibody (section 2.1.4.2) solution, which is coupled to a alkaline phosphatase, was applied to the membrane and incubated for additionally 1 h. The membrane was washed twice with 10 ml milk buffer and finally twice with 10 ml 0,1 M Tris-Base. The alkaline phosphatase-catalyzed color reaction was performed in freshly prepared development reaction buffer (50 mM $MgCl_2$; 100 mM NaCl; 100 mM Tris/HCl pH9.5; 0.015 % [w/v] of BCIP [5-bromo-4chloro-3-indolyl-phosphate] and 0.03 % [w/v] of NBT [nitroblue tetrazolium] [Bio-Rad Laboratories]) without shaking until the staining was clearly visible.

To detect ubiquitin it was necessary to autoclave (121 °C, 25 min, liquid cycle) the nitrocellulose membrane to improve detection of ubiquitin immunoreactivity (Swerdlow *et al.*, 1986). This had to be done immediately before the immunodetection. For that purpose the membrane was sandwiched in between of 12 layers Whatman paper and submerged in a plastic-box filled up with ddH_2O, weighted down with a 100 ml glass bottle filled with ddH_2O and autoclaved for around 30 min in the liquid cycle (according to Nathan Bays, Hampton Lab, UCSD; hamptonlab.ucsd.edu). The membrane was removed from the box directly at the end of autoclaving procedure at a temperature around 70 – 80 °C and transferred immediately into the milk buffer and blocked for 1 h. The incubation time with the mouse anti-ubiquitin antibody was 2 h.

2.2.4.2.2 Detection of phosphotyrosine

To verify phosphorylated tyrosine by Western blot analysis, it was necessary to proceed the immunodetection in TBST [5 % BSA (98 %, Sigma); 10 mM Tris (pH 7.5); 100 mM NaCl; 0,1 % Tween 20].

2.2.4.3 Expression and purification of GST fusion proteins in *E.coli*

For the expression of GST fusion proteins the protease deficient *E.coli* strain BL21 -(Novagene, Madinson, WI) was used. The plasmid pGEX5-3-CHC1-369 was transformed using heat shock and cells incubated over night at 37 °C. A positive clone was inocculated in 100 ml LB_{Amp} media and grown over night at 37 °C. Twenty-four ml of the overnight culture were used to inoculate 1,2 l LB_{Amp} media. This culture was incubated at 30 °C and at an optical density (OD_{600}) of 0,5 at 600 nm expression of the GST fusion proteins was induced by the addition of 0,5 mM IPTG. After 3,5 h of incubation at 30 °C cells were harvested at 4.000 x *g* for 10 min at room temperature and frozen at –20 °C. The pellet was resuspended in 30 ml ice-cold 1 x phosphate saline buffer (PBS) /5 mM EDTA buffer (2,7 mM KCl; 1,5 mM KH_2PO_4; 137 mM NaCl; 5,6 mM Na_2HPO_4; 1,4 mM NaH_2PO_4; 5 mM EDTA/NaOH pH8.0) containing 1 mM PMSF. The resuspended cells were transferred in a 30-ml Corex tube and

lysed by sonification (Supersonic Sonificator *Sonic Power*) for three times for 8-9 sec (level 4) on ice. The cell lysate was cleared at 12.000 rpm at 4 °C for 30 min (rotor SS-34). The supernatant was transferred to ultracentrifuge tubes and further cleared at 100.000 x *g* for 1 h at 4 °C. To isolate GST-fusion proteins the supernatant was added to 600 µl glutathion Sepharose beads in a 50-ml falcon tube and incubated for 1 h at 4 °C while overhead shaking. Glutathione Sepharose beads were spun down at 500 x *g* for 5 min and washed twice with 40 ml ice-cold 1 x PBS/5 mM EDTA transferred to a 15-ml falcon tube and washed twice with 14 ml 1 x PBS/5 mM EDTA. Bound proteins were eluted by three consecutive treatments with 250 µl of reduced glutathione buffer (20 mM reduced glutathione, 100 mM Tris/HCl pH 8.0). In the cold room, the three supernatants were dialysed separately in dialysis buffer (10 mM HEPES/NaOH pH7.8, 1mM $MgCl_2$, 1 mM DTT and 0,2 mM PMSF) with slow stirring. After 1h the samples were transferred in fresh dialysis buffer and remained therein over night. At the next day the samples were centrifuged for 1 min at 13.000 rpm at 4 °C to remove precipitates, respectively. The supernatants were frozen in liquid nitrogen in aliquots of 80 µg protein and stored at –80 °C.

The primers to generate GST fusions are listed below.

Primer	**Sequence**
Bam,aa1,CHC1,N-term	CGTGGGATCCCAATGAGTGACCTACCCAT
Sal,aa369Stop,CHC1,N	GCAAGTCGACTCATAAATCATCTGCACCTG
Sal,aa483Stop,CHC1	GCAAGTCGACTCAGTAGCAAGCTAGCGCTA

2.2.4.4 Co-immunoprecipitation experiments using Myc-Sjl2p and HA-Sla1p

Cells used for co-immunoprecipitation experiments were prepared in advance as follows. Cells grown in 1,6 l of YPD to an OD_{600} of 0,8-1 were harvested by centrifugation for 5 min at 4000 rpm (4°C). Cell pellets were washed twice with 200 ml ice-cold ddH_2O and once with 50 ml cold IP buffer (115 mM KCl, 5 mM NaCl, 2 mM $MgCl_2$, 1 mM EDTA/NaOH pH 8, 20 mM HEPES/KOH pH 7.8). Cells were resuspended in IP buffer to a concentration of 50 OD_{600} units of cells in 300 µl of total volume. Aliquots containing 300 µl of this cell suspension were frozen in liquid nitrogen and stored at –80°C for subsequent immunoprecipitations.

Alternatively, cells were grown till a given OD_{600} and harvested by centrifugation for 5 min at 4000 rpm at 4 °C. Cell pellets were washed twice with ice-cold ddH_2O and once with cold IP-buffer. After removing the complete supernatant cells were resuspended in 150 – 300 µl of IP-buffer and processed for immunoprecipitation as described below.

One aliquot of CB1 and BS1198 cells were lysed with glass beads (~ 483mg) in the presence of protease inhibitors (1 x CLAP; chymostatin, leupeptin, antipain, pepstatin, each 5 µg/ml final concentration) by vortexing for 45 sec and cooling on ice for 1 min for 10 rounds. Cell lysates were transferred to fresh precooled Eppendorf tubes and glass beads were washed with 800 µl IP buffer (by vortexing for 30 sec). DTT was added to 1 mM (final concentration) and proteins were extracted in the presence of 0,2 % (w/v) NP-40 (final concentration; FLUKA) for 20 min on ice. After 20 min of centrifugation at 13.000 rpm in a microcentrifuge, a mouse monoclonal anti-Myc antibody (5 µl; clone A-14, Santa Cruz) was added to the supernatant and incubated for 1 h at 4 °C on an overhead shaker. Protein concentrations of the supernatant fractions were determined using the Microassay Bradford procedure (Bradford, 1976) to verify equal protein concentrations in all samples. A 1:3 slurry of protein-A Sepharose beads (Pharmacia) was added and the affinity purification of Myc-Sjl2p assemblies were performed for 1 h at 4 °C on an overhead shaker. The protein-A Sepharose beads were washed four times with 500 µl IP buffer (containing 0,2% (w/v) NP40 and 1 mM DTT, respectively). Bound proteins were eluted in 140 µl of SDS-PAGE Laemmli sample buffer, containing 2,5 % β-ME, at 95 °C for 5 min and then centrifuged for 5 min at 13.000 x *g*. Twenty µl of the precipitates were separated by SDS-PAGE. Myc-Sjl2p and HA-Sla1p were detected by immunoblotting using as primary antibodies mouse anti-c-Myc (Oncogene) and mouse anti-HA (clone 16B12, Covance).

The same method was performed for experiments using Myc-Sla1p and HA-Bsp1p, Myc-Sjl3p and HA-Sla1p, Myc-Sjl2p and HA-Pan1p, but was also performed with mouse anti-HA (4 µl, clone 3F10, Roche) for isolating the protein assemblies via HA-epitopes.

To isolate Rvs167p by co-immunoprecipitation 5 µl of rabbit anti-Rvs167p serum were used, in 50 % (w/v) glycerol (final concentration).

2.2.4.4.1 CIP treatment of immunoprecipitates

To test whether some of the multiple bands of HA-Sla1p after separation by SDS-PAGE are due to phosphorylation, HA-Sla1p was co-isolated with Myc-Sjl2p. After incubation of protein extracts with protein-A Sepharose the beads were washed 5 times with 500 µl IP-buffer containing 0,2 % NP-40 and 1 mM DTT and were pre-equilibrated by washing in 1 ml 1 x NEBuffer 3 (100 mM NaCl, 50 mM Tris/HCl, 10 mM $MgCl_2$, 1 mM DTT [pH7.9 at 25 °C]) (New England biolabs). Sepharose beads were resuspended in 100 µl 1 x NEBuffer 3 and either 5 µl (≅ 50 U) of calf intestinal phosphatase (CIP, New England Biolabs) or 5 µl 1 x NEBuffer 3 (negative control) were added to the samples. After

incubation for 1 h at 37 °C while slow shaking on a rocker, 35 µl of 4 x Laemmli sample buffer containing 10 % β-ME were added and immunoprecipitates were released by boiling at 95 °C for 5 min.

In order to test if binding of Myc-Sjl2p to HA-Sla1p is abolished after de-phosphorylation, the immunoprecipitation was performed via the HA-epitope of Sla1p. After the 1h incubation with or without CIP, protein-A Sepharose beads were spun down and the supernatant was transferred to another reaction tube. Sepharose beads were washed 5 times with 500 µl 1 x NEBuffer 3 and resuspended in 140 µl of 1 x Laemmli sample buffer containing 2,5 % β-ME. Thirty-five µl of 4 x Laemmli sample buffer containing 10 % β-ME were added to the supernatant. All samples were boiled for 5 min at 95 °C and stored at –20 °C.

2.2.4.4.2 Co-immunoprecipitation of Sjl2p with Abp1p and Rvs167p

Different variations in the co-immunoprecipitation protocol were tested to verify the physical interaction of Sjl2p and Abp1p *in vivo*.

In strains carrying TAP-Sjl2p and HA-Abp1p immunoprecipitation was performed via the TAP epitope. After separation of the proteins by SDS-PAGE and immunoblotting, HA-Abp1p was shown to bind to the IgG-Sepharose in the negative control in similar amounts compared to the test conditions. Detergent concentrations of 0,1 % and 0,2 % of NP-40 did not result in a specific co-immunoprecipitation. Furthermore, neither the preincubation of the IgG-Sepharose beads with 1 % BSA and an *E.coli* extract nor the generation of a high-speed supernatant (70.000 rpm, TLA 120.2) containing 1 % NP-40 effected the specific co-precipitation of HA-Abp1p. It was also tested to precipitate HA-Abp1p via HA-antibodies either by the standard protocol or by usage of protein-A Sepharose preloaded with anti-HA antibodies prior to the incubation with the yeast lysate, but TAP-Sjl2p was found in equal amounts in both the test and the control precipitates. Upon immunoprecipitation of Myc-Sjl2p in the presence of 0,4, 0,8, and 1,2 % NP-40 HA-Abp1p was also not found to co-precipitate. In contrast, HA-Sla1p co-precipitated with Myc-Sjl2p under these conditions specifically. During this study it was shown by another group that GFP-Abp1p and Myc-Sjl2p interact with each other (Stefan *et al.*, 2005). According to the described protocol cells of the strains CB181 (GFP-Abp1p and Myc-Sjl2p) and CB178 (GFP-Abp1, negative control) were spheroblasted and hypotonically lysed before immunoprecipitation via the Myc epitope of Sjl2p. GFP-Abp1p was present in the precipitates in the negative control in equal amounts.

In order to determine the interaction of Rvs167p or End3p with Sjl2p, respectively, co-immunoprecipitation was performed via the Myc epitope using the strains CB1 (Myc-Sjl2p and HA-Sla1p) and BS1198 (HA-Sla1p). By using detergent concentrations of 0,25, 0,5, and 1 % NP-40, both Rvs167p and End3p were found to bind unspecifically to protein-A Sepharose beads. Therefore it was examined if immunoprecipitation by using TAP-Sjl2p results in the detection of a specific signal for Rvs167p. But Rvs167p was also found to bind unspecifically to IgG-Sepharose beads. Therefore, co-precipitation was performed via Rvs167p. For that purpose, an *Δrvs167* strain (BS1678) served as the negative control and the presence or absence of Sjl2p was examined after the IP by immunoblotting using an anti-Sjl2p antibody (serum). Performing the immunoprecipitation in the presence of 0,2 % NP-40, the anti-Sjl2p antibody revealed a high background staining. Therefore, different NP-40 concentrations were tested 0,4, 0,8, and 1,2 %. The background staining of the anti-Sjl2p antibody was apparently less at 1,2 % NP-40 and, although weak, Sjl2p showed a specific co-immunoprecipitation with Rvs167p. But this result remains to be confirmed.

2.2.4.4.3 Co-immunoprecipitation of Sla1p with Sjl2p after triggered endocytosis

Cells of the strain CB45 (Myc-Sjl2p and HA-Sla1p) were grown in 100 ml of YPD to 0,3-0,4 OD_{600} with shaking (125 r/min) at 30 °C. 30 OD_{600} units of cells were harvested by centrifugation, resuspended in 6 ml YPD and incubated for 5 min at 30 °C (waterbath, 140 rpm). Cycloheximide was added to a final concentration of 1,8 mM and the cell culture was well mixed. After 10 min of incubation 1 ml (≅ 5 OD_{600}) of the cell suspension was removed and poisoned with 10 mM NaN_3 and 10 mM NaF on ice. After triggering of endocytosis with 6 µl 10^{-4} α-factor, 1-ml samples were taken at 30, 60, 90 sec, and 15 min, transferred to a 15-ml falcon tube and poisoned. Cells were washed in 1 ml IP buffer and finally resuspended in 100 µl IP buffer. Immunoprecipitations of Myc-Sjl2p were performed under standard conditions, except that the scale of the procedure was reduced by the factor 4. For incubations with protein-A Sepharose beads, 15 µl bed volume (1:3 slurry) of beads were used and after the incubation with the protein extract they were washed 4 times with 500 µl IP-buffer containing 0,2 % NP-40 and 1 mM DTT. Bound proteins were released in 60 µl of 1 x Laemmli sample buffer containing 2,5 % β-ME. The immunodetection of HA-Sla1p revealed that the interaction of HA-Sla1p and Myc-Sjl2p is apparently unchanged during the endocytic process.

2.2.4.4.4 Co-immunoprecipitation of Flag-Rsp5p with HA-Sjl2p

In order to test a co-precipitation of Flag-Rsp5p with Myc-Sjl2p, co-immunoprecipitation was performed via the HA epitope using the strains expressing HA-Sjl2p, Flag-Rsp5p, and Myc-Sla1p (CB240), or Flag-Rsp5p and Myc-Sla1p (CB246, positive control strain). Flag-Rsp5p is present in the strains under the control of a Gal1-promotor (pRS415-Flag-RSP5).

At the OD_{600} of 0,4 the cells were shifted to SD media without leucin, containing 1 % raffinose instead of glucose and 2 % galactose to induce the expression of Flag-Rsp5p. After 12 h the 50 OD_{600} units of cells (OD_{600} 0,6-0,7 units of cells) were harvested by centrifugation for 5 min at 4000 rpm at 4 °C, respectively. Cell pellets were washed twice with ice-cold ddH_2O and once with cold IP-buffer. After removing the complete supernatant cells were resuspended in 300 µl of IP-buffer and processed for immunoprecipitation as described in section 2.2.4.4. Very briefly, cells were lysed with glass beads in the presence of 1x CLAP. Proteins were extracted in the presence of 0,4% or 0,8 % (w/v) NP-40, the cell lysate cleared and subsequently incubated with an anti-HA antibody and protein-A Sepharose. The isolated complexes were washed and released in 75 µl of 1x Laemmli sample buffer containing 2,5 % β-ME by boiling. The precipitates were analysed by SDS-PAGE and immunoblotting with anti-Myc-, anti-HA-, and anti-Flag antibodies.

2.2.4.5 *In vitro* actin polymerization assay

Actin polymerization assays were basically performed according to Goode (2002), scaling down the procedure by a factor of 10. Cells were grown in 1,6 l of YPD at 30 °C with shaking (125 r/min) to 0,8 OD_{600} units/ml. Cells from 4,8 liters were harvested by centrifugation at 4000 rpm for 5 min at 4 °C (Kontron A6.9) and washed twice with 200 ml ice-cold ddH_2O. The cells were resuspended in 40 ml HEK-A buffer (20 mM HEPES-KOH, pH 7.5; 1 mM EDTA; 50 mM KCl), transferred into a 50-ml Falcon tube, centrifuged at 4000 rpm for 5 min at 4 °C and again resuspended in 5,5 ml HEK-A buffer containing proteinase inhibitors 1 x Complete (Roche) and 1 x PMSF, (final concentration). Cells were lysed by high pressure with three rounds at 20.000 psi at 4 °C in a FrenchPress and collected in the 50-ml Falcon tube after each round. The French Press was washed with 500 µl HEK buffer, the lysate was transferred into a 30-ml Corex tube, and the 50-ml Falcon tube was washed with 5 ml HEK-A buffer, which was also transferred into the Corex tube. To generate the low-speed supernatant (LSS) the lysate was centrifuged at 13.000 rpm for 20 min at 4 °C (Sorvall, rotor SS-34) and the supernatant was poured through four layers of cheesecloth (1,5 x 1,5 cm). The

cheesecloth was wedged in a plastic funnel over a 50-ml graduated cylinder on ice. The total volume of the LSS was generally approximately (approx.) 13-14 ml. A 1-cm long stir bar was added and the graduated cylinder was transferred to a stir plate in the cold room. While mixing, drops of cold 100 % glycerol were added with a pipette to a final concentration of 10 % (approx. 10 min). Using a disposable pipette, the mixture was added to six 3,2 ml ultracentrifuge tubes and centrifuged at 82.000 rpm for 80 min at 4 °C (Beckman, rotor TLA 110). Only the clearest high speed supernatant (HSS1) was carefully harvested (approx. 7-8 ml), minimizing the uptake of the upper lipid phase and absolutely avoiding the lower debris. It was filtered again though cheesecloth (1,5 x 1,5 cm) in a funnel onto a graduated cylinder on ice with a final volume of approx. 7,5 ml. To trigger actin assembly 5 mM $MgCl_2$ and 0,2 mM ATP were added together with 1 x CLAP, inverted without stirring, and the mixture was incubated for 2 h in the cold room (HSS2). Isolation of actin structures was performed by centrifugation at 18.000 rpm for 90 min at 4 °C (Sorvall, rotor SS-34, 25.000 x *g*) in a 15-ml Corex tube. The resulting supernatant (HSS3) was decanted and the tubes were inverted on paper towels for 1-2 min. With a 1-ml pipette tip (terminal 5 mm removed) the pellet was completely resuspended by pipetting up and down in a total volume of 700 µl HEK-B buffer (20 mM HEPES-KOH, pH 7.5; 1 mM EDTA; 50 mM KCl; 5 % glycerol; 5 mM $MgCl_2$) and actin structures were repelleted at 77.000 rpm for 15 min at 4 °C (Beckman, rotor TLA 120.2). The supernatant (HSS4) was removed and the pellet very gently rinsed with 200 µl HEK-B buffer containing 0,2 mM ATP. To salt strip the actin-associated proteins, the pellet was resuspended in 180 µl HSB buffer (HEK-B buffer; 0,2 mM ATP; 0,5 M KCl) by using a 200-µl pipette tip (terminal 5 mm removed), transferred to a 1-ml dounce homogenizer on ice, and the centrifugation tube was rinsed with 30 µl HSB buffer to recover residual pellet material, and combined in the douncer. The material was homogenized with 12 strokes minimizing aeration of the sample (AP). Then it was transferred into a 1-ml thickwall-polycarbonat ultracentrifuge tube, the dounce homogenizer rinsed with 75 µl HSB buffer, combined and centrifuged at 88.000 rpm for 20 min at 4 °C (Beckman, rotor TLA 120.2) to sediment actin filaments. The supernatant (ASW) was transferred to a cold 1,5-ml tube and the pellet (rAP) was homogenized with approx. 50 strokes in HSB buffer to prepare the sample for SDS-PAGE analysis. Protein concentrations were determined by Bradford analysis, 5 µg of protein separated by SDS-PAGE and detected by immunoblotting.

2.2.4.6 Glycerol density gradient centrifugation

The glycerol density gradient centrifugation were basically performed according to Regelmann *et al*. (2003) (Regelmann *et al.*, 2003). CB72 cells were grown in 200 ml of YPD

to 0,3 OD_{600} units/ml at 25 °C with shaking (125 r/min). 50 OD_{600} units of cells were harvested by centrifugation at 4000 rpm for 5 min at 4 °C, washed twice in 20 ml ice-cold ddH_2O, and resuspended in 500 µl ice-cold IP-buffer (115 mM KCl, 5 mM NaCl, 2 mM $MgCl_2$, 1 mM EDTA/NaOH pH8, 20 mM HEPES/KOH pH7.8, 1-4 mM PMSF in DMSO, 1-8 x CLAP). Cells were mechanically lysed with 0,3 g glass beads by vortexing for 45 sec and cooling on ice for 1 min for 10 rounds and lysates were cleared by centrifugation at 13.000 rpm for 20 min at 4 °C. 200 µl of the resulting cell extract was layered over a freshly prepared cold glycerol step gradient [450 µl each of 50 %, 40 %, 30 %, 20 % and 10 % (w/w) or 35 %, 28,75 %, 22,5 %, 16,25 % and 10 % (w/w) of glycerol in IP-buffer] and centrifuged for 4 h at 55.000 rpm at 15 °C / 4 °C in a TLS 55 rotor (Beckman Instruments). Twelve 220 µl fractions were collected from the top and subjected to TCA-precipitation. After 30 min of incubation in the presence of cold 6 % TCA (w/v, final concentration) on ice, precipitates were centrifuged at 13.000 rpm for 20 min at 4 °C and supernatants were carefully discarded. Pellets were once washed with 1 ml of ice-cold acetone by incubation on ice for 5 min and centrifugation at 13.000 rpm for 20 min at 4 °C. After discarding the supernatant pellets were dried for approximately 15 min at 37 °C, resuspended in 50 µl of 1 x Laemmli sample buffer containing 2,5 % β-ME and dissolved by incubation for 20 min on a multivortexer at 37 °C. After boiling of the samples for 5 min at 95 °C and centrifugation at 13.000 rpm for 5 min at room temperature 10 µl per fraction were separated by SDS-PAGE. Proteins were detected by immunoblotting using anti-HA, anti-Myc, anti-PGK, anti-FAS and anti-Ape1p antibodies.

2.2.4.7 Isolation of clathrin-coated vesicles

The procedure used to isolate clathrin-coated vesicles was performed according to Mueller and Branton (1984). CB42 cells were grown in 1,0 l of YPD (or selective media) to 1.2 – 1.4 OD_{600} units/ml at 30°C with shaking (125 r/min). 2160 OD_{600} units of cells from 2 litres were harvested by centrifugation for 5 min at 4.000 rpm and washed twice with 200 ml ice-cold distilled water (wet weight of cells ~10g). The cells were resuspended in 360 ml of 0.8 M Sorbitol, 10 mM Tris (pH 7.5), 10 mM $CaCl_2$, 2 mM DTT, 0.6 mM PMSF and 10 µg/ml Zymolyase 100T (MS Biomedicals) from 1mg/ml stock solution in 4 M Sorbitol/1M Tris pH7.5, transferred into two 500-ml tubes, and incubated in a waterbath shaking at 80 r/min for 1 h at 30 °C. Spheroblast formation was monitored with hypotonical lysis of 20 µl of the cell suspension in ddH_2O. Spheroblasts were sedimented by centrifugation for 15 min at 200 x *g* (1.200 rpm, rotor A6.9), and washed twice with 200 ml 0.8 M Sorbitol, 100 mM MES (pH 6.5), 0.5 mM $MgCl_2$, 1mM EGTA, 0.2 mM DTT, 0.6 mM PMSF at 4 °C. Before

the second wash, spheroblast pellets were combined in one 500-ml centrifuge tube. The spheroblasts were then resuspended in 180 ml 100 mM MES (pH6.5), 0.5 mM $MgCl_2$, 1 mM EGTA, 0.02 % NaN_3, 0.2 mM DTT, 0.6 mM PMSF, 0.1 mg/ml RNase from a 10 mg/ml stock solution in ddH_2O, was added, and hypotonically lysed in a waterbath shaking at 80 r/min for 30 min. The yeast lysate was centrifuged in 30-ml Sorvall-centrifuge tubes for 30 min, 4°C at 21.000 x *g* (15.200 rpm, rotor SS-34). The pellet was discarded and the supernatant centrifuged for 60 min at 100.000 x *g* at 4 °C. The resulting highspeed membrane pellet was resuspended in 1 ml of isolation buffer containing 100 mM MES (pH6.5), 0.5 mM $MgCl_2$, 1 mM EGTA, 0.02% NaN_3 (w/v), 0.2 mM DTT, 0.6 mM PMSF, 1 x CLAP and homogenized with 12 strokes in a 2 ml-glass dounce homogenizer and centrifuged for 1 min at 13.000 rpm in a microcentrifuge at 4 °C. The supernatant (approx. 1,1-1,2 ml) was loaded on a Sephacryl S-1000 column (80 cm long, 10 mm wide) pre-equilibrated in isolation buffer. Twenty-five fractions were eluted at 16 ml/h, 4 ml each, of which #6 to #19 were analysed by SDS-PAGE and immunoblotting using antibodies against Chc1p (S. Lemmon), PGK (Molecular Probes), actin (Roche), HA- (16B12, Covance), and Myc-epitope (Oncogene).

Two milliliters of the samples were prepared for SDS-PAGE by TCA-precipitation, as described in section 2.2.4.6, but washed twice with 1 ml of ice-cold acetone. The precipitated proteins were resuspended in 90 µl of 1 x Laemmli sample buffer.

For electron microscopy 500 µl of fractions #10 to #13 were fixed overnight in the presence of 2.5% (w/v) glutaraldehyd, added from a 25 % (w/v) stock solution and stored at 4 °C. After adsorption to freshly glow-discharged grids coated with a carbon support film, the mounted samples were washed with water and negatively stained with 2% aqueous uranyl acetate. Micrographs were taken at a primary magnification of 52.000 x in a Philips CM 10 transmission electron microscope. Dr. Heinz Schwarz performed these steps (MPI, Tübingen).

Quantitative immunoblotting was performed by subsequent incubation of the nitrocellulose membrane with regular primary antibodies (see section 2.1.4.1) and, to improve signal intensity, with rabbit anti-mouse antibody if the primary antibody was generated in mice. Finally, IgGs were labelled by binding to [^{125}I]protein A (Molecular Probes), the nitrocellulose membrane was dried and fixed in a film cassette. To visualize radioactive signals a Phosphor Imager screen was exposed for 1-4 days, depending on the intensity of the signal. Screens were scanned with a Phosphor Imager (Storm 860) and quantified using the software ImageQuant 5.2 (Molecular Dynamics).

2.2.4.8 Pull-down experiments with Glutathione S-transferase (GST) fusion proteins

Soluble GST-Sjl2$_{890-1183}$ recombinant protein was expressed in the *E.coli* strain BL21 (Novagene, Madinson, WI) and was affinity purified using gluthathione-agarose as described in section 2.2.4.3. To generate the yeast protein extract, a total of 1,75 - 2 x 10^{10} cells (CB84) were spheroblasted at 30 °C for 1 h in 50 ml of 10 mM Tris/HCl (pH 7.5), 0.8 M sorbitol, 1 mM DTT, 0.5 mM PMSF, and 0.01 mg/ml Zymolyase 100T. Spheroblasts were sedimented by centrifugation (15 min, 200 x *g*, 4 °C) and resuspended in 7 ml ice-cold lysis buffer (20 mM HEPES/KOH [pH 7.2], 0.1 M KCl, 2 mM $MgCl_2$, 0.2 M sorbitol, 0.6% (w/v) Triton X-100, 1 mM DTT) containing protease inhibitors (0.5 mM PMSF, 1 x CLAP). The yeast lysate was then subjected to 15 strokes with a 7 ml dounce homogenizer and was centrifuged at 22.000 x *g* for 30 min at 4 °C (Sorvall, SS-34). One milliliter of the supernatant was carefully added. 1 x CLAP and 1 mM PMSF (in DMSO) were again added and the reaction tube was carefully inverted. The reaction mixture was incubated for 1 h on ice with 40 µl bed volume of glutathione-Sepharose 4B (Pharmacia) preloaded with 80 µg of GST-Sjl2$_{890-1183}$, GST and control GST-fusions without any movement. The beads were washed four times (200 rpm, 2 min) with lysis buffer and bound proteins were eluted by three consecutive treatments with 250 µl of reduced glutathione buffer (20 mM reduced glutathione, 100 mM Tris/HCl [pH 9.0], 0.2 M NaCl, 5 mM DTT, 0.1 % Triton X-100). The combined eluates were TCA precipitated (see section 2.2.4.6) and the resulting precipitates resuspended in 180 µl of 1 x Laemmli sample buffer, vortexed for 20 min at 37 °C, and boiled at 95 °C for 5 min. 30 µl per sample were analysed by SDS-PAGE and immunoblotting with an α-Chc1 antibody and 15 µl per sample were used for Coomassie Brilliant Blue staining.

2.2.4.9 Detection of ubiquitination of HA-Sjl2p after triggered endocytosis

Cells from the strain CB207 grown in 500 ml of YPD to 1 x 10^7 cells/ml at 30 °C were harvested by centrifugation for 5 min at 4.000 rpm at room temperature (approx. 83 OD_{600}). The cell pellet was resuspended in 16,6 ml of prewarmed YPD, transferred to a 100-ml flask and incubated for 10 min at 30 °C (waterbath, 140 rpm). Five ml (≅ 25 OD_{600}) were taken from the cell culture after strong shaking and poisoned with 10 mM NaN_3, 10 mM NaF, and containing 20 mM NEM (final concentration, on ice) to prevent de-ubiquitination. Addition of 50 µl 10^{-4} α-factor (final concentration approximately 4,3 x 10^{-7}) triggered endocytosis and 5-ml samples were taken after strong shaking at 1 min and 2,5 min after addition of pheromone and treated as described above. Sample were washed once with ice-cold ddH_2O containing 20 mM NEM and 10 mM NaN_3 and once with ice-cold IP buffer also containing 20 mM NEM

and 10 mM NaN_3. The inhibitors were added to all buffers during the subsequent immunoprecipitation. Cell pellets were resuspended in 150 µl IP buffer with inhibitors, and lysis and immunoprecipitation performed as described in section 2.2.4.4 using 4 µl of the anti-HA antibody to isolate HA-Sjl2p. After immunoprecipitation washed beads with bound assemblies were resuspended in 30 µl of 1 x Laemmli sample buffer containing 2,5 % β-ME and boiled at 95 °C. To retrieve the complete sample protein-A Sepharose were separated from the released precipitates by spinning in 1-ml Mobicol columns (MoBiTech). To separate the proteins by SDS-PAGE, 10 µl of each sample were loaded for detection of proteins by anti-HA and anti-Myc antibodies and 30 µl for detection of ubiquitin.

3 Results

3.1 The synaptojanin-like proteins physically associate with proteins of the actin cytoskeleton

3.1.1 Sjl1p, Sjl2p and Sjl3p co-sediment with *in vitro* polymerized actin

The *Saccharomyces cerevisiae* inositol polyphosphate 5´-phosphatases Sjl1p, Sjl2p, and Sjl3p each contain a conserved NH_2-terminal Sac1 domain, followed by a 5´-phosphatase domain and a highly variable C-terminal proline-rich domain (PRD). Because of the variability the PRD region of all three synaptojanins is suggested to function as a targeting domain. Sjl2p and Sjl3p exhibit Sac1 PPIPase activities (Guo *et al.*, 1999; Hughes *et al.*, 2000) and all three possess 5-Pase activity towards the inositol ring of phosphoinositides (PI). Phosphoinositides control numerous cellular processes including actin cytoskeletal arrangements, vesicular trafficking, cell signaling, and growth. While single deletions of synaptojanin-like phosphatases exhibited no phenotype, double mutations revealed functions in a variety of cellular processes. On the one hand, Δ*sjl1*Δ*sjl2* and Δ*sjl2*Δ*sjl3* cells were defective in the organization of the actin cytoskeleton. Additionally, Δ*sjl1*Δ*sjl2* showed an aberrant cell surface morphology (Singer-Krüger *et al.*, 1998; Srinivasan *et al.*, 1997; Stolz *et al.*, 1998), whereas the Δ*sjl1*Δ*sjl3* mutant was phenotypically similar to the wildtype. On the other hand, Δ*sjl2*Δ*sjl3* and more profoundly Δ*sjl1*Δ*sjl2* cells exhibited a defect in receptor-mediated and fluid-phase endocytosis, but Δ*sjl1*Δ*sjl3* cells did not (Singer-Krüger *et al.*, 1998). First evidence for an association of inositol polyphosphate 5-phosphatases with actin came from observations of a translocation of 5-phosphatases to actin patches in response to hyperosmotic stress (Ooms *et al.*, 2000). Significantly, in the lab of Birgit Singer-Krüger the proline-rich domain of Sjl2p was found to physically interact with Sla1p, a protein that links

actin and the clathrin-based endocytic machinery (Howard *et al.*, 2002) and the actin patch component Abp1p. Additionally, the Sac1-like domains, which exhibits the PPIP activities, of Sjl2p and Sjl3p, but not Sjl1p, were identified as direct interaction partners of the actin patch component Bsp1p (Wicky *et al.*, 2003).

To determine more precisely the physical association of synaptojanin-like proteins with actin an *in vitro* assay based on the reconstitution of actin assembly in membrane free soluble yeast extracts (Goode, 2002) was performed, scaling down the procedure by a factor of 10. After lysis of yeast cells a 255.000 x *g* supernatant was generated, that contained the vast majority of cellular actin in a monomeric form along with a free pool of soluble actin-filament associated proteins. Assembly of actin and associated proteins was triggered by the addition of 5 mM magnesium chloride, 10 % glycerol, and 0,2 mM ATP. Formed actin structures were isolated by centrifugation at 25.000 x *g*, washed, and homogenized in high salt buffer to wash off the actin-associated proteins from filaments (see section 2.2.4.5). The strains used for

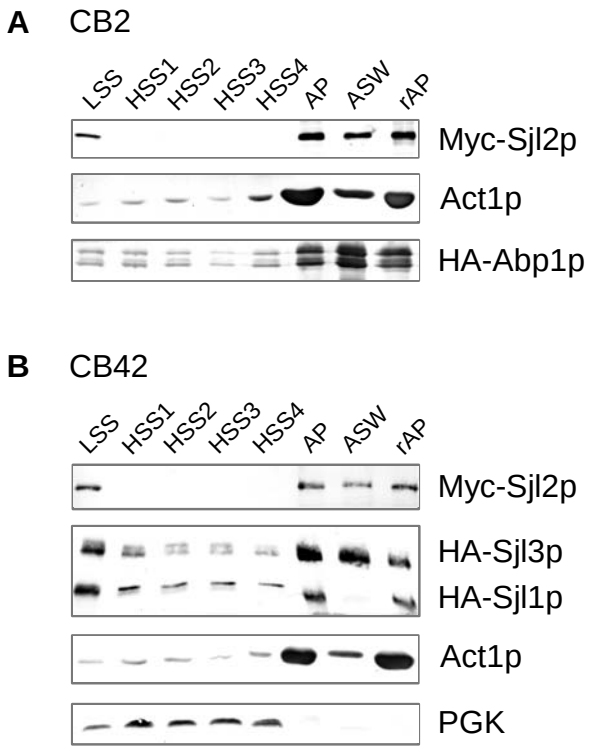

Fig. 1. All three synaptojanin-like proteins co-sediment with *in vitro* polymerized actin
(**A**) *In vitro* polymerization of actin was performed as follows: A cell lysate was clarified (LSS), 10 % glycerol added and mixed. A high speed supernatant was generated (HSS1) and 5 mM $MgCl_2$, and 0,2 mM of ATP triggered actin assembly (HSS2). After generation of a actin filaments pellet and the supernatant (HSS3) by centrifugation, the pellet was washed and repelleted (AP and HSS4). After homogenisation in high salt buffer, actin filaments were repelleted (rAP) and separated from soluble proteins (ASW). Five µg of each sample were separated by SDS-PAGE and analysed by immunoblotting. (**B**) Polymerization of actin was performed as described in (A), by using cell extracts of the strain CB42, carrying epitope tagged versions of all three synaptojanin-like proteins. Abbreviations: LSS: low speed supernatant; HSS: high speed supernatant; AP: actin pellet; rAP: repelleted actin; PGK: phosphoglycerate kinase

these experiments carried either the F-actin binding protein Abp1p (Quintero-Monzon *et al.*, 2005) tagged with three copies of the HA epitope and Sjl2p with 13 copies of the Myc epitope (CB2, control strain) (Fig. 1A) or epitope tagged versions of all three Sjl-proteins (CB42) whereby it was possible to detect the association of all three family members with actin in one and the same cell extract (Fig. 1B) Act1p and HA-Abp1p were used as control proteins indicating polymerized actin filaments during the assay. The actin-associated protein HA-Abp1p indicated the separation of actin-associated proteins from the actin filaments by high salt. Act1p and its binding protein HA-Abp1p were enriched in the actin pellet fraction (Fig. 1A; AP), while the cytosolic enzyme phosphoglycerate kinase (PGK; Fig. 1B) was absent and remained in the high speed supernatants (HSS1-HSS4). After homogenisation of the actin pellet (AP) in high salt buffer and subsequent centrifugation, Act1p was mainly found in the fraction of repelleted actin (rAP), confirming that actin filaments do not disassemble during this step. HA-Abp1p was largely detected in the supernatant (ASW) indicating a more loose association with actin filaments. Importantly, Myc-Sjl2p was enriched in the AP-sample that contains actin and associated proteins and was partially stripped from actin filaments (ASW). Both strains used, CB2 (Fig. 1A) and CB42 (Fig. 1B), showed reproducible results with respect to Act1p and Myc-Sjl2p. In CB42, a loss in the amounts of HA-Sjl3p and HA-Sjl1p was observed during experimental processing (HSS1-HSS4). In HSS3 it was most likely due to incomplete association with actin and in HSS4 probably due to detachment from actin filaments during the washing step. Loss of Myc-Sjl2p during the preparation was moderate. However, HA-Sjl3p and HA-Sjl1p were also found to be enriched and to co-sediment with assembled actin (Fig. 1B). Interestingly, while HA-Sjl3p could be partially stripped from actin structures by incubation with high salt buffer, similar to Myc-Sjl2p and HA-Abp1p, HA-Sjl1p could not be removed by the salt wash, but was quantitatively recovered together with the repelleted actin filaments (rAP; Fig. 1B). In sum, these results show an association of all three synaptojanin-like proteins with actin, because they were found to co-fractionate with *in vitro* assembled actin. But, since HA-Sjl1p could not be stripped from actin, these results also point to biochemical differences and modes of interaction of the synaptojanin-like family members with the actin cytoskeleton.

3.1.2 Sjl2p does not interact with Abp1p *in vivo*

A two-hybrid screen, performed in the Singer-Krüger lab, identified a physical interaction of the proline-rich domain of Sjl2p with Abp1p, an actin binding protein of the cortical actin cytoskeleton, implicated in the endocytosis (Fazi *et al.*, 2002). To verify this binding *in vivo* the same IP conditions as for co-precipitation of Sla1p with Sjl2p were used to

co-precipitate Abp1p with Sjl2p. Under these conditions, Abp1p was found to bind non-specifically with Sepharose beads. Therefore different protocols for co-immunoprecipitation were tested. First, it was checked if variations in the detergent concentration of NP-40 up to 1,2 % raise the stringency of binding. But this treatment did not result in a co-precipitation. Second, using Abp1p and Sjl2p tagged with different epitope combinations (TAP-Sjl2p/HA-Abp1; Myc-Sjl2p/HA-Abp1p; Myc-Sjl2p/GFP-Abp1p) showed still non-specific binding. Third, Sepharose beads were pre-incubated with a yeast cell-extract without tagged proteins or an *E.coli* cell extract, but none of these tests yielded a clear positive interaction with Abp1p. Furthermore, neither performing the IP with a high speed supernatant (70.000 rpm, TLA120.2), nor trying to reproduce the later published Abp1p/Sjl2p co-immunoprecipitation by hypotonical lysis of spheroblasted cells (Stefan *et al.*, 2005) caused specific co-precipitation of Abp1p with Sjl2p. In conclusion, the physical interaction could not be confirmed *in vivo*.

3.1.3 Sjl2p interacts with Abp1p in a two hybrid assay, independently of Sla1p

Therefore, it was tested if the interaction of Abp1p and the proline-rich domain of Sjl2p in the two-hybrid system is maybe mediated by Sla1p, which was also shown to interact physically with the proline-rich domain of Sjl2p (B. Singer-Krüger, unpublished results). Moreover, deletion of *SLA1* showed a synthetic lethal mutant phenotype together with a null mutation of *ABP1* (Holtzman *et al.*, 1993). Sla1p itself is known to interact with proteins regulating actin dynamics, with proteins required for endocytosis, and binds to the Ste2p receptor (Howard *et al.*, 2002; Warren *et al.*, 2002). It is suggested to appear early at punctuated cortical patches and is later joined by Abp1p, coexisting transiently at endocytic sites (Kaksonen *et al.*, 2003). Sla1p is present in the two-hybrid reporter strain Y190. To investigate the binding dependence of Sjl2p and Abp1p with Sla1p both the strain Y190 modified by deletion of *SLA1* (Y190Δsla1#12) as a well as the positive control strainY190 were subsequently transformed with pAS1-Sjl2-588, coding for the PRD of

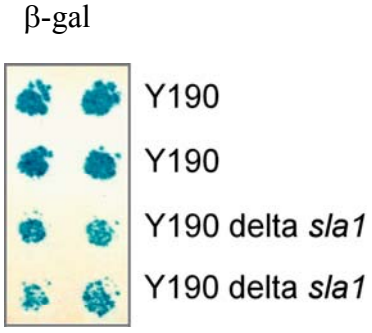

Fig. 2. The proline-rich domain of Sjl2p interacts with Abp1p in *Δsla1* mutants
Two-hybrid interactions between pAS1-Sjl2-588 and 3`Sjl2#19 in yeast two hybrid reporter strains Y190 and Y190Δsla1#12. The test was performed as outlined in the Materials and Methods.

Sjl2p and 3´Sjl2#19, containing the reading frame of *ABP1*. By using the β-galactosidase assay to test for a physical interaction between Sjl2p and Abp1p domains, a blue staining was visible in *Δsla1* and control cells (Fig. 2, four colony patches for each strain). This indicates that an interaction of the proline-rich domain of Sjl2p with Abp1p in a two-hybrid assay is not dependent on Sla1p.

3.2 Characterization of the interaction between Sjl2p and Sla1p *in vivo*

3.2.1 The endocytic linker protein Sla1p co-immunopecipitates with Sjl2p, but not with Sjl1p and Sjl3p

In the above described yeast two-hybrid screen it was found that the proline-rich domain of Sjl2p physically interacts with the N-terminal two SH3 domains of Sla1p (B. Singer-Krüger, unpublished data). Sla1p was shown to be essential for the proper formation of the cortical actin cytoskeleton (Holtzman *et al.*, 1993). In addition, it represents a novel type of endocytic adaptor that can link receptors with a $NPFX_{(1,2)}D$-motif to the clathrin/actin-based endocytic machinery (Howard *et al.*, 2002). To verify this interaction *in vivo* the binding of Sjl2p to Sla1p was analysed by co-immunoprecipitation. Co-immunoprecipitation experiments were carried out using cell extracts, preincubated with 0,2 % NP-40, expressing both Myc-Sjl2p and HA-Sla1p (CB1), or HA-Sla1p alone (BS1198, control strain). The functional proteins were expressed from the chromosome under the control of the endogenous promoters. Myc-Sjl2p assemblies were isolated from total cellular extracts by binding to an anti- Myc antibody and, in a second step, by associating this complex to protein-A covered Sepharose. Immunoprecipitates were analysed by immunoblotting using anti-Myc and anti-HA antibodies (see section 2.2.4.2.1). HA-Sla1p was detected in immunoprecipitates after isolation of Myc-Sjl2p, but not in the control lacking Myc-Sjl2p, suggesting that HA-Sla1p interacted with Myc-Sjl2p *in vivo* (Fig. 3A, lane 3). Later, another study verified this interaction in large scale protein complex analyses (Gavin *et al.*, 2006). Conversely, further experiments to test a binding of Sjl3p or Sjl1p with Sla1p unveiled no co-precipitation for HA-Sla1p or Myc-Sla1p after immunoprecipitation of Myc-Sjl3p (Fig. 3B) or HA-Sjl1p (Fig. 3C). The co-immunoprecipitated HA-Sla1p revealed three bands of slight different mobility. Together, these results indicate that the endocytic patch component HA-Sla1p interacts specifically with Myc-Sjl2p *in vivo*.

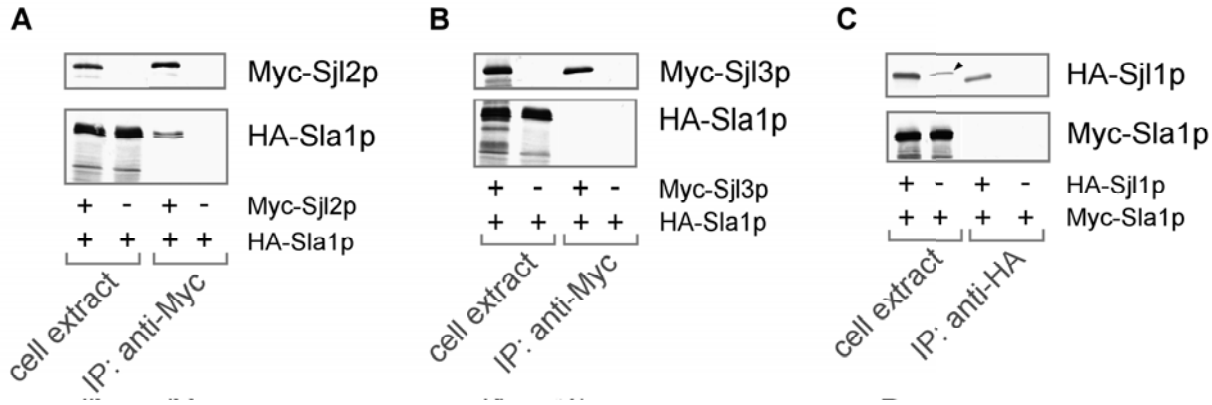

Fig. 3. Sla1p interacts exclusively with Sjl2p
(**A**) Co-immunoprecipitations were performed with an anti-Myc antibody using cell extracts (CB1 and BS1198 cells) containing the epitope-tagged proteins as indicated, in the presences of 0,2 % NP-40. Proteins bound to protein-A Sepharose were released by boiling in SDS-PAGE sample buffer, separated by SDS-PAGE and detected by immunoblotting using anti-Myc and anti-HA antibodies. (**B**) Co-immunoprecipitation was performed as described in (A) by using cell extracts of CB105 (Myc-Sjl3p and HA-Sla1p cells) and BS1198 (HA-Sla1p cells) (**C**) In this co-immunoprecipitation experiments cell extracts of CB136 (HA-Sjl1p and Myc-Sla1p) and CB137 (Myc-Sla1p) were incubated with an anti-HA antibody and further treated as described in (A). The band marked with an arrow is a cross reaction with the anti-HA antibody, also visible in other blots of cell extracts.

3.2.2 Sla1p immunoprecipitates with Sjl2p independently of its phosphorylation status

Recent experiments in *S. cerevisiae* have identified a number of proteins of the actin cytoskeleton and the endocytic machinery that are regulated by phosphorylation (Ficarro *et al.*, 2002). Examples for a phosphoregulation are Ent1p, Clc1p, Rvs167p, Pan1p and also Sla1p, which are implicated in the regulation of cortical actin patches and vesicle formation (Chu *et al.*, 1999; Friesen *et al.*, 2003; Watson *et al.*, 2001; Zeng and Cai, 1999; Zeng *et al.*, 2001). In particular, Sla1p is phosphorylated at the LxxQxTG repeat in its C-terminal domain by the serine/threonine kinases Ark1p and Prk1p (Zeng *et al.*, 2001). Thus, to ascertain whether the upper bands of HA-Sla1p after immunoprecipitation are caused by phosphorylation HA-Sla1p-immunoprecipitates were treated with calf intestinal phosphatase (CIP). Two control experiments were performed: the regular co-immunoprecipitation (Fig. 4A, lane 1) and a control to verify that an incubation only with CIP buffer cannot alter the band pattern of HA-Sla1p (lane 2). The resulting precipitates from the control experiments showed both the previously described mobility pattern of HA-Sla1p and the co-precipitation of Myc-Sjl2p (Fig. 4A, lanes 1 and 3). In contrast, treatment with CIP resulted in a conversion of the upper HA-Sla1p bands into a faster mobility band. (Fig. 4A, lane 5). Myc-Sjl2p was still detected in the precipitate of HA-Sla1p, although under these experimental conditions it was not distinguishable if Myc-Sjl2p still bound to the non-phosphorylated form of HA-Sla1p. These findings demonstrated that phosphorylation of HA-Sla1p effected the multiple

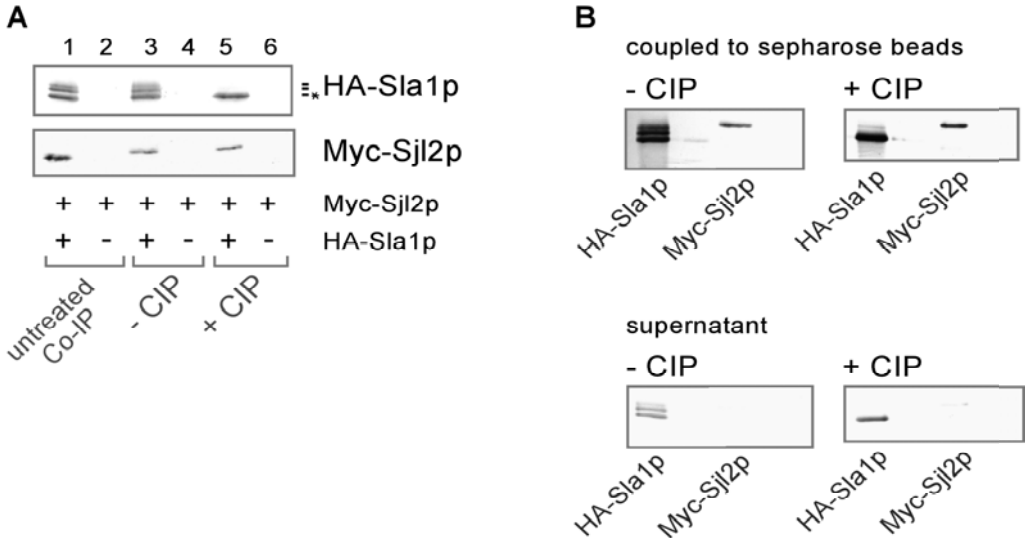

Fig. 4. Interaction of Myc-Sjl2p and HA-Sla1p is stable despite the de-phosphorylation of HA-Sla1p
(A) For co-immunoprecipitation cell extracts of strains expressing Myc-Sjl2p and HA-Sla1p (CB1) or Myc-Sjl2p (BS1248, control) were subsequently incubated with an anti-HA antibody and protein-A Sepharose. The bound complexes were washed and pre-equilibrated in CIP-buffer. Samples in lanes 1 and 2 were washed in IP-buffer, sample buffer was added, and boiled. Other immunoprecipitates were either incubated without (lanes 3 and 4) or with CIP for 1 h at 37 °C (lanes 5 and 6), beads were washed, sample buffer was added, and boiled. Analysis was processed by SDS-PAGE and immunoblotting with anti-Myc and anti-HA antibodies. (B) Co-immunoprecipitations were performed as described in (A). After incubation without or with CIP, protein-A Sepharose beads and supernatant were separated, and protein-A Sepharose beads were washed. All samples were resuspended in sample buffer to an equal volume and analysed by SDS-PAGE and immunoblotting. * indicates the faster mobility band of HA-Sla1p.

band pattern in a SDS gel. As a consequence, it was tested if Myc-Sjl2p interacts both with phosphorylated and non-phosphorylated forms of HA-Sla1p. GST-fusion proteins encompassing the three SH3 domains of Sla1p were shown not to be phosphorylated by the kinases Ark1p and Prk1p, while GST-fusions containing the C-terminal QxTG repeats were phosphorylated (Zeng *et al.*, 2001). *In vitro* an interaction of the proline-rich domain of Sjl2p with Sla1p takes place within the N-terminal two SH3 domains of Sla1p (B. Singer-Krüger laboratory). Therefore, it was likely that the binding of both proteins is independent on phosphorylation of Sla1p. To confirm this idea, HA-Sla1p was subsequently immunoprecipitated and the protein-A Sepharose beads, incubated either without (- CIP) or with calf intestinal phosphatase (+ CIP). After incubation, the supernatant and the protein-A Sepharose beads were separated and examined. In contrast to the control experiment incubated without CIP, it was confirmed that after treatment HA-Sla1p´s bands collapsed in one band to faster mobility (Fig. 4B). Comparing the amounts of Myc-Sjl2p in the supernatant fraction and in the HA-Sla1p assemblies at the protein-A Sepharose beads, it was further demonstrated that the major fraction of Myc-Sjl2p still bound to de-phosphorylated HA-Sla1p at the protein-A Speharose beads. Only a faint band of Myc-Sjl2p was visible in the supernatant fraction, likely to disassemble from the protein-A Sepharose beads together with

HA-Sla1p during the incubation step. Thus, Myc-Sjl2p seems to interact with phosphorylated and non-phosphorylated forms of HA-Sla1p. These results lead to the suggestion that the phosphoregulation of Sla1p via Ark1p and Prk1p might not interfere the interaction of Myc-Sjl2p and HA-Sla1p.

α-factor uptake assays were performed (see section 2.2.4.4.3) to further define a timing of the interaction between Sjl2p and Sla1p during triggered receptor-mediated endocytosis. The used strain CB45 expressed Myc-tagged Sjl2p and HA-tagged Sla1p. Thirty OD_{600} cells were harvested and subjected to treatment with cycloheximide to inhibit protein biosynthesis. Before (0 min) and after 30 sec, 60 sec, 90 sec and 15 min of pheromone α-factor addition, samples (5 OD_{600}) were taken and cells were energy-poisoned by the addition of NaF and NaN_3. Cells were lysed and Myc-Sjl2p was isolated in the presence of 0,2 % NP-40. Proteins of the cell extracts and the precipitates were separated by SDS-PAGE and analysed by immunoblotting. By using this assay it was not possible to recognize differences in the interaction of Myc-Sjl2p and HA-Sla1p during triggered endocytosis (data not shown).

3.2.3 Sjl2p interacts with Sla1p in cells lacking the actin patch component Abp1p

Stefan *et. al* (2005) described an *in vivo* interaction of Sjl2p and Abp1p. Although during this PhD work this interaction was not confirmed (see section 3.1.2), it was tested if the binding of Sjl2p and Sla1p depends on Abp1p. The cells used in this experiment expressed Myc-tagged Sjl2p and Sla1p tagged with HA epitopes either in a wildtype (CB1) or *Δabp1* background (CB128). Deletion of *ABP1* was confirmed by PCR. The control cells (BS1198) carried HA-tagged Sla1p in a wildtype background. In wildtype strain CB1, HA-Sla1p co-precipitated with Myc-Sjl2p specifically (Fig. 5, lane 5). No signal for HA-Sla1p was visible in the untagged control strain BS1198 (lane 6), although it was detected in the corresponding cell extract (lane 2). Comparably, in *Δabp1* cells HA-Sla1p was also found to

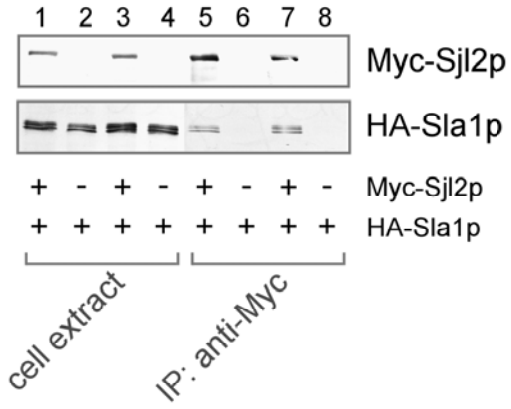

Fig. 5. Sjl2p and Sla1p interact in *Δabp1* cells
Co-immunoprecipitation was performed with cell extracts of wildtype strain CB1 (lane 1 and 5), *Δabp1* strain CB128 (lane 4 and 7) and control strain BS1198 (lane 2, 4, 6 and 8) containing the indicated tagged proteins. Cell extracts were incubated with a rabbit anti-Myc antibody in the presence of 0,2% NP-40. Proteins were detected by immunoblotting using anti-Myc and anti-HA antibodies.

co-immunoprecipitate with Myc-Sjl2p (lane 7), suggesting that Abp1p does not mediate the interaction of Myc-Sjl2p with HA-Sla1p *in vivo*.

3.2.4 Interaction of Sjl2p and Sla1p is not disturbed in *sec7* mutant cells, which form aberrant Golgi membrane structures

Sjl2p, but not Sjl3p and Sjl1p, localized to punctuated structures in *Δark1Δprk1* or *Δark1 prk1-as3* mutant cells, devoid of two actin-regulating kinases (Böttcher *et al.*, 2006). These punctuated structures are defined as actin clumps containing endocytic proteins and ~ 100-nm vesicles, likely representing the endocytic pool (Sekiya-Kawasaki *et al.*, 2003). Theses findings supported a major function of Sjl2p in endocytosis. Consistent with these results, it was found that in a temperature-sensitive *sec7* mutant, which forms aberrant Golgi membrane structures after shift to 0,1 % glucose at 37 °C (Novick *et al.*, 1980), the HA-Sjl2p staining pattern was not affected. In contrast, the staining of HA-Sjl3p was lost after the shift. To check the amounts of HA-Sjl3p and HA-Sjl2p in *sec7* mutants, strains carrying HA-epitope tagged Sjl2p or Sjl3p were incubated at 25 and 37 °C with the appropriate glucose concentrations and subjected to immunoblotting. The amounts of HA-Sjl2p were comparable at both temperature conditions, at 25 °C and 37 °C. Interestingly, a band shift of HA-Sjl2p to a decreased mobility was detectable after incubation at restrictive condition (37 °C; 0,1 % glucose). An additional upper band of HA-Sjl2p was detected also after growth at 25 °C (Fig. 5, lane 1). This band shift was frequently, but more faint, also observed in wildtype cells. Analogous to the lack of a HA-Sjl3p signal in *sec7* cells, observed by indirect immunofluorescence microscopy, the level of HA-Sjl3p was strongly reduced after incubation at restrictive conditions (lane 4), compared to the protein amounts at 25 °C (lane 3). The cytosolic enzyme PGK, was found in equivalent amounts in all four cell extracts (lanes 1-4). These observations further suggested a differential subcellular localization and function of Sjl2p and Sjl3p in membrane trafficking. Degradation of HA-Sjl3p may be a result of a defect in the biogenesis of phospholipids that may lead to the dissociation of the lipid phosphatase from the membrane, consistent with a function of HA-Sjl3p at the late Golgi.

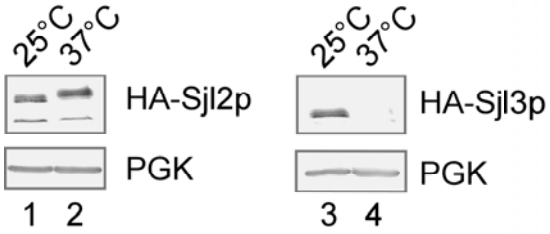

Fig. 6. In *sec7* cells HA-Sjl2p shows a band shift, while HA-Sjl3p is degraded at 37 °C
Temperature-sensitive *sec7* cells expressing either HA-Sjl2p (BS1175, lanes 1 and 2) or HA-Sjl3p (CB175, lanes 3 and 4) were harvested after growth at 25 °C in YPD medium and after 2 h incubation at 37 °C in medium containing 0,1 % glucose (lanes 2 and 4). Samples were lysed with glass beads and processed for immunoblotting with an anti-HA antibody and an anti-PGK antiserum (loading control).

To address whether parts of the biological functions of HA-Sjl2p are affected in *sec7* cells, binding to Myc-Sla1p was tested by co-immunoprecipitation. Both proteins, HA-Sjl2p and Myc-Sla1p still co-immunoprecipitated (Fig. 7, lanes 5-8) in *sec7* mutants. Furthermore, a slight mobility shift was also detected for Myc-Sla1p in cell extracts after incubation at restrictive conditions (lanes 1 and 3), in both strains CB195 expressing HA-Sjl2p and Myc-Sla1p, and CB197 expressing Myc-Sla1p alone. Interestingly, after co-immunoprecipitation, HA-Sjl2p and Myc-Sla1p showed a more pronounced staining of the upper band(s) (lane 5) at restrictive conditions.

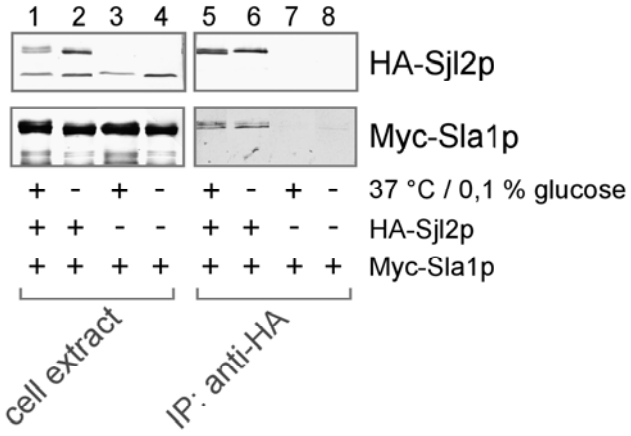

Fig. 7. Myc-Sla1 co-immunoprecipitates with HA-Sjl2 in *sec7* cells after shift for 2 h to 37°C in 0,1 % glucose medium
sec7 cells expressing HA-Sjl2p and Myc-Sla1p (CB195; lanes 1 and 2) or Myc-Sla1p alone (CB197, control strain; lanes 3 and 4) were subjected to co-immunoprecipitation with an anti-HA antibody as described in Fig. 3, except that 25 OD cells were used. Cells were harvested either after growing overnight at 25 °C (lanes 2+6 and 4+8) or after an additional incubation step for 2 h in 0,1 % glucose at 37 °C (lanes 1+5 and 3+7).

3.3 Sjl2p is found in complex with proteins of cortical actin patches and the endocytic machinery

3.3.1 Bsp1p, a cortical actin patch component, interacts with Sla1p *in vivo*

In a recent study, Sjl2p was described to interact with the newly identified cortical actin patch component Bsp1p *in vivo* (Wicky *et al.*, 2003). Most importantly, this interaction is mediated via the N-terminal Sac1/polyphosphoinositide phosphatase domain of Sjl2p, and requires the highly conserved $CX_5R(T/S)$ motif implicated in the PPIP-activity of Sjl2p. In the present PhD work it was shown that Myc-Sjl2p binds to HA-Sla1p *in vivo* (section 3.2.1). The physical interaction between Bsp1p and Sla1p was already proposed by two-hybrid analysis (Kübler and Riezman, 1993). Since Bsp1p is tightly coupled to the cortical actin cytoskeleton at the plasma membrane (Wicky *et al.*, 2003) and Sla1p acts as an adapter that links proteins of actin patches and proteins required for endocytosis (Warren *et al.*, 2002), the physical interaction of Sla1p and Bsp1p was examined *in vivo*. Myc-Bsp1p was found to co-precipitate with HA-Sla1p (Fig. 8, lane 1) as they did vice versa (Fig. 8, lanes 3 and 4). In support of this, the interaction was later confirmed in large scale protein complex analyses (Gavin *et al.*, 2006).

Interestingly, Sjl2p binds to both the two SH3 domains of Sla1p through the C-terminal proline-rich domain and to Bsp1p via the N-terminal Sac1-like domain. Thus, it remains to be elucidated if the interaction of HA-Sla1p and Myc-Bsp1p may depend on Sjl2p.

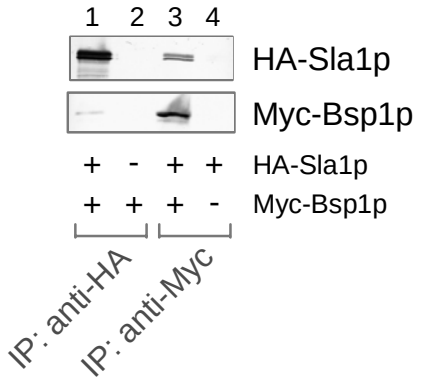

Fig. 8. HA-Sla1p interacts with Myc-Bsp1p *in vivo*
Co-immunoprecipitations were performed as described in Fig. 3A. Cell extracts, expressing the indicated proteins were incubated with an anti-HA antibody (lanes 1 and 2; strains CB47 and CB53) or an anti-Myc antibody (lanes 3 and 4; strains CB47 and BS1198). Analysis of proteins was performed by Western blotting and immunodetection.

3.3.2 Sjl2p is found in complex with Sla1p and Pan1p, which are essential for endocytosis

Sla1p, Pan1p and End3p form a heterotrimeric complex by physical interaction *in vivo*, which is required for normal actin cytoskeleton organization, endocytosis, and normal cell wall morphogenesis (Howard *et al.*, 2002; Tang *et al.*, 2000). This complex is believed to establish at cortical actin patches at an early stage of endocytosis (Kaksonen *et al.*, 2005). Since Sla1p was identified as an interaction partner of Sjl2p, it was tested if Pan1p is also present in Sjl2p/Sla1p complexes. By using standard immunoprecipitation conditions optimised for a detection of Sjl2p and Sla1p binding, HA-Pan1p was detected with an unspecific signal both in the test strain and the control stain (not shown). Therefore it was necessary to figure out the optimal experimental conditions for a co-precipitation of HA-Pan1p with Myc-Sla1p (Tang *et al.*, 2000). The used strains contained Sla1p tagged with Myc epitopes and Pan1p tagged with HA epitopes (CB77) or HA-Pan1p alone (CB58, control strain). Remarkably, the presence of 1,0 % NP-40 in the buffer during the immunoprecipitation (Fig. 9A, lanes 5 and 6, respectively) enhanced the efficiency of HA-Pan1p co-isolation with Myc-Sla1p compared to conditions with less detergent (0,25 and 0,5 % NP-40; lanes 1 to 4). To investigate if HA-Pan1p is present in a complex together with HA-Sla1p and Myc-Sjl2p co-immunoprecipitation experiments were performed using 1,0 % NP-40. The used strains carried Myc-Sjl2p, HA-Sla1p, and HA-Pan1p (CB72) or HA-Sla1p and HA-Pan1p (CB71, control strain). HA-Sla1p and HA-Pan1p were also detected after immunoprecipitation of Myc-Sjl2p (Fig. 9B), although the amounts of HA-Pan1p were strikingly smaller than those of HA-Sla1p. These data suggest that HA-Pan1p is present in

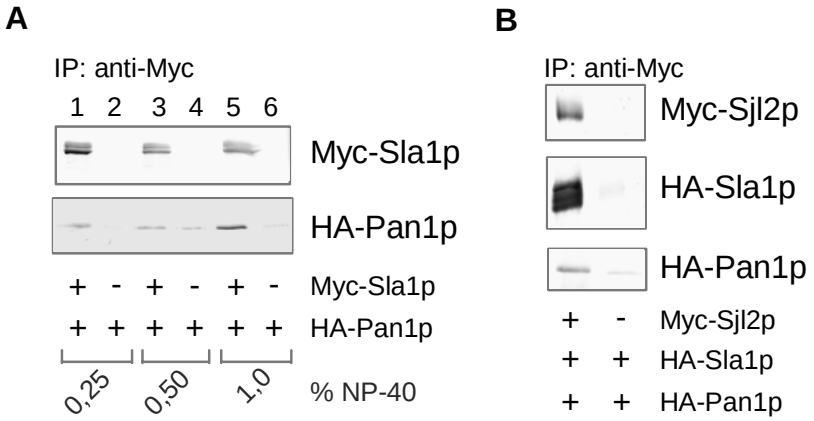

Fig. 9. Myc-Sjl2p interacts with the HA-Sla1p/Pan1p complex
(**A**) Co-immunoprecipitations of cell extracts containing either Myc-Sla1p and HA-Pan1p (CB77) or HA-Pan1p (CB58; control strain) were performed with an anti-Myc antibody as described in Fig. 3A. Concentrations of NP-40 were used as indicated. (**B**) Cell extracts, containing Myc-Sjl2p, HA-Sla1p and HA-Pan1p (CB72) or HA-Sla1p and HA-Pan1p (CB71; control strain) were processed for co-immunoprecipitation. In the presence of 1,0 % NP-40 cell extracts were incubated with anti-Myc antibody and, in the second step, with protein-A Sepharose beads. Bound proteins were analysed by immunoblotting using anti-Myc and anti-HA antibodies.

Myc-Sjl2p/HA-Sla1p assemblies. It is possible that either Pan1p resists solubilization by lower concentrations of the detergent NP-40 or that not all Myc-Sjl2p/HA-Sla1p complexes contain HA-Pan1p *in vivo*.

To confirm whether Sjl2p, Sla1p, and Pan1p physically associate *in vivo*, glycerol density gradients were performed as described in section 2.2.4.6. The sedimentation velocity of the three proteins was compared to the velocity of endogenous marker proteins with a known molecular size (PGK: M_r=42 kDa; Ape1p: M_r=600 kDa; FAS: M_r=2,4 MDa, respectively). The estimated molecular mass of Sjl2p is 133 kDa (approximately 147 kDa including 13 Myc epitopes, respectively) and would have been expected to peak in fractions with monomeric Pan1p, which has a molecular mass of 160 kDa (approx. 163 kDa including three HA-epitopes, respectively). The majority of HA-Pan1p sedimented (Fig. 10A, lanes 3 and 4) shortly after the 42-kDa cytosolic enzyme PGK (lanes 2 and 3) indicating a monomeric state. Interestingly, Myc-Sjl2p was mainly found to sediment in higher molecular weight fractions (lanes 4 and 5) than HA-Pan1p, partially co-fractionating with the 600-kDa marker protein aminopeptidase 1 (Ape1p) in lane 7. Similar to Myc-Sjl2p, HA-Sla1p showed a sedimentation pattern within the higher molecular size range compared to its protein mass of 135 kDa (138 kDa including three copies of the HA epitope), suggesting that both proteins associate in complexes. The phosphorylated forms of HA- Sla1p were detectable over its complete sedimentation profile, suggesting this state as its main form in the cell. To examine the sedimentation profiles of Myc-Sjl2p, HA-Sla1p, and HA-Pan1p in more detail the range

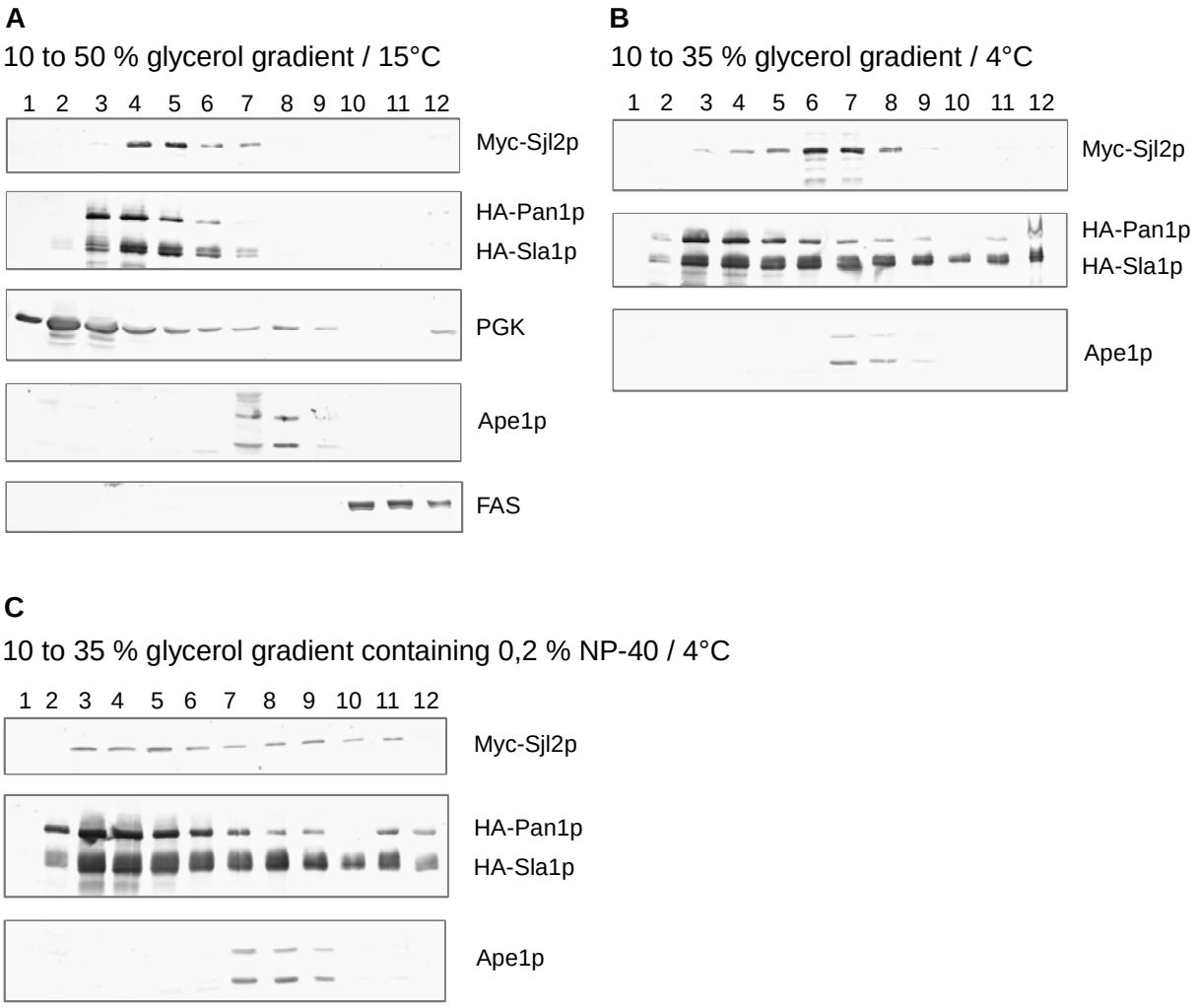

Fig. 10. Myc-Sjl2p is present in high-molecular-weight complexes
(**A**) Wildtype cells (CB72) expressing proteins as indicated were mechanically lysed in the presence of protease-inhibitors PMSF (1mM) and CLAP (1 x) and cleared by a 13.000 x *g* centrifugation step. Samples were loaded onto a 10 to 50 % glycerol gradient equilibrated in IP-buffer and were subjected to centrifugation at 100.000 x *g* (15 °C). Fractions were collected from top of the resulting gradient and analysed by Western blotting using anti-Myc, anti-HA, anti-Ape1p, and anti-FAS antibodies. Sizing standards are: PGK, phosphoglycerate kinase, M_r = 42 kDa; Ape1p, aminopeptidase 1, M_r = 600 kDa; FAS, fatty acid synthase, M_r = 2,4 MDa. (**B**) Preparation of the cell lysate was performed as described in (A), except that 4 mM PMSF and 8 x CLAP were added. Glycerol gradient compromised 10 to 35 % glycerol and centrifugation was performed at 4 °C. (**C**) Cells were lysed as described in (B) and incubated for 20 min with 0,2 % NP-40 before clearing the lysate. The glycerol gradient was performed as described in (B).

of the glycerol gradient was limited from 10 to 35 % of glycerol. Furthermore, since after a spin at 15 °C proteins were detected mainly at low molecular sizes, velocity gradients were performed at 4 °C to check for and possibly prevent complex dissociation (Fig. 10B). Using these conditions, in relation to the marker protein Ape1p (lanes 7 and 8) the sedimentation profile of Myc-Sjl2p was shifted to a higher-molecular-size range with peaks in lanes 6 and 7. HA-Sla1p and HA-Pan1p showed also considerable protein amounts dispersed through the whole gradient, indicating a faster sedimentation rate and maybe higher complex stability. The peaks of HA-Sla1p and HA-Pan1p still remained in lanes 3 and 4, possibly present as the monomeric form. Finally, the distribution of Myc-Sjl2p was tested after incubation of the cell

lysate in 0,2 % of the detergent NP-40 (Fig. 10C) to solubilize membrane associated complexes. As a control, compared to Fig. 10B the distribution of the 600-kDa protein Ape1p remained similar in this experiment (Fig. 10C). However, incubation of the cell extract with 0,2 % NP-40 for 20 min (Fig. 10C) before clearing the lysate and loading onto the glycerol gradient resulted in a dispersal of the sedimentation profile of Myc-Sjl2p both to lower- and higher-molecular-size ranges, while the profiles of HA-Sla1p and HA-Pan1p were similar to conditions without detergent. This may indicate a solubilization of larger complexes containing Myc-Sjl2p. Altogether, as observed by glycerol gradient centrifugation, Myc-Sjl2p obviously associates with other proteins resulting in a faster sedimentation rate than in its monomeric form. HA-Sla1p and HA-Pan1p sediment to some extend in the same fractions than Myc-Sjl2p.

3.3.3 The proline-rich domain of Sjl2p associates with the clathrin heavy chain (Chc1p) *in vitro*

The proline-rich domain of Sjl2p contains the protein sequence LIDLD at amino acid positions 944-948 that matches the L(L/I)(D/E/N)(L/F)(D/E) consensus motif, defined as a clathrin-binding box, for binding to the amino terminal domain of clathrin heavy chain 1 (Chc1p) (Dell'Angelica *et al.*, 1998; ter Haar *et al.*, 1998). To integrate and confirm a function of Sjl2p to clathrin-mediated transport it was essential to examine an interaction between Sjl2p and Chc1p. To address this question, GST pull-down experiments were performed. The glutathione S-transferase (GST) Sjl2p fusion protein contained amino acids 890-1183 spanning the proline-rich domain (GST-Sjl2$_{890\text{-}1183}$). The Singer-Krüger lab provided the purified protein expressed in *E. coli*. GST alone and GST-Ypt7p fusions were also provided and served as negative controls during the subsequent binding studies. From each fusion protein 80 µg were immobilized on 40 µl bed volume of glutathione-Sepharose beads and washed after binding. Meanwhile, cells from strain CB84, carrying the N-terminal 3 x HA epitope tagged version of clathrin light chain (Clc1p), were spheroblasted and lysed in the presence of 0,6 % Triton-X 100. The yeast lysate was then homogenized and cleared. One milliliter of the supernatant was carefully added to each GST fusion coupled to the glutathione Sepharose affinity matrix. After incubation the beads were extensively washed and bound proteins were eluted by three consecutive treatments with reduced glutathione buffer. Eluates were subjected to TCA-precipitation and prepared for separation by SDS-PAGE. The separated proteins were either stained with Coomassie Brilliant Blue or transferred to nitrocellulose for immunoblotting. Importantly, a specific binding of the proline-rich domain of Sjl2p to Chc1p was detected *in vitro* (Fig. 11A, lane 1). No binding of

Chc1p to the control proteins GST alone (lane 2) or the GST-Ypt7p fusion (lane 3) was observed. Less amounts of GST-Sjl2$_{890\text{-}1183}$ were bound to glutathione-Sepharose beads compared to GST alone and GST-Ypt7p as shown in the Coomassie Brilliant Blue staining. Conversely, N-terminally tagged HA-Clc1p did not bind specifically to glutathione-Sepharose beads, since background levels were detected in all three samples (data not shown).

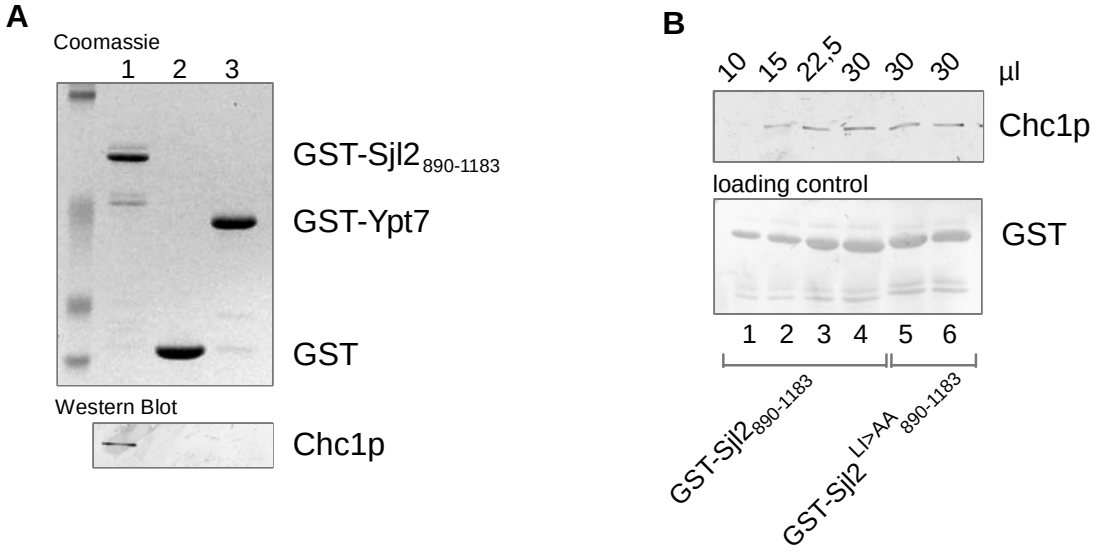

Fig. 11. The proline-rich domain of Sjl2p binds to clathrin heavy chain (Chc1p) *in vitro*
(**A**) GST and GST-fusions were expressed in *E.coli* and purified as described in section 2.2.4.3. To perform the GST pull-down experiments 80 µg of each fusion protein were immobilized to glutathione-Sepharose beads and washed. To generate the protein extract CB84 cells were spheroblasted in the presence of 0,8 M sorbitol and proteinase inhibitors. Spheroblasts were lysed in buffer containing 0,2 % sorbitol, 0,6 % Triton-X 100 and proteinase inhibitors. After incubation of the fusion proteins with the protein extract, beads were extensively washed and bound proteins eluted by reduced glutathione buffer. TCA-precipitates were separated by SDS-PAGE. Coomassie Brilliant Blue staining visualized GST-Sjl2$_{890\text{-}1183}$, GST, and GST-Ypt7. Chc1p was detected by immunoblotting with anti-Chc1p antibodies. (**B**) GST pull-down assays were performed as described in (A) using GST-Sjl2$_{890\text{-}1183}$ and GST-Sjl2$^{LI>AA}_{890\text{-}1183}$. As indicated, different amounts of eluates were loaded onto the SDS-PAGE and analysed by immunoblotting using an anti-Chc1p antibody.

To verify these results by reverse GST pull-down experiments, two different GST fusions of the N-terminal domain of Chc1p were prepared, representing the binding platform for the clathrin box motif. One fragment of yeast *CHC1* included amino acids 1 to 369 (GST-Chc1p$_{1\text{-}369}$) corresponding to the seven-bladed β-propeller and the first α-zigzag of residues 1-363 in rat (Drake and Traub, 2001). The larger fragment encompassed the β-propeller plus five α-helical zigzags (GST-Chc1p$_{1\text{-}483}$), which comprises the complete linker that joins the β-propeller to the distal leg (Kirchhausen, 2000). Although in small amounts, recombinant proteins were expressed in *E. coli* cells and purified by glutathione-Sepharose affinity purification. After GST-pulldown experiments both GST-Chc1p fusion proteins did not bind to Myc-Sjl2p using the strain CB1 (data not shown). In a second set of experiments a lysate of the strain CB42, carrying Myc-epitope tagged Sjl2p, HA-tagged Sjl3p and HA-tagged Sjl1p,

was used in binding experiments to GST-Chc1p$_{1-369}$ coupled to glutathione-Sepharose beads. Preliminary results showed small amounts of HA-Sjl3p bound to Chc1p$_{1-369}$, but not to GST alone or GST-Ypt7p (data not shown). HA-Sjl1p and Myc-Sjl2p were not detected in the precipitates. GST pull-down experiments using GST-Chc1p$_{1-483}$ did not show an interaction with any of the synaptojanin-like proteins. This may be explained by an incorrect folding of the N-terminal Chc1p domain.

Next it was examined if the clathrin-binding box LIDLD$_{948}$ is essential for binding of the proline-rich domain of Sjl2p with Chc1p. A similar five-amino acid consensus sequence motif for binding to the terminal domain of clathrin heavy chain, LLDID$_{919}$ has also been identified in the proline-rich domain of Sjl3p and the deletion of this motif reduced the binding to Chc1p (Ha *et al.*, 2003). But Ha *et al*. (2003) cannot exclude that a reduction of binding to Chc1p was caused from an altered domain structure after deletion of the binding motif. In mammalian cells the minimal consensus sequence defining a clathrin box LLpL(-) was revealed by comparing protein sequences of clathrin-binding proteins, like amphipysin 1 and 2, epsin 1, and adaptors AP-1, AP-2, and AP-3. L typically denotes a leucine, and p and (-) denote a polar and a negatively charged residue, respectively (Kirchhausen, 2000). Therefore, in the present PhD work leucine and isoleucine, the first conserved residues in the clathrin box LIDLD$_{948}$ of Sjl2p were changed by site-directed mutagenesis to alanines, resulting in AADLD$_{948}$, respectively (pGEX5-3-SJL2-3´end-LI>AA). Mutagenesis was performed according to the manufacturer´s protocol (see section 2.2.1.1) and the correct nucleotide substitutions were confirmed by DNA sequencing. Subsequently the fusion protein GST-Sjl2$^{LI>AA}_{890-1183}$ was expressed and purified by glutathione-Sepharose affinity purification (section 2.2.4.3). GST pull-down experiments were performed as described in Figure 11A with immobilized wildtype GST-Sjl2$_{890-1183}$ and mutant GST-Sjl2$^{LI>AA}_{890-1183}$ (Figure 11B). Obviously, conversion of leucine and isoleucine to alanines was not sufficient to impair the binding of the proline-rich domain of Sjl2p to Chc1p. Maybe additional binding motifs are present in the proline-rich domain of Sjl2p and Sjl3p, which are yet unknown to be recognized by the structurally complex N-terminal domain of Chc1p.

3.3.4 Rvs167p and End3p, which are known to act at endocytic sites, are found in association with the proline-rich domain of Sjl2p *in vitro*

To further elucidate proteins that interact with the PRD of Sjl2p and strengthen a putative association of Sjl2p with clathrin-coated endocytic vesicles, GST pull-down precipitates from the strain CB1 (Fig. 12) were checked preferentially for the presence of proteins that act as part of the endocytic machinery and regulate the assembly of the actin

cytoskeleton. First, the binding of HA-Sla1p to the PRD of Sjl2p was confirmed by the GST-pulldown. Sla1p is a multivalent adaptor that binds a large number of proteins involved in endocytosis and actin organization, including Pan1p, End3p, Las17p, and Sla2p, and Rvs167p (Holtzman *et al.*, 1993; Li, 1997; Stamenova *et al.*, 2004; Tang *et al.*, 2000). Using a specific anti-Rvs167p antibody, Rvs167p was also found to associate with GST-Sjl2$_{890\text{-}1183}$ (lane 1) but not with GST alone (lane 2). Detection of End3p with a specific antibody discovered also an association of this protein with GST-Sjl2$_{890\text{-}1183}$. Remarkably, since the strain CB1 used for these experiments also contained Myc-Sjl2p, the very same protein could also be detected to

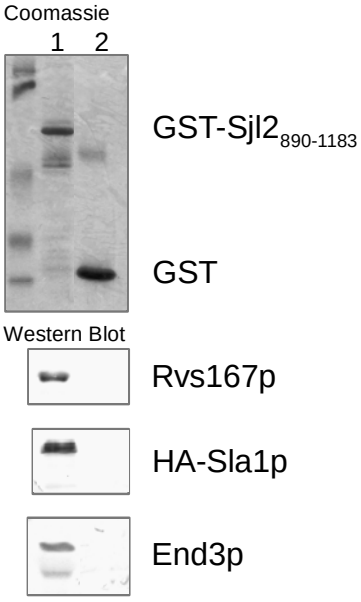

Fig. 12. The proline-rich domain of Sjl2p associates with different proteins involved in actin organization and endocytosis
GST pull-down experiments were accomplished as described in Fig. 11A, except that GST-fusion proteins GST-Sjl2$_{890\text{-}1183}$ and GST alone were incubated with protein extracts of the strain CB1 expressing HA-Sla1p and Myc-Sjl2p. TCA-precipitates were analysed by SDS-PAGE and subsequent immunoblotting using anti-Rvs167p, anti-HA, and anti-End3p antibodies.

bind to Sjl2p PRD (data not shown), suggesting a network of proteins probably with repeating modules or an evenly distribution of Sjl2p at different sides of the endocytic vesicle. Moreover, preliminary results point to a possible interaction of Sjl2p and Rvs167p using co-immunoprecipitation, but remain to be confirmed (data not shown). Notably, it was shown that Sjl2p is found in association with proteins affecting endocytic progressing and actin reorganization. Association of Sjl2p to Rvs167p and End3p targets it to essential processes in the formation of a clathrin-coated vesicle, like the initiation of endocytosis (Kaksonen *et al.*, 2005). In summary, these results strengthen the evidence for a subcellular localization of Sjl2p at endocytic sites during the process of vesicle formation at the plasma membrane.

3.4 Sjl2p and Sjl3p co-fractionate with clathrin-coated vesicles, distinct to Sjl1p

3.4.1 Sjl1, Sjl2p, and Sjl3p display distinct elution profiles from a Sephacryl S-1000 gel filtration column

In mammalian cells synaptojanin 1 is suggested to play a role in the un-coating step of clathrin-coated vesicles, since nerve terminals of synaptojanin 1 knock-out mice contain an increased number of clathrin-coated vesicles, correlating with an accumulation of PtdIns(4,5)P_2 and PtdIns(3,4,5)P_3 (Cremona *et al.*, 1999). The yeast synaptojanins have been suggested to control two clathrin-mediated pathways by the regulation of PtdIns(4,5)P_2, endocytosis and sorting between the TGN and endosomes (Ha *et al.*, 2003; Stefan *et al.*, 2002). Furthermore, it was shown that the yeast synaptojanins are membrane associated and Sjl3p interacts genetically with clathrin (Bensen *et al.*, 2000; Ha *et al.*, 2001; Stolz *et al.*, 1998), but evidence for an association of any of the yeast synaptojanin-like 5`-phosphatases with clathrin-coated vesicles was still lacking. Thus, clathrin-coated vesicles were isolated (Mueller and Branton, 1984) from a yeast strain carrying epitope tagged versions of all three synaptojanin-like proteins, HA-Sjl1p, Myc-Sjl2p, and HA-Sjl3p (CB42). Cells were grown to an OD_{600} of approximately 1,1 and a total of approx. 10 g (wet weight) cells and were subjected to spheroblasting. After hypotonical lysis of the spheroblasts, clearing of the lysate at low speed and centrifugation at 100.000 x *g*, the microsomal pellet was homogenized and cleared at 13.000 x *g*. The isolated vesicles were size fractionated by a Sephacryl S-1000 column and twenty-five 4 ml fractions were collected. Two milliliters of fractions #6 to #19 were TCA-precipitated and analysed by SDS-PAGE and immunoblotting. All three synaptojanin-like proteins were enriched in the 100.000 x *g* pellet (P), similar to Chc1p and the CPY receptor Vps10p (Fig. 13A) (Cereghino *et al.*, 1995). The main amounts of the cytosolic marker protein PGK were found in the supernatant after centrifugation at

A

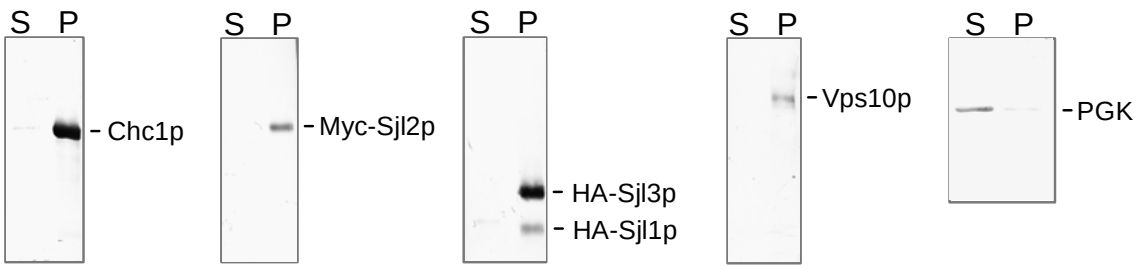

S = supernatant

P = 100.000 x *g* pellet

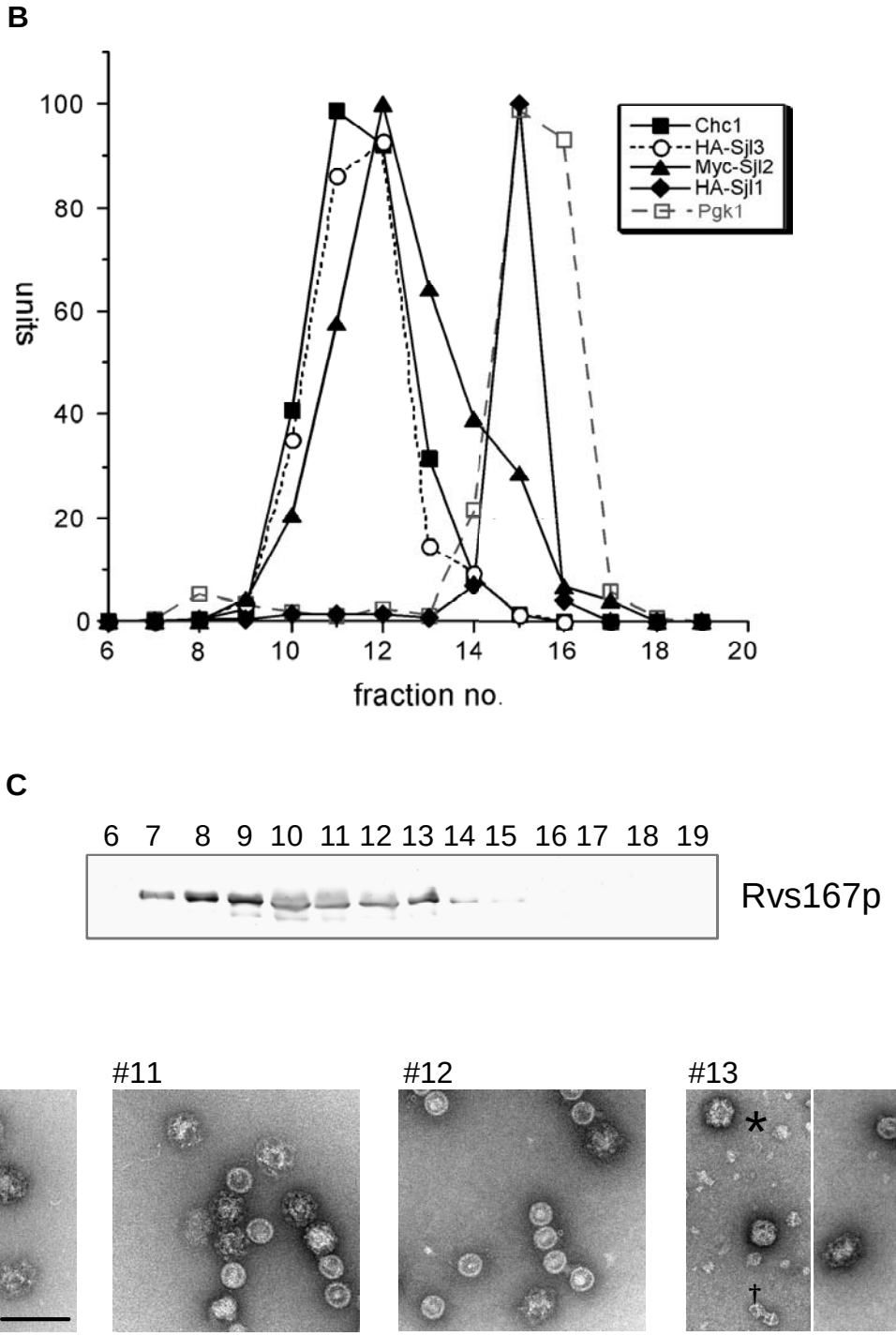

Fig. 13. Myc-Sjl2p and HA-Sjl3p fractionate similar to clathrin-coated vesicles, while HA-Sjl1p does not
(**A**) Cells of strain CB42 carrying epitope tagged versions of all three synaptojanin-like proteins were spheroblasted, hypotonically lysed and cleared before centrifugation at 100.000 x *g*, generating the pellet (P) and supernatant (S) fraction. Equal protein amounts were analysed by immunoblotting. (**B**) Isolation of clathrin-coated vesicles was performed as described in section 2.2.4.7 and portions of the fractions #6 to #19 were analysed by immunoblotting. Quantitation of immunoreactive bands was performed with [^{125}I] protein A and analysed with the PhosphoImager. The isolation was repeated seven times. (**C**) Elution profile of Rvs167p after the experimental procedure described in (A) (**D**) Portions of fractions #10 to #13 were fixed with 2,5 % glutaraldehyde. After negative staining, samples were viewed in the electron microscope at the magnification of 52.000; bar, 100 nm; *, densely coated vesicle; †, fatty acid synthase particles.

100.000 x *g*. After gel filtration chromatography on the Sepharcryl S-1000 column, clear differences among Myc-Sjl2p, HA-Sjl1p, and HA-Sjl3p were detectable (Fig. 13B). Myc-

Sjl2p and HA-Sjl3p eluted from the column very similar to Chc1p. The elution profile of HA-Sjl3p perfectly matched the profile of Chc1p. Following the major Myc-Sjl2p-peak in fractions #12 and #13, significant amounts were still detectable in fractions #14 and #15, likely to represent a small soluble pool of proteins. This may indicate a dissociation of Myc-Sjl2p from the membranes during the preparation. The HA-Sjl1p peak was clearly separated from Chc1p, corresponding to the profiles of cytosolic PGK (Fig. 13B) and actin (not shown) peaking in fraction #15. The amounts of the indicated proteins within the fractions were highly reproducible among various experiments, as determined by quantitative immunoblotting. The elution profile of Rvs167p revealed protein peaks in fractions #10 and #11 (Fig. 13C), corresponding with high protein amounts of Chc1p. Interestingly, in fractions #7 to #9 considerable amounts of Rvs167p were also detectable, in which most of the other proteins appeared in minor amounts. For this experiment the elution profiles of Myc-Sjl2p and Chc1p were not checked. Although the elution profile of Rvs167p appears to be similar in the strain CB228 (Myc-Sjl2p and *pik1-83*) (data not shown), it is necessary to verify this result with wildtype cells. Rvs167p contains N-BAR domains which can tubulate membranes *in vitro* (Peter *et al.*, 2004) and it is suggested to function in the process of vesicle scission at the plasma membrane (Kaksonen *et al.*, 2005; Takei *et al.*, 1999). Thus, detection of Rvs167p strongly indicated the isolation of plasma membrane-derived clathrin-coated vesicles (Balguerie *et al.*, 1999; Gourlay *et al.*, 2003).

It was of great interest to explore the presence of authentic clathrin-coated vesicles in clathrin-containing fractions. Portions of fractions #10 to #13 were fixed with 2,5 % glutaraldehyde and analysed by electron microscopy (EM) after negative staining. Figure 13D shows vesicles with the typical structure of a clathrin coat in fractions #10 and #11, confirming the presence and high enrichment of authentic clathrin-coated vesicles with an average diameter of 64 ± 7 nm (Mueller and Branton, 1984). The average diameter of smooth membrane vesicles in fractions #10 to #13 was 38 ± 3 nm. Due to the size fractionation of the Sephacryl S-1000 column smooth membrane vesicles were found in all fractions with enrichment in fraction #12. Additionally, some of the few vesicular structures found in fraction #13 contained coats that appeared to be more dense than those of authentic clathrin-coated vesicles. In this fraction an high enrichment of a symmetric protein structure was visible, most likely fatty acid synthase (Fig. 13D) (Kolodziej *et al.*, 1996).

To address the question on which type of vesicles Myc-Sjl2p resides to CCVs, immunodetection of Myc-Sjl2p was performed on fixed fraction by using antibodies coupled to gold particles for detection by EM. For that purpose, the homogenized and cleared

microsomal pellet was pre-incubated for 1 h with a mouse anti-Myc antibody and loaded onto the Sephacryl S-1000 column. After fixation of the resulting fractions #10 to #13 with 2,5 % glutaraldehyde, vesicles were subsequently incubated with either swine or goat anti-mouse antibodies, in the second step with protein-A-10 nm gold and finally negative stained. However, gold-particles were detected rarely and unspecific distributed on the grid by EM. Most likely the glutaraldehyde fixation does not impair binding of the immunoreagent (H. Schwarz, personal communication).

Since an immunodetection of Myc-Sjl2p on clathrin-coated or smooth vesicles was not successful, the cleared 100.000 x *g* microsomal pellet (see section 2.2.4.7) (Mueller and Branton, 1984), was tested for a flotation of the clathrin-coated vesicles and Myc-Sjl2p by different density gradients. Neither a sucrose gradient (steps 53 %, 35 %, 20 %, 10 %), a Nycodenz gradient (steps 37 %, 31 %, 27 %, 20 %, 13 %) nor an Iodixanol gradient (steps 40 %, 30 %, 25 %, 20 %, 15 %, 10 %) showed a floatation of the synaptojanin-like proteins or clathrin-coated vesicles into the gradient. This may indicate that the protocol for the generation of the microsomal pellet prevents a flotation in the different gradients. Therefore, the vesicle pellet was prepared by subcellular fractionation and subjected to flotation on a discontinuous Nycodenz gradient. Similar to the other gradients, Myc-Sjl2p and Vps10p were not detected to flotate into the gradient. As a third method, whole-cell extracts were prepared by gentle osmotic lysis followed by a differential centrifugation. Afterwards an antibody and protein-A Sepharose were used to immunoisolate clathrin-coated vesicles (Deloche *et al.*, 2001). The procedure was performed as described, but an anti-Myc antibody was used for the isolation of intact clathrin-coated vesicles via Myc-Sjl2p. This method did not succeed to precipitate clathrin-coated vesicles. These results may be due to a very fragile consistence of the clathrin coat.

Nevertheless, the elution of Myc-Sjl2 and HA-Sjl3p, but not Sjl1p, in fractions containing authentic clathrin-coats with a diameter close to that of clathrin-coated vesicles (Mueller and Branton, 1984) provide a strong argument for an association of these synaptojanin-like proteins with such vesicles, supporting the proposed role in un-coating of yeast clathrin-coated vesicles.

3.4.2 Sjl2p is maybe targeted to clathrin-coated vesicles by multiple recruiting factors

Next, it was addressed which domains or interaction partners of Sjl2p are sufficient to recruit the PI phosphatase to its proposed site of action at clathrin-coated vesicles. By taking advantage of the described protocol to isolate clathrin-coated and Sjl2p-positive vesicles, elution profiles of epitope tagged versions of Sjl2p were generated from different mutant

strains. These strains either lacked known interaction partners of Sjl2p or expressed a truncated version of Sjl2p (HA-Sjl2p-Δprd). Additionally, the fractionation profile of HA-Sjl2p was examined in a *pik1-83* mutant strain in which the levels of PtdIns(4)P and PtdIns(4,5)P_2 are reduced by 45 – 60 % compared to wildtype cells. A typical example for the distribution of the marker proteins Chc1p and PGK from a wildtype strain after isolation of clathrin-coated vesicles and immunoblotting of fractions #6 to #19 is shown in Figure 14A. The peak of Chc1p was found in fractions #11 and #12, but PGK peaked clearly separated in fraction #15. In all mutant strains elution profiles of Chc1p and PGK were largely similar to wildtype cells (not shown). The elution profiles of Sjl2p in the analysed mutant strains indicated an association with and recruitment to fractions #11 and #12, containing clathrin-coated vesicles (Fig. 14), as shown in wildtype cells (Fig. 13C). Interestingly, in contrast to a recent study (Stefan *et al.*, 2005) that described a diffuse staining of GFP-Sjl2p after indirect immunofluorescence in cells lacking *ABP1*, data of this PhD work showed a recruitment of Myc-Sjl2p to clathrin-containing fractions in *Δabp1* cells (Fig. 14C), similar to wildtype cells. Moreover, analysis of all mutants did not reveal an obvious recruiting factor, since in all strains Sjl2p seemed to associate with vesicular structures. Thus, it appears that Sjl2p is recruited to clathrin containing vesicular structures by multiple factors. The deletion of

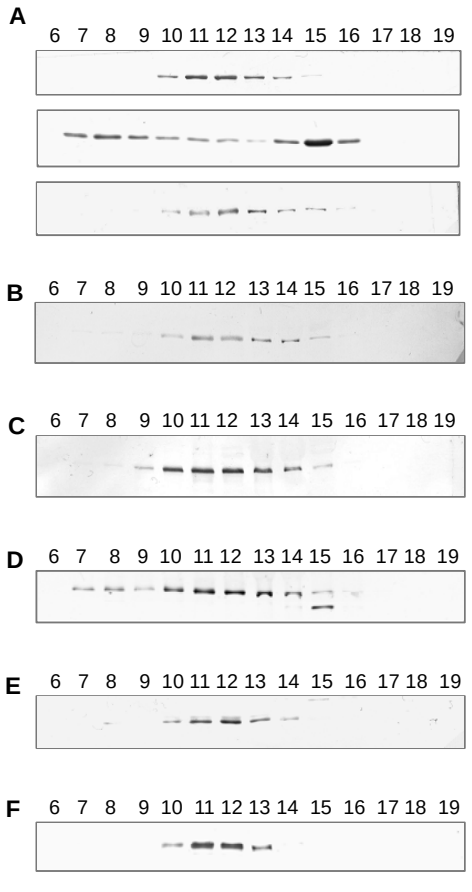

Fig. 14. Elution profiles of Sjl2p in different mutant strains
(**A**) to (**F**) Cells were grown either in YPD or selective media to an OD_{600} of approx. 1,1. Isolation of clathrin-coated vesicles from the indicated strains was performed as described in section 2.2.5.7. Fractions #6 to #19 were collected, precipitated by TCA in the presence of DOC and analysed by SDS-PAGE and immunoblotting. Strains used for these studies: (A) CB42; (B) CB164; (C) CB131; (D) SK94; (E) SK3; (F) CB228

identified binding partners, the proline-rich domain, or reduction in PtdIns(4)P and PtdIns(4,5)P_2 levels are individually not sufficient to abolish a proposed association with clathrin-coated vesicles.

Interestingly, Myc-Sjl2p bands showed a slight mobility shift in clathrin-coated vesicles containing fractions #10, #11 and #12, while the bands in fractions #13 and #14 were sharper. This mobility shift was reproducible in experiments using wildtype cells and was also detectable in *Δsla1Δbsp1* cells expressing Myc-Sjl2p (Fig. 14B), *Δabp1* cells expressing Myc-Sjl2p (Fig 14C), *Δsjl1Δsjl2Δsjl3* cells expressing HA-Sjl2p from a *LEU2*-based plasmid (Fig. 14D), and *Δsjl2* cells expressing HA-Sjl2p-Δprd (Fig. 14E). These reproducible observations indicate posttranslational modifications in Sjl2p, likely phosphorylation or ubiquitination.

3.5 Sjl2p and Sjl3p are posttranslationally modified, but Sjl1p is not

3.5.1 Tyrosine phosphorylation

Posttranslational modifications are known as upstream signaling event for regulation of activity, stability, localization and binding properties of proteins (Barriere *et al.*, 2006; Hicke, 2001b; Seet *et al.*, 2006). In eukaryotes, phosphorylation of specific residues is, beside ubiquitination, one of the most important regulatory mechanism by which the activity of enzymes and receptors can be regulated. In yeast, phosphorylation is well known to regulate actin polymerization during vesicle formation at the plasma membrane (Toshima *et al.*, 2005; Zeng *et al.*, 2001). It has been shown to be important for routing of cell surface transporters and pheromone receptors into ubiquitin-dependent degradative vacuolar pathways (Hicke *et al.*, 1998) and to influence trafficking of the resident TGN membrane protein Ste13p (Johnston *et al.*, 2005).

Whereas in yeast cells tyrosine phosphorylation is rarely described, in mammalian cells it is known as a powerful regulator for protein activity (Bonifacino and Traub, 2003; Confalonieri *et al.*, 2000; Girault *et al.*, 1992; Pang *et al.*, 1988). During the present PhD work Irie *et al*. described a stimulation of early phases of endocytosis as an effect of tyrosine phosphorylation in three tyrosine residues in the proline-rich domain of synaptojanin 1 and the requirement of its de-phosphorylation in later stages to facilitate the un-coating process (Irie *et al.*, 2005). Multiple band pattern of yeast Sjl2p observed in immunoprecipitates (section 3.1.1, 3.3.2, and 3.2.3), or after isolation of clathrin-coated vesicles (see section 3.4.2), or of Sjl3p during assembly of actin (see section 3.1.1) suggested the existence of (a) posttranslational modification(s). Moreover, Sjl2p also contains three tyrosine residues in the

proline-rich domain at the amino acids 901, 904 and 1123, similar to mammalian synaptojanin 1 (Irie *et al.*, 2005). To verify tyrosine phosphorylation of yeast synaptojanins, immunoprecipitation experiments were performed using the strain CB207 expressing functional HA-Sjl2p clearly distinguishable from Myc-Sla1p by size after separation by SDS-PAGE. Myc-Sla1p is a known substrate of the serine/threonin kinases Ark1p and Prk1p (Zeng *et al.*, 2001). Therefore it is suggested that the anti-phosphotyrosine antibody does not detect Myc-Sla1p. To discover a possible tyrosine phosphorylation of Myc-Sjl3p, strain CB105 was used expressing also HA-Sla1p, while strain CB136 carried HA- Sjl1p and Myc-Sla1p. The strain BS64 was subjected to immunoprecipitation as a negative control, since it does not carry any epitope tagged protein and thus indicates unspecific bands pattern after immunoblotting. Immunoprecipitation was accomplished as described in section 2.2.4.4, except that $25OD_{600}$ cells were harvested freshly at an OD_{600} of 0,2-0,3. The synaptojanin-like proteins were precipitated with antibodies directed against the epitopes, with which they were tagged. After separation in SDS-PAGE and immunoblotting, immunoprecipitates of all three synaptojanin-like proteins were clearly detected (Fig. 15A). These results confirmed once again the specific interaction of Sla1p with Sjl2p (lane 9), while no signal for Sla1p was detected in strains expressing HA-Sjl1p (lane 8) or Myc-Sjl3p (lanes 6 and 7). Immunoprecipitates of strain BS64 did not result in detection of unspecific signals. Immunodetection using a phosphotyrosine antibody resulted in a specific staining of bands at the molecular sizes of Myc-Sjl3p (lane 11) and HA-Sjl2p (lane 13). At these molecular masses no signal was detected in the control strain BS64 (lane 14). As expected, no signal was examined at the molecular size of Myc-Sla1p (lanes 11-13). Differences in the intensity of the phosphotyrosine staining between Myc-Sjl3p and HA-Sjl2p are likely caused by higher amounts of Myc-Sjl3p versus HA-Sjl2p in the cell extract (lanes 2 and 4) and after immunoprecipitation (lanes 6 and 9). Several background bands were observed in the precipitate of BS64 and similarly in the precipitates of the other strains. Beside these unspecific signals, no band was visible at the molecular size of HA-Sjl1p (lane 12), although the protein could be clearly detected in the cell extract (lane 3) and the immunoprecipitate (lane 8). Remarkably, although threefold amounts of each sample were analysed by SDS-PAGE for detection of phosphotyrosine residues, the phosphorylated protein amounts of HA-Sjl2p and Myc-Sjl3p are minor, suggesting that this modification is possibly a regulation factor. It cannot be excluded that phosphorylation of Sjl1p occurs at low level or under restricted conditions.

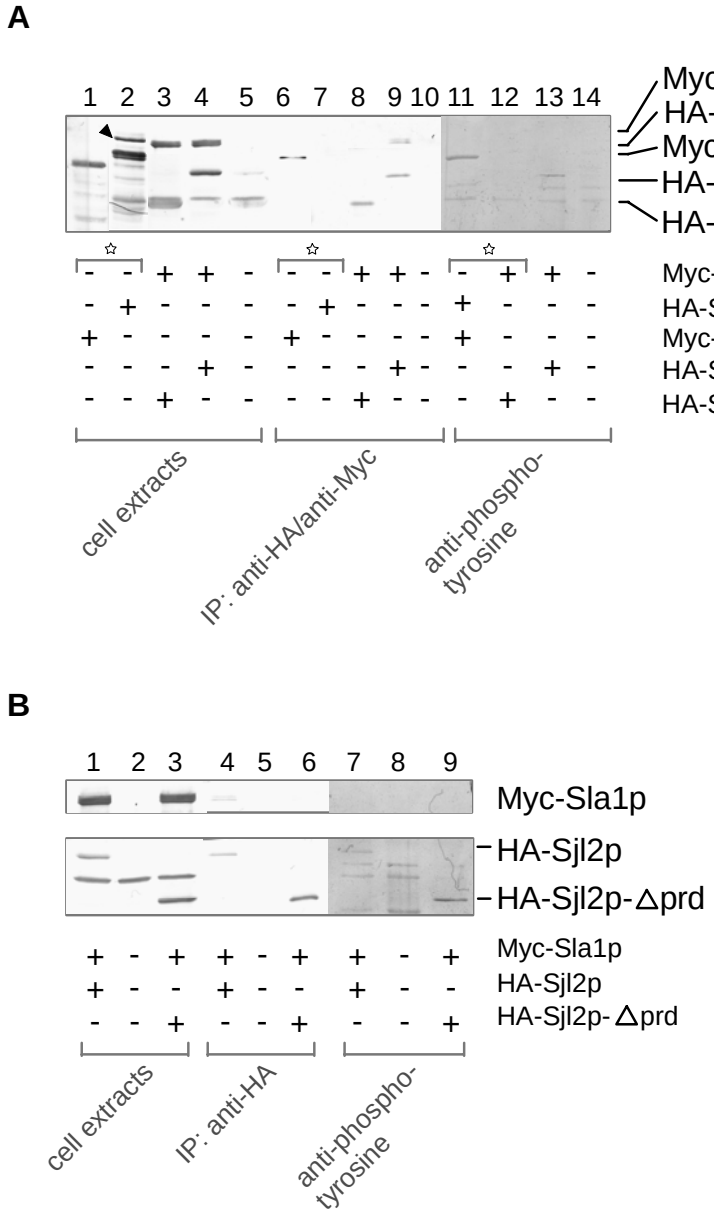

Fig. 15. Sjl2p, Sjl3p, and Sjl2pΔprd are modified by tyrosine phosphorylation, while Sjl1p is not
(**A**) To perform immunoprecipitations 25 OD_{600} units of cells were lysed per sample. HA- or Myc-protein complexes were isolated by binding to anti-HA antibody and, in the second step, to protein-A Sepharose. After washing, 30 µl of 1 x sample buffer containing 2,5 % β-mercaptoethanol were added to the samples and boiled. To retrieve the complete sample protein-A Sepharose were separated from the released proteins by spinning in Mobicol columns (MoBiTech). Samples were analysed by immunoblotting with anti-HA, anti-Myc, and anti-phosphotyrosine (PY-20) antibodies. Used strains: CB105 (Myc-Sjl3p + HA-Sla1p + HA-Pan1p), CB136 (HA-Sjl1p + Myc-Sla1p), CB207 (HA-Sjl2p + Myc-Sla1p), BS64 (control strain) (**B**) For immunoprecipitation, cells were used expressing either HA-Sjl2p and Myc-Sla1p (CB207) or HA-Sjl2p-Δprd and Myc-Sla1p (SK22). The control strain BS64 did not carry tagged proteins. Experimental conditions were performed as described in (A). ⭑: both proteins are expressed in CB105, arrow: HA-Pan1p

Irie *et al.* (2005) demonstrated that three tyrosine phosphorylation sites in the proline-rich domain of mammalian synaptojanin 1 are responsible for a selective inhibition of the interaction with endophilin, which stimulates the 5`-phosphatase activity of synaptojanin 1. Therefore it was investigated if tyrosine phosphorylation is still detectable for Sjl2p lacking its proline-rich domain (Fig. 15B). HA-Sjl2p-Δprd was expressed from a plasmid (pRS315-

HA-SJL2-Δprd) in *Δsjl2* cells that expressed Myc-Sla1p from the chromosomal locus (SK22). Due to the expression from a plasmid, higher protein amounts of HA-Sjl2p-Δprd were detected in the cell extract (lane 3) and after immunoprecipitation (lane 6). The levels of the chromosomally tagged HA-Sla1p were comparable in both strains SK22 (lane 1) and the positive control strain CB207 (lane 3). Strain CB207 expressed HA-Sjl2p and Myc-Sla1p from the endogenous promoters (lanes 1 and 4). Strain BS64 served as the negative control, since it does not express epitope tagged proteins (lanes 2 and 5). Myc-Sla1p is again detected with HA-Sjl2p after co-immunoprecipitation (lane 4). HA-Sjl2p-Δprd (lane 6) is clearly visible in immunoprecipitates together with less amounts of Myc-Sla1p. Results from the diploma student Svenja Kaden confirmed that Sla1p does not interact with Sjl2p lacking its proline-rich domain (unpublished data). Compared to the band pattern from the precipitates of strain BS64, a signal was detected at the molecular sizes of HA-Sjl2p (lane 7) and HA-Sjl2p-Δprd (lane 9) after incubation with anti-phosphotyrosine antibodies. The same background staining was detected as described in Fig. 15A.

Taken together, theses results point to an attachment of a phosphate group to tyrosine residues in HA-Sjl2p and Myc-Sjl3p, but not HA-Sjl1p. In contrast to published data of Irie *et al* (2005) from the mammalian system, Sjl2 lacking its proline-rich domain, HA-Sjl2p-Δprd, was still phosphorylated at tyrosine residues within the domains responsible for the PPIP- and 5´Pase- activity of Sjl2p. Whether these modifications represent a regulation mechanism, as described for synaptojanin 1 (Irie *et al.*, 2005), remains to be examined.

3.5.2 Ubiquitination

Ubiquitination acts as a reversible modification similar to phosphorylation. Moreover, it is suggested that phosphorylation and ubiquitination are in tight cooperation in cells (Haglund and Dikic, 2005). A hierarchical cascade of enzymes executes ubiquitination. E3 ligases, the final effector of the cascade, can append ubiquitin to intracellular targets either as a single moiety (mono-ubiquitination), or as chains of ubiquitin (polyubiquitination) (Hochstrasser, 2006). Mono-ubiquitination is well known to be required for the internalization and hence down-regulation of several plasma membrane proteins in both yeast and mammalian cells. But it becomes more and more evident that also proteins of the endocytic machinery are mono-ubiquitinated in yeast (Hicke, 2001a; Sigismund *et al.*, 2004). For example, Rvs167p is ubiquitinated by the essential ubiquitin ligase Rsp5p. Rsp5p interacts with its substrates via a WW motif, which are 33-amino acid blocks (Sudol *et al.*, 1995) that bind to the PPLP, PPxY, or PxY motifs (reviewed in Chang *et al.*, 2000). Sjl1p, Sjl2p, and

Sjl3p each contain two conserved PxY binding motifs short before the proline-rich domains (Sjl1p: PTY_{773} and PVY_{817}; Sjl2p: PTY_{828} and PVY_{878}; and Sjl3p: PTY_{803} and PVY_{853}, respectively). Therefore it was likely that the yeast synaptojanins-like proteins are modified by ubiquitin, in addition to their phosphorylation on tyrosine residues. Immunoprecipitation experiments were performed as described in section 2.2.4.9 using the appropriate antibodies to isolate the synaptojanin-like proteins in the presence of 0,2 % NP-40. Strains used in these studies were the same as for the tyrosine phosphorylation experiments, strain CB207 expressing HA-Sjl2p and Myc-Sla1p, strain CB105 carrying Myc-Sjl3p and HA-Sla1p, and CB136 carrying HA-Sjl1p and Myc-Sla1p. Myc-Sla1p co-precipitates with HA-Sjl2p, but not with HA-Sjl1p or Myc-Sjl3p. Another study could not detect ubiquitination of Sla1p (Stamenova *et al.*, 2004), thus serves as a possible negative control for an unspecific binding of the anti-ubiquitin antibody. As a second negative control, the lysate of CB140 cells was also subjected to immunoprecipitations, since it carries only Myc-tagged Sla1p. Although the amounts of proteins varied after the different immunoprecipitations, all three synaptojanin-like proteins were clearly visible after immunoblotting with anti HA- and Myc-antibodies (Fig.16A, lanes 6-8). Co-immunoprecipitation of Myc-Sla1p with HA-Sjl2p was also confirmed (lane 8). Prior to probing the nitrocellulose membrane with the anti-ubiquitin antibody, the membrane was autoclaved to improve the detection (section 2.2.4.2.1) (Swerdlow *et al.*, 1986). Compared to the band pattern after separation of immunoprecipitates from CB140 cells (lane 13), a pronounced staining was examined at the molecular size of HA-Sjl2p (lane 12) and Myc-Sjl3p (lane 10) after immunodetection of the precipitates with the anti-ubiquitin antibody. The appearance of one single band at the same molecular size of the tagged protein suggests a low ubiquitination state of HA-Sjl2p and Myc-Sjl3p. Despite the fact that three times more sample was analysed by SDS-PAGE, no signal for ubiquitination was observed at a detectable level at the size of monomeric HA-Sjl1p (lane 11) and HA-Sla1p (lane 12). The unspecific background bands had the same intensity in lanes 10 to 14, which excludes mistakes in the experimental procedure. This result is strengthened by the observation that compared to HA-Sjl2p (lane 8) higher HA-Sjl1p amounts (lane 7) were detected in the immunoprecipitates after incubation with anti-HA-antibodies. It was striking that the precipitates of Myc-Sjl3p (lane 10) and HA-Sjl1p (lane 11) showed more background labelling in the higher and lower molecular weight range, compared to the HA-Sjl2p immunoprecipitates (lane 12), after detection with the anti-ubiquitin antibody. This indicates the presence of further ubiquitinated binding partners of Myc-Sjl3p and HA-Sjl1p, since it

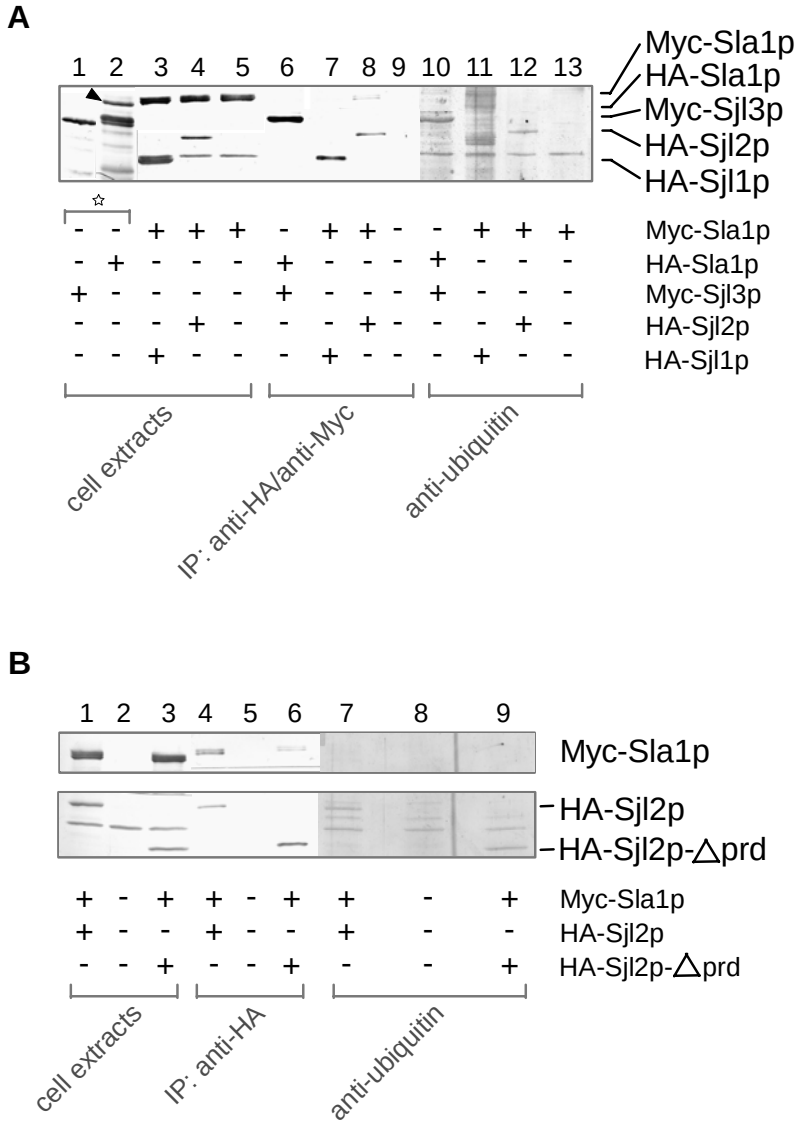

Fig. 16. Sjl2p, Sjl3p, and Sjl2pΔprd are ubiquitinated, whereas Sjl1p is not
(**A**) Cells were grown to 0,5-0,8 OD_{600} cells/ml and immunoprecipitation was performed as described. Precipitates were analysed by immunoblotting with anti-HA, anti-Myc and anti-ubiquitin antibodies. The used strains expressed Myc-Sjl3p, HA-Sla1p, and HA-Pan1p (CB105), HA-Sjl2p and Myc-Sla1p (CB207), HA-Sjl1p and Myc-Sla1p (CB136). CB140 (control strain) expresses Myc-Sla1p. (**B**) In this immunoprecipitation experiment, cells were used expressing HA-Sjl2p and Myc-Sla1p (CB207) or HA-Sjl2p-Δprd and Myc-Sla1p (SK22). The control strain BS64 did not carry tagged proteins. Experimental conditions were organized as described in fig. 14A. ⭑: both proteins are expressed in CB105, arrow: HA-Pan1p

cannot be explained by an unspecific binding of proteins to protein-A Sepharose beads. Moreover, analysis of the immunoprecipitates via antibodies against the epitopes discovered only the proteins at the expected molecular size.

It was furthermore interesting to address if the modification of HA-Sjl2p by ubiquitin is restricted to its proline-rich domain (Fig. 16B). Thus, *Δsjl2* cell containing HA-Sjl2p-Δprd and Myc-Sla1p were analysed (lane 3). Strain CB207 expressing the full length HA-Sjl2p and Myc-Sla1p served as a positive control for ubiquitination (lane 1), while BS64 was used as a negative control to identify the unspecific band pattern after immunoblotting (lane 2).

Subsequent immunoprecipitation via the HA-epitopes was performed as described in section 3.5.1 in the presence of 0,2 % NP-40. After separation of the isolated proteins by SDS-PAGE and immunoblotting with anti-HA antibodies, HA-Sjl2p (lane 4) and HA-Sjl2p-Δprd (lane 6) were clearly visible. An unspecific staining of Myc-Sla1p appeared at higher levels (lane 6) after immunoprecipitation of HA-Sjl2p-Δprd, but the amounts were lower than compared to Myc-Sla1p co-immunoprecipitated with HA-Sjl2p (lane 4). After incubation with the anti-ubiquitin antibody two unspecific bands were detected in precipitates from strain BS64, but they were distinct from the bands at the molecular size of HA-Sjl2p and HA-Sjl2p-Δprd, respectively. Appearance of a band at the molecular size of HA-Sjl2p-Δprd indicates that ubiquitination of HA-Sjl2p also or only occurs at the catalytic domains.

The lower ubiquitination state of Sjl2p and Sjl3p suggests mono- or multi-ubiquitination. In yeast, the E3 ligase Rsp5p is the unique member of the conserved Rsp5p/Nedd4 HECT-family that is proposed to ubiquitinate components of the receptor internalization machinery (Rotin *et al.*, 2000; Stamenova *et al.*, 2004). To investigate the possibility that Sjl2p is a substrate of Rsp5p, co-immunoprecipitations were carried out. Strains used for that purpose expressed either Flag-Rsp5p from an inducible plasmid (pRS415-Flag-RSP5), Myc-Sla1p and HA-Sjl2p (CB240), or Flag-Rsp5p and Myc-Sla1p (CB246, control strain). After the induction of Flag-Rsp5p expression by galactose cells were grown over night, harvested and lysed by glass beads. Cell extracts were preincubated with 0,4 % or 0,8 % NP-40. HA-Sjl2p complexes were isolated from total cellular extracts by binding to rabbit anti-HA antibody and, in a second step, by associating this complex to Protein-A covered Sepharose. Immunoprecipitates were analysed by immunoblotting using anti-Myc, anti-HA, and anti-Flag antibodies (see section 2.2.4.4.4). Preliminary results did not show a specific binding of Flag-Rsp5p to HA-Sjl2p (data not shown). Recent studies described that the interaction of Rsp5p/Nedd4p HECT-family members with its substrate could be rather transient (Woelk *et al.*, 2006). Further optimising of the experimental conditions, like stabilizing the supposed interaction between the proteins, or the use of a chromosomally tagged version of Rsp5p may result in the successful co-immunoprecipitation of Rsp5p. Since only small amounts of Sjl2p are present in the cell, scaling up of the co-immunoprecipitation procedure may result in a specific signal.

In sum, HA-Sjl2p and Myc-Sjl3p show modification by appended ubiquitin, maybe due to a regulation mechanism. It is currently unclear if the tyrosine phosphorylation and ubiquitination are influenced by each other or represent different steps as described for receptor endocytosis (Haglund and Dikic, 2005). HA-Sjl1p seems not to be a substrate for

tyrosine kinases as well as ubiquitin ligases. However, it cannot be ruled out if posttranslational modifications of HA-Sjl1p occur at very low levels or only in the response to specific stimuli.

3.5.3 Time course experiment

Previous studies demonstrated that endocytic proteins are concerted at endocytic sites in a highly regulated order and timing (Kaksonen *et al.*, 2003; Kaksonen *et al.*, 2005). Posttranslational modifications are supposed to play a major role in these regulation mechanisms. Recently, it became clear that the role of ubiquitin in promoting internalization is not restricted to tagging cargo molecules at the plasma membrane, ubiquitination appears to regulate the activity of components of the endocytic machinery as well (Hicke, 2001a; Stamenova *et al.*, 2004). Reconsidering a proposed regulation mechanism of mammalian synaptojanin 1 by tyrosine phosphorylation and de-phosphorylation cycles during the different stages of endocytosis (Irie *et al.*, 2005), it was intriguing to investigate if ubiquitination of Sjl2p is altered after triggering receptor-mediated endocytosis.

In yeast, it is supposed that 2-5 min after initiating endocytic internalization vesicles form and bud off the plasma membrane (Toshima *et al.*, 2006). Therefore, it was decided to assay the ubiquitination status of Sjl2p at early timepoints after triggering receptor-mediated endocytosis by adding the α-factor pheromone. To determine the ubiquitination status, HA-Sjl2p was subsequently immunoprecipitated. The used strain CB207 (*MAT***a**) carried Sjl2p tagged with HA epitopes and Sla1p tagged with Myc epitopes. Cells were grown to a density of 10^7 cells per ml and harvested. Before and after addition of α-factor, 25 OD_{600} were collected at 0 min, 1 min, and 2,5 min and energy-poisoned by adding NaN_3 and NaF. To minimize a possible de-ubiquitination of HA-Sjl2p during the subsequent immuno-precipitation steps, N-ethylmaleimide (NEM) was added to all buffers (see section 2.2.4.9). Precipitates were prepared as described and proteins were detected using anti-HA, anti-Myc, and anti-ubiquitin antibodies. Although preliminary results indicated increased amounts of ubiquitin-modified HA-Sjl2p 1 min after triggering endocytosis (data not shown), this result was observed inconsistently. Detection of small amounts of ubiquitinated proteins in yeast is very difficult, since antibodies do not bind so well as in other optimised systems. Since the preliminary results point to a possible and yet unknown regulation mechanism for Sjl2p, it would be worth to optimise the assay conditions.

3.6 Analysis of the chimeric Sjl2/3p protein (Sjl2/3p)

3.6.1 Sjl2/3p does not interact with Sla1p

The C-terminal proline-rich domains of Sjl1p, Sjl2p, and Sjl3p do not share an extensive identity as the Sac1-like and 5`Pase domains do. One of their suspected functions is to target specific synaptojanin-like family members to distinct subcellular sites. A recent study has shown that the localization of Sjl2p to cortical actin patches depends on the PRD of Sjl2p, actin filaments, and the actin patch component Abp1p (Stefan *et al.*, 2005). It was of interest to clarify if replacement of the proline-rich domain from the endocytic protein Sjl2p by the PRD of Sjl3p effects changes in function and targeting. To test an interaction of HA-Sjl2/3p with Myc-Sla1p, pRS315-HA-SJL2/3 was transformed in a *Δsjl2* strain expressing Myc-Sla1p (CB185). As a positive control served a strain carrying full length HA-Sjl2p and Myc-tagged Sla1p (CB207), while the negative control strain expressed only Myc-Sla1p (CB140, control strain). Co-immunoprecipitations were accomplished as described above, in the presence of 0,2 % NP-40 using the anti-HA antibody. HA-Sjl2p and HA-Sjl2/3p and their interacting proteins were bound to protein-A Sepharose and analysed by immunoblotting. Myc-Sla1p was detected in immunoprecipitates from HA-Sjl2p expressing cells (Fig. 17, lane 4), clearly above the unspecific staining (lane 5), again confirming co-precipitation by the used conditions. By contrast, low quantities of Myc-Sla1p were detected after precipitation of HA-Sjl2/3p (lane 6) similar to the negative control (lane 5), indicating for an unspecific

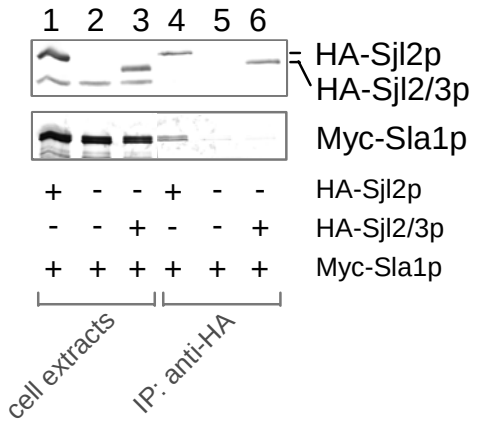

Fig. 17. HA-Sjl2/3p and Myc-Sla1p do not associate with each other *in vivo*
Co-immunoprecipitations were performed with the anti-HA antibody using cell extracts (CB207, CB233 and CB140) containing the epitope-tagged proteins as indicated, in the presences of 0,2 % NP-40. HA complexes were immobilized on protein-A Sepharose, washed and boiled with sample buffer for release. Proteins were separated by SDS-PAGE and analysed by immunoblotting using anti-HA and anti-Myc antibodies.

binding of Myc-Sla1p to protein-A Sepharose beads. These results imply a loss of binding capacity with Myc-Sla1p if the proline-rich domain of Sjl3p is fused to the PPIP- and 5´Pase-domains of Sjl2p. This observation is consistent with a lack of an interaction of Sjl3p with Sla1p revealed during this PhD work (see section 3.2.1), but the validity of this comparison remained to be scrutinised.

3.6.2 Sjl2/3p co-elutes with Chc1p containing fractions from a Sephacryl S-1000 gel filtration column

It was of further interest to reveal the subcellular localization of the chimeric HA-Sjl2/3p. After isolation of clathrin-coated vesicles (Mueller and Branton, 1984) from *Δsjl2* cells carrying pRS315-HA-SJL2/3 and Myc-tagged Sla1p, the elution profiles revealed that HA-Sjl2/3p co-elutes with Chc1p in fractions # 10 to # 13 (Fig. 18), distinct from the cytosolic marker protein PGK. Interestingly, HA-Sjl2/3p exhibited several bands after

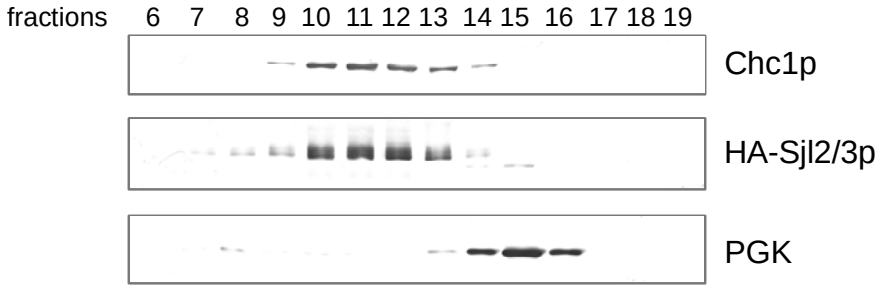

Fig. 18. HA-Sjl2/3p is found in fractions containing Chc1p after isolation of clathrin-coated vesicles
Isolation of clathrin-coated vesicles was performed as described in section 2.2.4.7 Resulting fractions #6 to #19 were subjected to TCA-precipitation, portions of the precipitates were separated by SDS-PAGE and analysed by immunoblotting using anti-Chc1p, anti-HA and anti-PGK antibodies. The used strain CB233 expressed HA-Sjl2/3p (pRS315-HA-SJL2/3) and Myc-Sla1p.

separation by SDS-PAGE, also observed after separation of crude cell extracts expressing HA-Sjl2/3p (not shown). This was maybe due to posttranslational modifications. The result indicated that the chimeric protein HA-Sjl2/3p localizes to vesicular structures, similar to Sjl2p and Sjl3p. Again, it should be noted that large protein aggregates contain HA-Sjl2/3p, which co-elute with Chc1p containing fractions, but independent from clathrin-coated vesicles, (advised in section 3.4.2).

3.6.3 The Sjl2/3p chimeric protein is posttranslationally modified

Since a multiple band pattern was detected for HA-Sjl2/3p after isolation of CCVs, it was straightforward to test, whether HA-Sjl2/3p is posttranslational modified by tyrosine phosphorylation and ubiquitination. After transformation of pRS315-SJL2/3 in *Δsjl2* cells expressing Myc-Sla1p (CB233) immunoprecipitations (see section 3.5.2) with the anti-HA antibody and analysis of the precipitates were performed (see section 2.2.4.2.1). The control strain CB140 carried Myc-epitope tagged Sla1p (CB140, not shown). After precipitation of HA-Sjl2/3p, a faint signal for tyrosine phosphorylation was detected, but clearly visible above the background staining (Fig. 19A, lane 5). Furthermore, ubiquitination (Fig. 19B, lane 5) was

detected (Fig. 19B, lane 5). These posttranslational modifications suggest that the chimeric HA-Sjl2/3p folds properly to be recognized by the modifying enzymes.

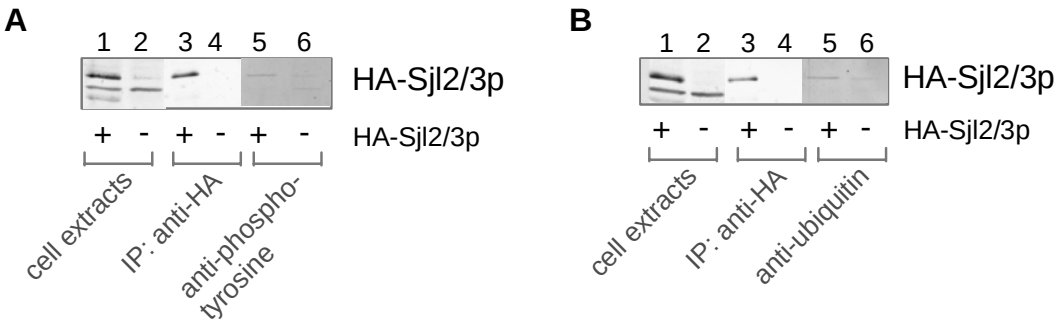

Fig. 19. Sjl3/3p is modified by tyrosine phosphorylation and ubiquitination
(**A**) Immunoprecipitations were performed as described (section 2.2.4.9). The used strains contained HA-Sjl2/3p and Myc-Sla1p (CB233) and Myc-Sla1p (CB140, control strain). Precipitates were separated by SDS-PAGE and analysed by immunoblotting using anti-HA and anti-phosphotyrosine antibodies. (**B**) The experiments were performed as described in (A), but precipitates were analysed using anti-HA and anti-ubiquitin antibodies.

3.6.4 Sjl2/3p does not rescue lethality of *Δsjl1Δsjl2Δsjl3* cells

Several studies revealed that single null mutants of the synaptojanin-like proteins (*sjl1*, *sjl2* and *sjl3*) are viable, while deletion of all three proteins (*SJL*) genes is lethal suggesting that the yeast synaptojanins have essential but overlapping functions. However, double mutants demonstrated several phenotypes including defects in endocytosis, impaired cell growth, defects in actin cytoskeletal organization, and aberrant cell surface and vacuole morphologies (Singer-Krüger *et al.*, 1998; Srinivasan *et al.*, 1997; Stefan *et al.*, 2002; Stolz *et al.*, 1998). Together, expression of Sjl2p as the only yeast synaptojanin phosphatase resulted in minor phenotypes than compared to the sever defects if only Sjl3p or Sjl1p were expressed. Therefore, it was examined if the chimeric protein HA-Sjl2/3p is able to rescue the *Δsjl1Δsjl2Δsjl3* lethal phenotype, as Sjl2p does. For that reason, pRS315-HA-SJL2/3 was transformed in *Δsjl1Δsjl2Δsjl3* cells containing the *URA3*-based vector pRS316-SJL2 (BS1561). Control strains were triple null mutants of the synaptojanin-like proteins (*Δsjl1Δsjl2Δsjl3*) carrying either pRS315-SJL2 and pRS316-SJL2 (SK7), or pRS315-HA-SJL2-Δprd and pRS316-SJL2 (SK9). After plasmid shuffling by counterselection with 5-FOA, either pRS315-HA-SJL2/3, pRS315-SJL2, or pRS315-HA-SJL2-Δprd were the only copies of synaptojanin-like proteins in the mutant strains. After 3 days of incubation at 25 °C single colonies of *Δsjl1Δsjl2Δsjl3* + pRS315-SJL2 cells were visible (Fig. 20), but *Δsjl1Δsjl2Δsjl3* cells, expressing HA-Sjl2/3p or HA-Sjl2p-Δprd showed still the lethal phenotype of *Δsjl1Δsjl2Δsjl3* cells. These data confirmed that the proline-rich domain of Sjl2p

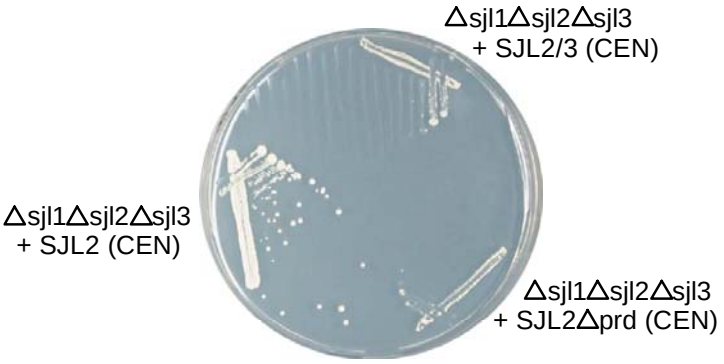

Fig. 20. *SJL2/3* does not rescue the lethality of a *Δsjl1Δsjl2Δsjl3* mutant
Growth on YPD + 5-FOA plates at 25 °C of *Δsjl1Δsjl2Δsjl3* + pRS316-SJL2 cells (BS1561) transformed with pRS316-SJL2 (SK7), pRS315-HA-SJL2-Δprd (SK9), or pRS315-HA-SJL2/3 (CB248).

is necessary for the survival of *Δsjl1Δsjl2Δsjl3* cells (unpublished results). Furthermore, fusion of the proline-rich domain of Sjl3p to the PPIP- and 5-Ptase-catalytic domains of Sjl2p is not sufficient to rescue lethality of *Δsjl1Δsjl2Δsjl3* cells. It is conceivable that an altered molecular environment to which the chimeric protein HA-Sjl2/3p may localize might prevent PI phosphatase activity. Lipids, peripheral, and integral proteins that are either at the plasma membrane or at the TGN may act either at Sjl2p or Sjl3p, thus might together not be able to stimulate the enzymatic activity of the chimeric protein HA-Sjl2/3p. Transformation of both catalytic domains of Sjl2p in the triple mutant could be a tool to test validity of this hypothesis. Furthermore, whether the fusion of the PRD of Sjl2p to the PPIP/5-Pase domains of Sjl3p results in the same phenotype remains to be determined.

3.6.5 Sjl2/3p only partially rescues the synthetic growth defect of a *Δgga1Δgga2Δsjl3* mutant at 39 °C

The elution profile of HA-Sjl2/3p indicated a proper recruitment to clathrin-coated vesicles containing fractions (see section 3.6.2). Despite this fact, HA-Sjl2/3p does not rescue the lethality of *Δsjl1Δsjl2Δsjl3* cells, similar to Sjl2p (see section 3.6.4), thus does not exhibit its function at sites of endocytosis. Since the loss of an interaction of HA-Sjl2/3p with Myc-Sla1p indicated a feature observed for Sjl3p (see section 3.6.1), it was investigated if HA-Sjl2/3p is able to alleviate the growth phenotype in *Δgga1Δgga2Δsjl3* cells at 39 °C by complementing *Δsjl3* (Ha *et al.*, 2003). *GGA1* and *GGA2* encode adaptor proteins that contain clathrin-binding motifs and thus are necessary for clathrin-mediated transport from the TGN directly to the (late) endosomes (Black and Pelham, 2000; Costaguta *et al.*, 2001). The synthetic growth defect at 37 °C visible after deletion of *SJL3* in a *Δgga1Δgga1* double mutant strain suggests that Sjl3p probably mediates a distinct pathway into the endosomal system, presumably to early endosomes (Ha *et al.*, 2003).

Plasmids encoding either HA-Sjl2/3p or Sjl3p were transformed in *Δgga1Δgga2Δsjl3* mutant cells and growth was assessed at the permissive (25 °C) and restrictive (39 °C) temperature (Fig. 21). The dramatic growth defect of *Δgga1Δgga2Δsjl3* mutant cells at 39 °C confirmed the expected phenotype. Compared to wildtype cells no synthetic growth defect was observed at 39 °C in *Δgga1Δgga2Δsjl3* cells expressing Sjl3p. It was not unexpected that *Δgga1Δgga2Δsjl3* cells carrying HA-Sjl2/3p showed a clear impairment of growth at the restrictive temperature. The lack of a complete growth rescue at 39 °C by expression of HA-Sjl2/3p in *Δgga1Δgga2Δsjl3* cells could be interpreted by that the chimeric protein HA-

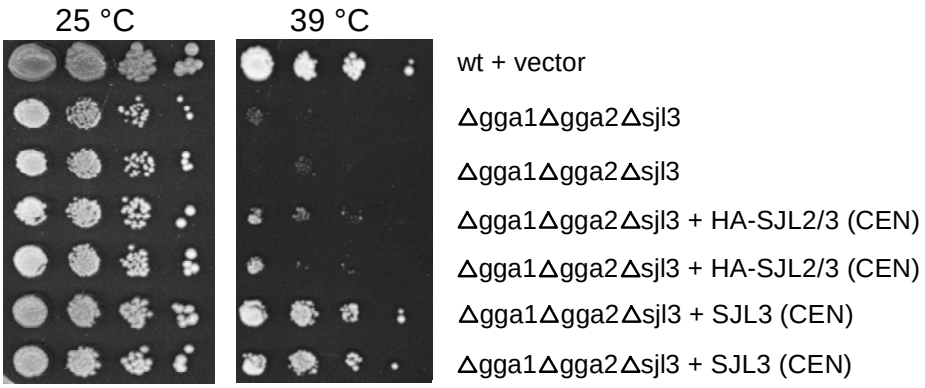

Fig. 21. Expression of HA-Sjl2/3p rescues only partially the synthetic phenotype of *Δgga1Δgga2Δsjl3* cells
Growth at the indicated mutant strains (from top to bottom: CB260, CB270, CB272, CB263, CB266, CB276, CB278) was assessed by spotting 10-fold serial dilutions onto YPD plates and growing for 3 days at the indicated temperature.

Sjl2/3p is not sufficiently functional to restore the role of the Sjl3p in the transport pathways between TGN and endosomes. Since Sjl2p is still present in *Δgga1Δgga2Δsjl3* cells, it remains open if a slight overexpression of Sjl2p from a CEN plasmid has the same growth effect as expression of HA-Sjl2/3p. Again, it could be argued that the molecular environment of HA-Sjl2/3p inhibits the catalytic domains.

4 Discussion

4.1 All synaptojanin-like proteins associate with polymerized actin

In the present study, Sjl1p, Sjl2p, and Sjl3p were found to co-sediment with *in vitro* polymerized actin. The first indication for an association of the yeast synaptojanin-like (Sjl) proteins with the cortical actin cytoskeleton originated from a study, in which GFP-tagged PPIP- and proline-rich domains of Sjl2p and Sjl3p showed a transient co-localization with actin patches under hyperosmotic stress conditions. These findings implicated Sjl2p and Sjl3p in the cell integrity pathway (Ooms *et al.*, 2000). Subsequent work has discovered that elevated PtdIns(4,5)P_2 levels in cells lacking the 5-Pase activities of the synaptojanin-like proteins cause, beside defects in endocytic and intracellular traffic, also defects in actin filament organization (Stefan *et al.*, 2002). Moreover, yeast two-hybrid screens and biochemical interaction studies led to the identification of the actin patch component Bsp1p as a direct binding partner of the PPIP domains of Sjl2p and Sjl3p *in vivo* (Wicky *et al.*, 2003), and the interaction of the proline-rich domain (PRD) of Sjl2p with the actin patch components Sla1p and Abp1p *in vitro* (Fazi *et al.*, 2002; Stamenova *et al.*, 2004).

Taking advantage of the possibility to detect physiological quantities of each yeast synaptojanin protein in one and the same cell extract, the association of Sjl1p, Sjl2p, and Sjl3p with actin, whose polymerization was triggered *in vitro*, was investigated using an established biochemical assay (Goode, 2002). Since the cell lysate was precleared by centrifugation at 255.000 x *g*, only the non-membrane-associated pools of Sjl1p, Sjl2p, and Sjl3p were followed during these experiments. Each of the polyphosphoinositide phosphatases co-sedimented with polymerized F-actin at 25.000 x *g*. Similar to Abp1p, both Sjl2p and Sjl3p could be washed off from actin structures by high salt concentrations, while Sjl1p remained tightly bound to actin under similar conditions.

Sjl1p and Sjl2p/Sjl3p also differ in respect to the absence or presence of a PPIP activity (Guo *et al.*, 1999) and all three family members vary considerably in the amino acid sequence of their proline-rich domains. Furthermore, unlike Sjl2p and Sjl3p, Sjl1p contains an asparagine-proline-phenylalanine (NPF_{934}) binding motif C-terminal in its proline-rich domain (Wendland *et al.*, 1998), similar to the mammalian synaptojanin 170 kDa isoform (Haffner *et al.*, 1997). This short motif results in an exclusive physical interaction of Sjl1p with the EH-domain containing proteins Tax4p and Irs4p, implicated in the actin-based cell integrity pathway (Morales-Johansson *et al.*, 2004). More evidence for a closer actin relation came from the observations that deletion of *SJL1*, but not of *SJL2* and *SJL3*, leads to the

suppression of the temperature-sensitive growth defect of a *sac6* mutant (Singer-Krüger *et al.*, 1998) and deletion of Sjl1p shows synthetic lethality with loss of the actin nucleation factor *PAN1*, that links actin filaments to the endocytic coat (Kaminska *et al.*, 2005; Wendland and Emr, 1998). Sac6p is an actin-filament-cross-linking protein that is essential for the progress of membrane tubulation (Kaksonen *et al.*, 2005). Suppression of the *sac6* phenotype by a deletion of *SJL1* points to the possible requirement of balanced PtdIns(4,5)P_2 levels for the growing actin network during the internalization process at the plasma membrane. However, the association of Sjl1p with specific binding partners that do not interact with Sjl2p/Sjl3p might explain the tight association with F-actin.

The detachment of Sjl2p and Sjl3p from filamentous actin by high salt indicates similar biochemical features for both proteins. It is conceivable that since vesicle formation and actin are intrinsically tied and Sjl2p interacts with the actin linked components Abp1p, Bsp1p, and Sla1p (Gavin *et al.*, 2006, and this work; Stefan *et al.*, 2005; Wicky *et al.*, 2003), association to and detachment from *in vitro* polymerized filamentous actin at least partially occurs through intermediary proteins resulting in a more loose association. Interestingly, during this PhD thesis it was shown that Sjl2p also associates with Pan1p *in vivo*, but maybe not with a similar tight and/or direct binding, as Sjl1p via its NPF motif. Given the similarities in the vesicle formation machinery at the plasma membrane and the *trans*-Golgi network (TGN) (reviewed in McNiven and Thompson, 2006) a comparable mechanism may cause the biochemical association of Sjl3p with *in vitro* polymerized actin at its subcellular site.

These results allow the conclusion that Sjl1p stably localizes to actin structures, while Sjl2p and Sjl3p bind weaker to actin filaments, probably via interaction partners. In mammalian cells synaptojanin 1 resides along the tubular invagination of the plasma membrane, apparently not as an intrinsic component of the coat similar to dynamin and amphiphysin (Haffner *et al.*, 1997). This observation also supports the finding that the yeast synaptojanin proteins are associated with filamentous actin, since a current model for actin-driven endocytic internalization proposes a branched network of filamentous actin around the coated invagination (Kaksonen *et al.*, 2006). The challenge will be to elucidate how the synaptojanins are integrated in the upcoming models in regard to their actin and membrane association. As a first clue to solve this challenge, it becomes more and more relevant that many types of protein-protein interaction via different motifs are rather weak. This indicates dynamic/fluid protein networks, like for example during vesicle budding. This system may have a built-in `dynamic instability´ (Hicke *et al.*, 2005) which might allow the synaptojanin

proteins to fulfil their different functions at distinct microdomains along the evolving transport vesicle.

4.2 Sjl2p associates specifically with proteins of the endocytic machinery

A significant finding in this PhD thesis was the specific interaction of Sjl2p with the clathrin cargo adaptor Sla1p *in vivo* (Howard *et al.*, 2002; Tan *et al.*, 1993). A physical interaction of both proteins was already described *in vitro* (Stamenova *et al.*, 2004) and further restricted for the minimal interacting domains (B. Singer-Krüger), whereas the *in vivo* proof was still lacking. During the present PhD work this interaction was confirmed by large scale protein complex analyses (Gavin *et al.*, 2006). Sla1p localizes to cortical actin patches, at an early stage during the invagination step of endocytosis, and moves toward the interior of the cell together with other coat proteins before the latter disassembles (Ayscough *et al.*, 1999; Kaksonen *et al.*, 2003; Kaksonen *et al.*, 2005). An implication of Sjl2p in the endocytic processes was already suggested, because, remarkably, *Δsjl1* or *Δsjl3* mutants lacking also *SJL2* displayed severe endocytic defects in both receptor-mediated and fluid-phase uptake (Singer-Krüger *et al.*, 1998; Stolz *et al.*, 1998). The interaction between Sjl2p and Sla1p suggests a role of Sjl2p during early steps of endocytosis when Sla1p participates as well. At that point Sjl2p might function rather as a regulatory component than as a phosphatase, maybe similar to an inhibition of the 5-Pase activity of mammalian synaptojanin 1 during early steps of endocytosis (Irie *et al.*, 2005).

The C-terminal fourteen LxxQxTG- and QxTG-motifs of Sla1p are targets for phosphorylation by the protein kinases Ark1p and Prk1p (Zeng *et al.*, 2001). In accordance, the staining pattern of Sla1p revealed multiple bands after immunoprecipitation. Treatment with calf intestinal phosphatase (CIP) of isolated Sla1p verified that two bands are due to protein phosphorylation. Interestingly, the binding of Sjl2p to the N-terminal two SH3 domains of Sla1p (B. Singer-Krüger, unpublished data) seems not to be influenced or regulated by the C-terminal phosphorylation of Sla1p. The possible regulation and implication of this interaction awaits to be discovered. Interestingly, the same two SH3 domains of Sla1p are binding sites for Las17p, an Arp2/3p complex activator (Rodal *et al.*, 2003), and all three SH3 domains of Sla1p interact with Rvs167p, a possible vesicle scission component at the plasma membrane (Stamenova *et al.*, 2004). The binding of Las17p to Sla1p inhibits the Arp2/3p complex activation and consequently actin polymerization. The question whether the three proteins, Sjl2p, Las17p, and Rvs167p, compete for binding to Sla1p or whether the bindings occur in sequence as part of a signaling cascade will be important to address in future research.

A recent study demonstrated that Sjl2p is recruited to cortical actin patches dependent on Abp1p (Stefan *et al.*, 2005). In contrast, a finding of this PhD thesis instead indicates that Sjl2p and Sla1p still co-precipitate in *Δabp1* cells. Since another group showed that Sla1p resides to cortical actin patches in *Δabp1* cells (Kaksonen *et al.*, 2005), Sjl2p is at least partially recruited to sites of endocytosis. The phenotype of *Δabp1* cells suggests a role for Abp1p in the disassembly of endocytic structures after vesicle internalization, because of longer-lived endocytic patches relative to wild-type cells (Kaksonen *et al.*, 2005). The study interprets this observation with a lack of recruitment of Ark1p and Prk1p by Abp1p, based on results of Fazi *et al*. (2002), and of Sjl2p, based on results of Stefan *et al*. (2005), to sites of endocytosis. A possible scenario based on the results of this PhD thesis and of Kaksonen *et al*. (2005) could be that the deletion of *ABP1* directly or indirectly rather influences Sjl2p activity than recruiting Sjl2p to sites of endocytosis. In light of the proposed role of the synaptojanin proteins in the uncoating of CCVs, a delayed activity of Sjl2p might delay the turnover of PtdIns(4,5)P_2 and thus lead to a prolonged lifetime of endocytic patches. Together, the results from Stefan *et al*. (2005) are controversial to the results in the present PhD work, since an interaction of Abp1p and Sjl2p was not confirmed *in vivo* and deletion of *ABP1* did not disturbed an interaction between Sjl2p and Sla1p. The apparent discrepancies might be explained by different strain backgrounds.

Sla1p functions in a complex with Pan1p and End3p (Tang *et al.*, 2000; Zeng *et al.*, 2001). To examine if Pan1p is also found in complex with Sjl2p/Sla1p, co-immuno-precipitation experiments and glycerol density gradients were performed. Strikingly, the amounts of Pan1p that co-immunoprecipitated with Sjl2p were smaller than the amount of Sla1p detected in the Sjl2p complex. Assuming that no destabilization of Sjl2p/Sla1p/Pan1p complex occurs during the isolation, it is possible that not all of the Sla1p/Sjl2p complexes contain also HA-Pan1p. The necessity to treat the cell lysates with high concentrations of NP-40 to detect a specific co-precipitation of Pan1p may indicate a strong membrane association of the putative Sjl2p/Sla1p/Pan1p complex. A possible interaction of Sjl2p/Sla1p/Pan1p was further suggested by sedimentation profiles of the three proteins in glycerol gradients. The majority of Sla1p and Pan1p were sedimented accordingly to their calculated molecular masses, whereas Sjl2p was largely detected at a higher molecular size. The calculated molecular mass of a putative Sjl2p/Sla1p/Pan1p complex is approximately 450 kDa including the appended epitopes. The interaction of Sjl2p/Sla1p/Pan1p is indicated with the appearance of all three proteins at a molecular mass slightly before the 600-kDa marker protein Ape1p. It was surprising that Sjl2p showed a strong dispersal to lower and apparently higher molecular

size complexes after treatment of the lysate with 0,2 % NP-40. This result supports the notion that Sjl2p is part of a very large membrane associated protein network of interacting proteins, most likely, at endocytic sites. It remains to be clarified if the putative subcomplexes represent different stages during the protein assembly and disassembly of protein networks during endocytosis. Unlike Sjl2p, the sedimentation of Sla1p and Pan1p remained similar after treatment with 0,2 % NP-40 suggesting that both proteins bind weaker to the membrane than Sjl2p. The observation that Sla1p is mainly found in its phosphorylated state in all fractions of the glycerol density gradients implicates that the de-phosphorylation and hence binding to Pan1p and End3p is tightly regulated. Taken together, these findings point to the existence of a Sjl2p/Sla1p/ Pan1p complex *in vivo*. It has yet to be established whether the interaction of these three proteins has a regulatory function in the progression of vesicle formation and maturation.

The GST-pulldown experiments have revealed that Chc1p, Rvs167p, and End3p associate with the proline-rich domain of Sjl2p *in vitro*. These proteins are required for actin organization at the plasma membrane and clathrin-mediated membrane traffic. The coat protein End3p is recruited early to sites of endocytosis, where it participates in the initiation of clathrin- and actin-mediated endocytosis, while Rvs167p arrives at a later stage due to an assumed requirement in the scission of endocytic vesicles (Kaksonen *et al.*, 2005). Clathrin heavy chain (Chc1p) is the major coat component at endocytic sites (Kirchhausen, 2000; Newpher *et al.*, 2005). Thus, Sjl2p associates with proteins of the endocytic machinery *in vitro*. These findings strengthen the evidence for an implication of Sjl2p in clathrin-mediated endocytosis.

Similar to Sjl3p, Sjl2p contains a clathrin-binding box $LIDLD_{948}$ in its proline-rich domain. The presence of this motif points to a direct interaction of Sjl2p with Chc1p for which some evidence was obtained in this work. In contrast to results after deletion of this motif in Sjl3p (Ha *et al.*, 2003), point mutations in the Sjl2p clathrin-binding box did not result in a decrease of the binding to Chc1p. Thus, additional, but yet unidentified, Chc1p-binding motifs may be present in the proline-rich domain of both Sjl2p and Sjl3p that participate in the association to Chc1p. Alternatively, it is supposable that Sjl2p interacting proteins and Sjl2p´s clathrin-binding box together establish a stable binding to Chc1p. Surprisingly, GST-pulldown experiments with the proline-rich domain of Sjl2p also recruited full-length Sjl2p. Since, as described, the PRD of Sjl2p leads to the isolation of proteins that localize to distinct sites at the evolving membrane invagination, it is possible that Sjl2p localizes to several microdomains at the endocytic tube. In agreement with this hypothesis is

the observation that the mammalian synaptojanin 1 resides along clathrin-coated membrane invaginations (Haffner *et al.*, 1997).

In sum, the data strengthen the argument that Sjl2p exhibits functions in an intricate network of proteins, implicated in clathrin-mediated endocytosis and actin organization at the plasma membrane. Since Sjl2p associates with proteins that localize to distinct subdomains at the membrane invagination, a distribution of Sjl2p at various sites of the evolving tube/vesicle is very likely.

4.3 Sjl2p and Sjl3p function at distinct subcellular sites

The finding that the PRD of Sjl2p, but not Sjl3p and Sjl1p, interacts with Sla1p further supports the idea of distinct subcellular localizations of the three family members. Although Sla1p was also identified to associate with Sjl1p *in vitro* (Stamenova *et al.*, 2004) this interaction was not confirmed *in vivo* during this PhD thesis. Several lines of evidence propose that Sjl3p functions in clathrin-mediated traffic between the TGN and endosomes (Bensen *et al.*, 2000; Ha *et al.*, 2001; Ha *et al.*, 2003). In this PhD work, no evidence for a co-fractionation of Sjl1p with clathrin-coated vesicles has been obtained. Sjl1p is believed to be generally implicated in regulating actin cytoskeletal organization, endocytosis and delivery of endocytic vesicles to the vacuole via control of phosphatidylinositol-4,5-bisphosphate levels (Stefan *et al.*, 2002).

Further evidence for a localization of Sjl2p and Sjl3p to distinct compartments came from the analysis of *sec7* cells under non-permissive conditions. In *sec7* mutant cells the Golgi compartment forms aberrant membrane structures (Schekman and Novick, 2004), resulting in a block of intra-Golgi transport (Hicke *et al.*, 1997). While Sjl3p was degraded after a shift to the non-permissive temperature, neither the protein amounts of Sjl2p were affected nor its interaction with Sla1p. The observed degradation of Sjl3p may be a result of an altered lipid composition of the Golgi complex. A stable interaction between Sjl2p and Sla1p in this mutant indicates an undisturbed recruitment to their sites of function, clearly distinct from the TGN. This interpretation is also supported by the finding that Sjl2p resides mainly on plasma membrane-derived vesicles that are generated prior to the activity of Sec18/NSF during endocytosis (Böttcher *et al.*, 2006).

Interestingly, both Sjl2p and Sla1p showed an altered mobility in a SDS-PAGE after incubation at the non-permissive temperature. The nature of these modifications is currently unknown.

4.4 Sjl2p associates with clathrin-coated vesicles

Clues regarding the roles of the synaptojanin family members in clathrin-mediated membrane traffic have emerged in a variety of model organisms. Given their enzymatic activity, synaptojanins are expected to be negative regulators of membrane-coat interactions implicating a function during the un-coating of endocytic vesicles. This prediction was supported in mammalian cells (Cremona *et al.*, 1999), *C. elegans* (Harris *et al.*, 2000), and *Drosophila melanogaster* (Verstreken *et al.*, 2003).

In *S. cerevisiae*, several studies have proposed a function of Sjl2p in endocytosis, due to phenotype analyses (Singer-Krüger *et al.*, 1998; Srinivasan *et al.*, 1997). As a further indication, Sjl2p, but not Sjl3p and Sjl1p, was found to aggregate together with endocytic components of the clathrin-mediated pathway upon loss of the kinases *ARK1* and *PRK1* (Böttcher *et al.*, 2006). An implication of Sjl3p in clathrin-mediated traffic between the TGN and endosomes was suggested by genetic and biochemical work (Bensen *et al.*, 2000; Ha *et al.*, 2001; Ha *et al.*, 2003). To unveil whether the Sjl family members localize to clathrin-coated vesicles a strain was analysed which contained tagged versions of all three synaptojanin-like proteins. Clathrin-coated vesicles were isolated according to Mueller and Branton (1984) and examined by electron microscopy (EM) and immunoblotting. In fact, clathrin-coated vesicles were highly enriched and Sjl2p and Sjl3p co-eluted with the clathrin-coated vesicles. Furthermore, Rvs167p, which participates in the scission of endocytic vesicles at the plasma membrane, also co-eluted in fractions containing clathrin-coated vesicles, Sjl2p, and Sjl3p. Significantly, Sjl1p was clearly separated from Chc1p with the main peak similar to cytoplasmic PGK. These results support the idea of distinct biochemical features of Sjl2p/Sjl3p versus Sjl1p. Unfortunately, various tests failed to demonstrate a direct binding of Sjl2p to clathrin-coated vesicles by EM immunotechniques. Furthermore, various density gradients failed to demonstrate a flotation of Sjl2p with clathrin-coated vesicles. Nevertheless, most likely the isolated Sjl2p-positive structures represent, or are derived from, clathrin-coated vesicles generated after budding from the plasma membrane. Altogether, these results are most consistent with a role of the lipid phosphatases Sjl2p and Sjl3p, but not Sjl1p, at yeast clathrin-coated vesicles.

Analysis of different mutant stains lead to the proposition that Sjl2p is recruited to endocytic sites/clathrin-coated vesicles by a variety of components. Neither the deletion of specific interacting partners, such as Sla1p and Bsp1p, or the proposed binding partner Abp1p, nor reducing PtdIns(4,5)P_2 levels abolished the co-elution of Sjl2p with clathrin-coated vesicles. But it should be cautioned that an unimpaired co-fractionation of Sjl2p with

clathrin-coated vesicles in all analysed mutants could also point to an unspecific co-elution with clathrin-coated vesicles. One possible explanation for that scenario is the presence of large Sjl2p- and Sjl3p-positive aggregates, which were not detectable by electron microscopy after negative staining. It will be a major point to address the direct binding of Sjl2p and Sjl3p to clathrin-coated vesicles, derived from the plasma membrane or the TGN.

Nonetheless, the finding that also the deletion of Sjl2p´s PRD was not sufficient to abrogate its vesicle association is consistent with the membrane association of Sjl3p lacking its proline-rich domain. Most likely, also the catalytic domains are involved in general membrane association of Sjl3p (Ha *et al.*, 2003) and Sjl2p. Together, these data suggest that the presence of the PPIP and 5-Pase domains of Sjl2p and Sjl3p are sufficient to allow a recruitment to membrane domains. The proline-rich domain may then specify the binding to defined membrane domains via their interaction with other specificity factors, such as Sla1p.

4.5 Sjl2p and Sjl3p are substrates for tyrosine phosphorylation and ubiquitination, while Sjl1p is not

It becomes more and more evident that posttranslational modifications of proteins are key factors in regulating cellular processes. Recent experiments in *S. cerevisiae* have identified a number of proteins implicated in the regulation of cortical actin patches and vesicle formation that are regulated by phosphorylation, in particular Ent1p, Clc1p, Rvs167p, Pan1p, and Sla1p (Chu *et al.*, 1999; Friesen *et al.*, 2003; Watson *et al.*, 2001; Zeng and Cai, 1999; Zeng *et al.*, 2001). This PhD work demonstrated that the yeast synaptojanin family members Sjl2p and Sjl3p are phosphorylated at tyrosine residues, whereas Sjl1p and, as expected, Sla1p are not. Although no signal was detectable, it cannot be excluded that Sjl1p is phosphorylated under certain conditions. Nevertheless, the lack of tyrosine phosphorylation of Sjl1p under the used conditions underlines once more a biochemical difference between Sjl2p/Sjl3p and Sjl1p. Reconsidering the 5-Pase regulation of synaptojanin 1 by tyrosine phosphorylation, a tight regulation of Sjl2p and Sjl3p may also be required during traffic events. Since the deletion of *SJL1* results in an apparent increase in PtdIns(4,5)P_2 levels (Stolz *et al.*, 1998), the 5-Pase activity of Sjl1p may function rather constitutively than regulated during the complex traffic processes.

Irie *et al*. (2005) have described that the 5-Pase activity of mammalian synaptojanin 1 is stimulated by the binding of endophilin to its proline-rich domain. This binding is negatively regulated by the phosphorylation of three tyrosine residues in the proline-rich domain of synaptojanin 1. The deletion of its proline-rich domain demonstrated that the tyrosine phosphorylations are present exclusively in this domain (Irie *et al.*, 2005). In contrast to the

results of their work, phosphorylated tyrosine residues were still detected in Sjl2p lacking the proline-rich domain. Two possible explanations are conceivable: either the proline-rich domain itself is not the target for the yet unidentified tyrosine kinase or the PRD and the enzymatic domains are phosphorylated. Although the conserved family members Sjl2p and Sjl3p are considered to reside at distinct subcellular compartments, the mechanism regulating their activity may be similar.

De-phosphorylation of Sla1p by incubation with CIP revealed that its interaction with Sjl2p is independent from the phosphorylation state of Sla1p. CIP removes phosphates from serine, threonine, as well as tyrosine residues. Regarding the discovered tyrosine phosphorylation of Sjl2p, its binding to Sla1p is likely independent of Sjl2p´s phosphorylation state. Since Sla1p also functions as an endocytic cargo adaptor, it will be exciting to investigate if this interaction links Sjl2p to a receptor tyrosine kinase, as described for mammalian synaptojanin 1 (Irie *et al.*, 2005).

Recent findings indicate that the phosphorylation of a protein can directly regulate the activity of ubiquitin ligases (E3s) (Gao and Karin, 2005). In particular, phosphorylation of some receptor cytoplasmic tails positively regulates ubiquitination at neighbouring lysines and these modifications are required for both constitutive and stimulated receptor internalization (Hicke *et al.*, 1998; Seet *et al.*, 2006). Both mechanisms are not yet well understood and vary largely in their signal cascades. Concomitantly to putative phosphorylation sites, Sjl1p, Sjl2p, and Sjl3p contain two PxY motifs, respectively. PPLP, PPxY, or PxY motifs are known binding motifs for Nedd4/Nedd4-like family (reviewed in Chang *et al.*, 2000; Staub and Rotin, 2006). Consistent with that, Sjl2p and Sjl3p were clearly detected to be ubiquitinated. Again, in spite of the presence of binding motifs no signal was examined for Sjl1p, whereas the negative result for Sla1p (Stamenova *et al.*, 2004) was expected. An earlier study described Sjl1p as an ubiquitinated and membrane-associated ERAD substrate in *npl4ubc7* yeast mutants (Hitchcock *et al.*, 2003). However, under physiological conditions, used in this PhD work, the incubation with an anti-ubiquitin antibody did not reveal a signal at the molecular size of Sjl1p. Nevertheless, Sjl1p is possibly a component of a putative multiprotein complex, including Rsp5p (Wendland *et al.*, 1998). Thus, it cannot be fully excluded that Sjl1p is ubiquitinated in un-detectable minor amounts under physiological conditions or after specific stimuli. Analyses of the precipitates of Sjl3p and Sjl1p with the anti-ubiquitin antibody unveiled additional bands of bigger and smaller molecular sizes, but this multiple band pattern did not appear after incubation with anti-HA or anti-Myc antibodies. Consequently, it is more likely that these bands represent other ubiquitinated

proteins that are associated rather than ubiquitinated intermediates of Sjl3p and Sjl1p. Adding a single ubiquitin moiety results in a size shift of approx. 8 kDa. Since Sjl2p and Sjl3p are high molecular weight proteins of approx. 133 kDa and 124 kDa, it is yet unclear if the detected, prominent ubiquitin band is due to a mono- or multi-ubiquitination. Appearance of a major single band close to the size of Sjl2p or Sjl3p suggests that both exist rather in a low ubiquitination status, whereas intermediates may exist transiently. It is unclear to which domain the ubiquitin moiety(s) is (are) added, since deletion of the proline-rich domain of Sjl2p also results in the appearance of a single ubiquitinated band.

In mammalian and yeast cells there is evidence that members of the Rsp5p/Nedd4 HECT-family ubiquitinate proteins, which usually contain conserved PPLP, PPxY or PxY motifs (Chang *et al.*, 2000; Stamenova *et al.*, 2004). Because Rsp5p is the only member of the Rsp5p/Nedd4 HECT-family in yeast, it is reasonable to assume that it is responsible for the ubiquitination of Sjl2p and Sjl3p. Rsp5p is an essential, peripheral membrane protein believed to regulate the internalization step of endocytosis and the sorting from the TGN to the vacuole by mono- and/or poly-ubiquitination (Dunn *et al.*, 2004; Galan *et al.*, 1996; Helliwell *et al.*, 2001). But not only receptors, channels, and transporters are mono-ubiquitinated as a signal for internalization or intracellular sorting, but also *trans*-acting proteins of the endocytic and biosynthetic/secretory pathways are targets of the ubiquitin ligase Rsp5p (Stamenova *et al.*, 2004; Staub and Rotin, 2006). The role of this modification in proteins of the *trans*-acting signaling network is yet unclear. It is currently unknown if Sjl2p and Sjl3p are ubiqitinated by Rsp5p, because co-immunoprecipitation experiments failed to show a clear interaction. Since only small amounts of ubiquitinated Sjl2p are present in the cell, it might be difficult to detect this transient interaction.

In sum, phosphorylation of Sjl2p and Sjl3p is probably a similar regulation mechanism for their activities, as described for mammalian synaptojanin 1 (Irie *et al.*, 2005). Importantly, ubiquitination of the yeast PI phosphatases Sjl2p and Sjl3p is demonstrated for the first time. Very recent studies recommend a tight regulation of membrane sorting reactions and the transport machinery by ubiquitination (Bonifacino, 2004; Stamenova *et al.*, 2004). Sjl3p represents the first member of the TGN transport machinery that is posttranslationally modified by phosphorylation and ubiquitination. The finding that Sjl2p and Sjl3p are both modified, strongly supports the idea of differences but also similarities in the vesicle formation at the plasma membrane and the TGN (McNiven and Thompson, 2006). The synaptojanin-like family members Sjl2p and Sjl3p likely display differences in their subcellular localization and participate in the vesicle-formation at distinct compartments (this

work and Ha *et al.*, 2001; Ha *et al.*, 2003), but they appear to be structurally similar , exhibit the same enzymatic activities (Guo *et al.*, 1999), and are modified by tyrosine phosphorylation and ubiquitination (this work).

Clearly, the major question is how the phosphorylation and ubiquitination signals of Sjl2p and Sjl3p are propagated and interpreted in the cell to regulate downstream transport events, and which upstream events trigger their generation. Preliminary evidence exists that the level of ubiquitinated Sjl2p increases after triggering α-factor internalization, but this result remains to be verified. Mass spectrometry could be a versatile tool to uncover the phosphorylated as well as the ubiquitinated residues as the first step toward a systematic effort.

4.6 Fusion of the Sjl3p proline-rich domain to the catalytic domains of Sjl2p impairs dramatically the function of Sjl2p

This study provided evidence that the C-terminal, highly variable proline-rich domains of the synaptojanin proteins are implicated in their distinct subcellular localization. In yeast, this idea is further supported by the finding that Sjl1p explicitly interacts with EH-containing proteins, such as Tax4p, via a NPF motif in its PRD (Morales-Johansson *et al.*, 2004), and that Sjl2p exclusively interacts with Sla1p (this work; B. Singer Krüger lab) via the proline-rich domain. Sjl3p has been shown to function in CCV formation from the TGN (Bensen *et al.*, 2000; Ha *et al.*, 2001), but specific interaction partners are unknown. In order to test the idea of the PRD as a specificity factor for its subcellular localization, a chimeric synaptojanin protein was studied. Since it was apparent that Sjl2p and Sjl3p localize to distinct subcellular localizations, the proline-rich domain of Sjl3p was fused to the enzymatic domains of Sjl2p. All performed experiments showed that the chimeric protein is not capable to substitute either Sjl2p or Sjl3p. It was not unexpected that the interaction of Sjl2/3p with Sla1p was abolished, because this interaction takes place only with the PRD of Sjl2p. Co-elution of Sjl2/3p with clathrin-coated vesicles indicated the recruitment to membranes similar to both Sjl2p and Sjl3p, but also Sjl2p-Δprd. But it should be mentioned that it is still possible that also Sjl2/3p is present in a large protein complex or aggregate just co-eluting with clathrin-coated vesicles. Most strikingly the lack of Sjl2/3p to rescue the lethality of *Δsjl1Δsjl2Δsjl3* cells, as Sjl2p does (Singer-Krüger *et al.*, 1998), and to rescue the temperature sensitivity of *Δgga1Δgga2Δsjl3* mutants, as Sjl3p does (Ha *et al.*, 2003), implicates a strong functional impairment of the Sjl2/3p chimeric protein. It is proposed that a SacI domain-defective form of Sjl2p is sufficient for the viability of the *Δsjl1Δsjl2Δsjl3* triple mutant (Stefan *et al.*, 2002).

Notably, a SacI domain-defective form of Sjl2p still contains the proline-rich domain and hence the possibility to interact with other proteins, like Sla1p. Since *Δsjl1Δsjl2Δsjl3* cells are inviable if Sjl2/3p is present as the only synaptojanin phosphatase, it appears as if the 5-Pase domain may not be active in the chimeric protein. The synthetic growth defect of *Δgga1Δgga2Δsjl3* mutants at 37 °C is likely the result of a defect of clathrin-mediated transport between the TGN and endosomal compartments (Ha *et al.*, 2003). Interestingly, although Sjl1p and Sjl2p are still present in this mutant, they apparently are not able to replace Sjl3p, again pointing toward mainly separated functions of the three yeast synaptojanin family members. Results of this PhD thesis show that the chimeric protein Sjl2/3p is not able to rescue the synthetic growth defect as Sjl3p does in the same strain background at 39 °C. It is tempting to speculate that the molecular environment of Sjl2/3p is not suitable to stimulate its 5-Pase activity, although it still has to be shown that it contains this activity *in vitro*. Possible scenarios are that Sjl2/3p is either recruited to the plasma membrane or to the TGN, but does exhibit enzymatic function at none of both compartments due to missing "regulatory factors". In fact, the incapacity to rescue *Δsjl1Δsjl2Δsjl3* cells might be due to wrong molecular environments at both subcellular sites. As a possible explanation, it would be conceivable that the three different domains of each synaptojanin-like family member recruit individual proteins. Moreover, proteins of the proline-rich domain might be linked to the proteins of the PPIP and/or 5-Pase domain. Therefore, the fusion of the proline-rich domain of Sjl3p to the catalytic domains of Sjl2p could prevent the link between the recruited proteins and hence result in significantly decreased or abolished phosphatase activities. Since Sjl2/3p is still tyrosine phosphorylated and ubiquitinated, it can be argued that the chimeric protein is still recognized by the responsible protein kinase and ubiquitin ligase. Thus, it might be possible that the posttranslational modifications are appended by a factor that functions independently from the interconnection of the three domains. Sjl2/3p shows a single band after incubation with the ubiquitin antibody, indicating a low ubiquitination status. A similar result is obtained after incubation with the phosphotyrosine antibody.

In sum, several lines of evidence support the conclusion that Sjl2/3p is a non-functional chimeric protein. If the functionality is abrogated by an inefficient activation of the enzymatic activity, for example because of the wrong molecular environment, or by conformational deficiencies awaits to be elucidated.

4.7 Future projects

Results obtained in this PhD suggest that Sjl2p localizes to primary endocytic vesicles, but the proof for a direct binding is still lacking. It is further highly interesting to reveal the detailed role of Sjl2p during early steps of clathrin-mediated endocytosis.

Results of this work further implicated Sjl3p in clathrin-mediated membrane traffic, likely by an association with TGN-derived clathrin-coated vesicles. PtdIns(4)P is the major phosphoinositide isoform found at the TGN. Therefore, it could be assumed that Sjl3p exhibits a different main function at the TGN than Sjl2p at the plasma membrane. Moreover, since PtdIns(4)P recruits mainly distinct peripheral proteins, the binding partners of Sjl3 might differ. Further binding studies and PI analyses could give insights into the proposed functional differences of the synaptojanin family members *in vivo*.

Data from this study biochemically separate Sjl1p from Sjl2p and Sjl3p. Whereas Sjl2p and Sjl3p are apparently integrated in protein networks, less is known about the cellular role of Sjl1p within the cell and if or how it may support Sjl2p/Sjl3p function.

Both Sjl2p and Sjl3p are targets of (a) tyrosine kinase(s) and most likely the E3 ligase Rsp5p, but the responsible enzymes remain to be elucidated. It is assumed that the phosphorylation of tyrosine residues within Sjl2p and Sjl3p has a regulatory function, as described for mammalian synaptojanin 1. The role of ubiquitin in their function is yet unclear. One key question will concern the regulatory impact of the tyrosine phosphorylation and ubiquitination for Sjl2p and Sjl3p function. Steps to answer this question will comprise for example: (i) to discover the modified amino acids by mass spectrometry, (ii) to determine the enzymatic activities of the modified synaptojanin-like proteins by phosphatase assays, or (iii) to examine the stimuli that result in the attachment of the phosphates or ubiquitin moieties. Analysis of the additional bands in the precipitates of Sjl1p and Sjl3p that appeared after detection with an anti-ubiquitin antibody may integrate these proteins in their functional networks. Maybe these analyses will explain why the precipitate of Sjl2p did not reveal additional bands (see section 3.5.2).

The interaction of the proline-rich domain of Sjl2p, but not of Sjl3p and Sjl1p, with the endocytic component Sla1p demonstrates that indeed the proline-rich domains of the three synaptojanin-like family members affect specific interaction partners. To support this conclusion, GST-pulldowns could be performed using the proline-rich domains of Sjl1p and Sjl3p to examine for a possible binding to interaction partners of Sjl2p. Additionally, new binding partners for Sjl3p and Sjl1p could be discovered by mass spectrometry after immunoprecipitation or by tagging proposed interaction partners basing on the genetic data of

other laboratories. It is also of interest to reveal specific binding partners of the Sac1-like domains and the 5-Pase domains of all three family members. Altogether, these binding studies may then explain the molecular basis for the missing activity of the chimeric protein Sjl2/3p. Whether *in vivo* the chimeric protein Sjl2/3p causes elevated PtdIns(4,5)P_2 levels because of inactive catalytic domains, could be examined by PI analysis and phosphatase activity assays.

Literature

Aguilar, R.C., Watson, H.A. and Wendland, B. (2003) The yeast Epsin Ent1 is recruited to membranes through multiple independent interactions. *J Biol Chem*, **278**, 10737-10743.

Audhya, A., Foti, M. and Emr, S.D. (2000) Distinct roles for the yeast phosphatidylinositol 4-kinases, Stt4p and Pik1p, in secretion, cell growth, and organelle membrane dynamics. *Mol Biol Cell*, **11**, 2673-2689.

Ayscough, K.R. (2000) Endocytosis and the development of cell polarity in yeast require a dynamic F-actin cytoskeleton. *Curr Biol*, **10**, 1587-1590.

Ayscough, K.R., Eby, J.J., Lila, T., Dewar, H., Kozminski, K.G. and Drubin, D.G. (1999) Sla1p is a functionally modular component of the yeast cortical actin cytoskeleton required for correct localization of both Rho1p-GTPase and Sla2p, a protein with talin homology. *Mol Biol Cell*, **10**, 1061-1075.

Ayscough, K.R., Stryker, J., Pokala, N., Sanders, M., Crews, P. and Drubin, D.G. (1997) High rates of actin filament turnover in budding yeast and roles for actin in establishment and maintenance of cell polarity revealed using the actin inhibitor latrunculin-A. *J Cell Biol*, **137**, 399-416.

Balguerie, A., Sivadon, P., Bonneu, M. and Aigle, M. (1999) Rvs167p, the budding yeast homolog of amphiphysin, colocalizes with actin patches. *J Cell Sci*, **112 (Pt 15)**, 2529-2537.

Barriere, H., Nemes, C., Lechardeur, D., Khan-Mohammad, M., Fruh, K. and Lukacs, G.L. (2006) Molecular basis of oligoubiquitin-dependent internalization of membrane proteins in Mammalian cells. *Traffic*, **7**, 282-297.

Bensen, E.S., Costaguta, G. and Payne, G.S. (2000) Synthetic genetic interactions with temperature-sensitive clathrin in Saccharomyces cerevisiae. Roles for synaptojanin-like Inp53p and dynamin-related Vps1p in clathrin-dependent protein sorting at the trans-Golgi network. *Genetics*, **154**, 83-97.

Black, M.W. and Pelham, H.R. (2000) A selective transport route from Golgi to late endosomes that requires the yeast GGA proteins. *J Cell Biol*, **151**, 587-600.

Bonifacino, J.S. (2004) The GGA proteins: adaptors on the move. *Nat Rev Mol Cell Biol*, **5**, 23-32.

Bonifacino, J.S. and Rojas, R. (2006) Retrograde transport from endosomes to the trans-Golgi network. *Nat Rev Mol Cell Biol*, **7**, 568-579.

Bonifacino, J.S. and Traub, L.M. (2003) Signals for sorting of transmembrane proteins to endosomes and lysosomes. *Annu Rev Biochem*, **72**, 395-447.

Böttcher, C., Wicky, S., Schwarz, H. and Singer-Krüger, B. (2006) Sjl2p is specifically involved in early steps of endocytosis intimately linked to actin dynamics via the Ark1p/Prk1p kinases. *FEBS Lett*, **580**, 633-641.

Bradford, M.M. (1976) A rapid and sensitive method for the quantitation of microgram quantities of protein utilizing the principle of protein-dye binding. *Anal Biochem*, **72**, 248-254.

Carreno, S., Engqvist-Goldstein, A.E., Zhang, C.X., McDonald, K.L. and Drubin, D.G. (2004) Actin dynamics coupled to clathrin-coated vesicle formation at the trans-Golgi network. *J Cell Biol*, **165**, 781-788.

Castellanos, R.M. and Mazon, M.J. (1985) Identification of phosphotyrosine in yeast proteins and of a protein tyrosine kinase associated with the plasma membrane. *J Biol Chem*, **260**, 8240-8242.

Cereghino, J.L., Marcusson, E.G. and Emr, S.D. (1995) The cytoplasmic tail domain of the vacuolar protein sorting receptor Vps10p and a subset of VPS gene products regulate receptor stability, function, and localization. *Mol Biol Cell*, **6**, 1089-1102.

Chang, A., Cheang, S., Espanel, X. and Sudol, M. (2000) Rsp5 WW domains interact directly with the carboxyl-terminal domain of RNA polymerase II. *J Biol Chem*, **275**, 20562-20571.

Chen, L. and Davis, N.G. (2000) Recycling of the yeast a-factor receptor. *J Cell Biol*, **151**, 731-738.

Chu, D.S., Pishvaee, B. and Payne, G.S. (1999) A modulatory role for clathrin light chain phosphorylation in Golgi membrane protein localization during vegetative growth and during the mating response of Saccharomyces cerevisiae. *Mol Biol Cell*, **10**, 713-726.

Chvatchko, Y., Howald, I. and Riezman, H. (1986) Two yeast mutants defective in endocytosis are defective in pheromone response. *Cell*, **46**, 355-364.

Confalonieri, S., Salcini, A.E., Puri, C., Tacchetti, C. and Di Fiore, P.P. (2000) Tyrosine phosphorylation of Eps15 is required for ligand-regulated, but not constitutive, endocytosis. *J Cell Biol*, **150**, 905-912.

Cope, M.J., Yang, S., Shang, C. and Drubin, D.G. (1999) Novel protein kinases Ark1p and Prk1p associate with and regulate the cortical actin cytoskeleton in budding yeast. *J Cell Biol*, **144**, 1203-1218.

Costaguta, G., Stefan, C.J., Bensen, E.S., Emr, S.D. and Payne, G.S. (2001) Yeast Gga coat proteins function with clathrin in Golgi to endosome transport. *Mol Biol Cell*, **12**, 1885-1896.

Cousin, M.A., Tan, T.C. and Robinson, P.J. (2001) Protein phosphorylation is required for endocytosis in nerve terminals: potential role for the dephosphins dynamin I and synaptojanin, but not AP180 or amphiphysin. *J Neurochem*, **76**, 105-116.

Cremona, O. and De Camilli, P. (2001) Phosphoinositides in membrane traffic at the synapse. *J Cell Sci*, **114**, 1041-1052.

Cremona, O., Di Paolo, G., Wenk, M.R., Luthi, A., Kim, W.T., Takei, K., Daniell, L., Nemoto, Y., Shears, S.B., Flavell, R.A., McCormick, D.A. and De Camilli, P. (1999) Essential role of phosphoinositide metabolism in synaptic vesicle recycling. *Cell*, **99**, 179-188.

Dell'Angelica, E.C., Klumperman, J., Stoorvogel, W. and Bonifacino, J.S. (1998) Association of the AP-3 adaptor complex with clathrin. *Science*, **280**, 431-434.

Deloche, O., Yeung, B.G., Payne, G.S. and Schekman, R. (2001) Vps10p transport from the trans-Golgi network to the endosome is mediated by clathrin-coated vesicles. *Mol Biol Cell*, **12**, 475-485.

Dhavan, R. and Tsai, L.H. (2001) A decade of CDK5. *Nat Rev Mol Cell Biol*, **2**, 749-759.

D'Hondt, K., Heese-Peck, A. and Riezman, H. (2000) Protein and lipid requirements for endocytosis. *Annu Rev Genet*, **34**, 255-295.

Dickman, D.K., Lu, Z., Meinertzhagen, I.A. and Schwarz, T.L. (2006) Altered synaptic development and active zone spacing in endocytosis mutants. *Curr Biol*, **16**, 591-598.

Drake, M.T. and Traub, L.M. (2001) Interaction of two structurally distinct sequence types with the clathrin terminal domain beta-propeller. *J Biol Chem*, **276**, 28700-28709.

Duncan, M.C., Cope, M.J., Goode, B.L., Wendland, B. and Drubin, D.G. (2001) Yeast Eps15-like endocytic protein, Pan1p, activates the Arp2/3 complex. *Nat Cell Biol*, **3**, 687-690.

Dunn, R., Klos, D.A., Adler, A.S. and Hicke, L. (2004) The C2 domain of the Rsp5 ubiquitin ligase binds membrane phosphoinositides and directs ubiquitination of endosomal cargo. *J Cell Biol*, **165**, 135-144.

Engqvist-Goldstein, A.E. and Drubin, D.G. (2003) Actin assembly and endocytosis: from yeast to mammals. *Annu Rev Cell Dev Biol*, **19**, 287-332.

Engqvist-Goldstein, A.E., Kessels, M.M., Chopra, V.S., Hayden, M.R. and Drubin, D.G. (1999) An actin-binding protein of the Sla2/Huntingtin interacting protein 1 family is a novel component of clathrin-coated pits and vesicles. *J Cell Biol*, **147**, 1503-1518.

Fazi, B., Cope, M.J., Douangamath, A., Ferracuti, S., Schirwitz, K., Zucconi, A., Drubin, D.G., Wilmanns, M., Cesareni, G. and Castagnoli, L. (2002) Unusual binding properties of the SH3 domain of the yeast actin-binding protein Abp1: structural and functional analysis. *J Biol Chem*, **277**, 5290-5298.

Ferro-Novick, S. and Jahn, R. (1994) Vesicle fusion from yeast to man. *Nature*, **370**, 191-193.

Ficarro, S.B., McCleland, M.L., Stukenberg, P.T., Burke, D.J., Ross, M.M., Shabanowitz, J., Hunt, D.F. and White, F.M. (2002) Phosphoproteome analysis by mass spectrometry and its application to Saccharomyces cerevisiae. *Nat Biotechnol*, **20**, 301-305.

Fields, S. and Song, O. (1989) A novel genetic system to detect protein-protein interactions. *Nature*, **340**, 245-246.

Flanagan, C.A. and Thorner, J. (1992) Purification and characterization of a soluble phosphatidylinositol 4-kinase from the yeast Saccharomyces cerevisiae. *J Biol Chem*, **267**, 24117-24125.

Foti, M., Audhya, A. and Emr, S.D. (2001) Sac1 lipid phosphatase and Stt4 phosphatidylinositol 4-kinase regulate a pool of phosphatidylinositol 4-phosphate that functions in the control of the actin cytoskeleton and vacuole morphology. *Mol Biol Cell*, **12**, 2396-2411.

Friesen, H., Murphy, K., Breitkreutz, A., Tyers, M. and Andrews, B. (2003) Regulation of the yeast amphiphysin homologue Rvs167p by phosphorylation. *Mol Biol Cell*, **14**, 3027-3040.

Gad, H., Ringstad, N., Low, P., Kjaerulff, O., Gustafsson, J., Wenk, M., Di Paolo, G., Nemoto, Y., Crun, J., Ellisman, M.H., De Camilli, P., Shupliakov, O. and Brodin, L. (2000) Fission and uncoating of synaptic clathrin-coated vesicles are perturbed by disruption of interactions with the SH3 domain of endophilin. *Neuron*, **27**, 301-312.

Galan, J.M., Moreau, V., Andre, B., Volland, C. and Haguenauer-Tsapis, R. (1996) Ubiquitination mediated by the Npi1p/Rsp5p ubiquitin-protein ligase is required for endocytosis of the yeast uracil permease. *J Biol Chem*, **271**, 10946-10952.

Gao, M. and Karin, M. (2005) Regulating the regulators: control of protein ubiquitination and ubiquitin-like modifications by extracellular stimuli. *Mol Cell*, **19**, 581-593.

Gary, J.D., Wurmser, A.E., Bonangelino, C.J., Weisman, L.S. and Emr, S.D. (1998) Fab1p is essential for PtdIns(3)P 5-kinase activity and the maintenance of vacuolar size and membrane homeostasis. *J Cell Biol*, **143**, 65-79.

Gavin, A.C., Aloy, P., Grandi, P., Krause, R., Boesche, M., Marzioch, M., Rau, C., Jensen, L.J., Bastuck, S., Dumpelfeld, B., Edelmann, A., Heurtier, M.A., Hoffman, V., Hoefert, C., Klein, K., Hudak, M., Michon, A.M., Schelder, M., Schirle, M., Remor, M., Rudi, T., Hooper, S., Bauer, A., Bouwmeester, T., Casari, G., Drewes, G., Neubauer, G., Rick, J.M., Kuster, B., Bork, P., Russell, R.B. and Superti-Furga, G. (2006) Proteome survey reveals modularity of the yeast cell machinery. *Nature*, **440**, 631-636.

Geli, M.I. and Riezman, H. (1996) Role of type I myosins in receptor-mediated endocytosis in yeast. *Science*, **272**, 533-535.

Girault, J.A., Chamak, B., Bertuzzi, G., Tixier, H., Wang, J.K., Pang, D.T. and Greengard, P. (1992) Protein phosphotyrosine in mouse brain: developmental changes and regulation by epidermal growth factor, type I insulin-like growth factor, and insulin. *J Neurochem*, **58**, 518-528.

Goffeau, A., Barrell, B.G., Bussey, H., Davis, R.W., Dujon, B., Feldmann, H., Galibert, F., Hoheisel, J.D., Jacq, C., Johnston, M., Louis, E.J., Mewes, H.W., Murakami, Y.,

Philippsen, P., Tettelin, H. and Oliver, S.G. (1996) Life with 6000 genes. *Science*, **274**, 546, 563-547.
Goode, B.L. (2002) Purification of yeast actin and actin-associated proteins. *Methods Enzymol*, **351**, 433-441.
Goode, B.L., Rodal, A.A., Barnes, G. and Drubin, D.G. (2001) Activation of the Arp2/3 complex by the actin filament binding protein Abp1p. *J Cell Biol*, **153**, 627-634.
Gourlay, C.W., Dewar, H., Warren, D.T., Costa, R., Satish, N. and Ayscough, K.R. (2003) An interaction between Sla1p and Sla2p plays a role in regulating actin dynamics and endocytosis in budding yeast. *J Cell Sci*, **116**, 2551-2564.
Guo, S., Stolz, L.E., Lemrow, S.M. and York, J.D. (1999) SAC1-like domains of yeast SAC1, INP52, and INP53 and of human synaptojanin encode polyphosphoinositide phosphatases. *J Biol Chem*, **274**, 12990-12995.
Ha, S.A., Bunch, J.T., Hama, H., DeWald, D.B. and Nothwehr, S.F. (2001) A novel mechanism for localizing membrane proteins to yeast trans-Golgi network requires function of synaptojanin-like protein. *Mol Biol Cell*, **12**, 3175-3190.
Ha, S.A., Torabinejad, J., DeWald, D.B., Wenk, M.R., Lucast, L., De Camilli, P., Newitt, R.A., Aebersold, R. and Nothwehr, S.F. (2003) The synaptojanin-like protein Inp53/Sjl3 functions with clathrin in a yeast TGN-to-endosome pathway distinct from the GGA protein-dependent pathway. *Mol Biol Cell*, **14**, 1319-1333.
Haffner, C., Takei, K., Chen, H., Ringstad, N., Hudson, A., Butler, M.H., Salcini, A.E., Di Fiore, P.P. and De Camilli, P. (1997) Synaptojanin 1: localization on coated endocytic intermediates in nerve terminals and interaction of its 170 kDa isoform with Eps15. *FEBS Lett*, **419**, 175-180.
Haglund, K. and Dikic, I. (2005) Ubiquitylation and cell signaling. *Embo J*, **24**, 3353-3359.
Harris, T.W., Hartwieg, E., Horvitz, H.R. and Jorgensen, E.M. (2000) Mutations in synaptojanin disrupt synaptic vesicle recycling. *J Cell Biol*, **150**, 589-600.
Heese-Peck, A., Pichler, H., Zanolari, B., Watanabe, R., Daum, G. and Riezman, H. (2002) Multiple functions of sterols in yeast endocytosis. *Mol Biol Cell*, **13**, 2664-2680.
Helliwell, S.B., Losko, S. and Kaiser, C.A. (2001) Components of a ubiquitin ligase complex specify polyubiquitination and intracellular trafficking of the general amino acid permease. *J Cell Biol*, **153**, 649-662.
Henry, K.R., D'Hondt, K., Chang, J., Newpher, T., Huang, K., Hudson, R.T., Riezman, H. and Lemmon, S.K. (2002) Scd5p and clathrin function are important for cortical actin organization, endocytosis, and localization of sla2p in yeast. *Mol Biol Cell*, **13**, 2607-2625.
Hicke, L. (2001a) A new ticket for entry into budding vesicles-ubiquitin. *Cell*, **106**, 527-530.
Hicke, L. (2001b) Protein regulation by monoubiquitin. *Nat Rev Mol Cell Biol*, **2**, 195-201.
Hicke, L. and Riezman, H. (1996) Ubiquitination of a yeast plasma membrane receptor signals its ligand-stimulated endocytosis. *Cell*, **84**, 277-287.
Hicke, L., Schubert, H.L. and Hill, C.P. (2005) Ubiquitin-binding domains. *Nat Rev Mol Cell Biol*, **6**, 610-621.
Hicke, L., Zanolari, B., Pypaert, M., Rohrer, J. and Riezman, H. (1997) Transport through the yeast endocytic pathway occurs through morphologically distinct compartments and requires an active secretory pathway and Sec18p/N-ethylmaleimide-sensitive fusion protein. *Mol Biol Cell*, **8**, 13-31.
Hicke, L., Zanolari, B. and Riezman, H. (1998) Cytoplasmic tail phosphorylation of the alpha-factor receptor is required for its ubiquitination and internalization. *J Cell Biol*, **141**, 349-358.
Hitchcock, A.L., Auld, K., Gygi, S.P. and Silver, P.A. (2003) A subset of membrane-associated proteins is ubiquitinated in response to mutations in the endoplasmic reticulum degradation machinery. *Proc Natl Acad Sci U S A*, **100**, 12735-12740.

Hochstrasser, M. (2006) Lingering mysteries of ubiquitin-chain assembly. *Cell*, **124**, 27-34.
Holler, D. and Dikic, I. (2004) Receptor endocytosis via ubiquitin-dependent and -independent pathways. *Biochem Pharmacol*, **67**, 1013-1017.
Holtzman, D.A., Yang, S. and Drubin, D.G. (1993) Synthetic-lethal interactions identify two novel genes, SLA1 and SLA2, that control membrane cytoskeleton assembly in Saccharomyces cerevisiae. *J Cell Biol*, **122**, 635-644.
Hopper, N.A. and O'Connor, V. (2005) Ephrin tempers two-faced synaptojanin 1. *Nat Cell Biol*, **7**, 454-456.
Howard, J.P., Hutton, J.L., Olson, J.M. and Payne, G.S. (2002) Sla1p serves as the targeting signal recognition factor for NPFX(1,2)D-mediated endocytosis. *J Cell Biol*, **157**, 315-326.
Huckaba, T.M., Gay, A.C., Pantalena, L.F., Yang, H.C. and Pon, L.A. (2004) Live cell imaging of the assembly, disassembly, and actin cable-dependent movement of endosomes and actin patches in the budding yeast, Saccharomyces cerevisiae. *J Cell Biol*, **167**, 519-530.
Hughes, W.E., Woscholski, R., Cooke, F.T., Patrick, R.S., Dove, S.K., McDonald, N.Q. and Parker, P.J. (2000) SAC1 encodes a regulated lipid phosphoinositide phosphatase, defects in which can be suppressed by the homologous Inp52p and Inp53p phosphatases. *J Biol Chem*, **275**, 801-808.
Hunter, T. (2000) Signaling--2000 and beyond. *Cell*, **100**, 113-127.
Hurley, J.H. and Meyer, T. (2001) Subcellular targeting by membrane lipids. *Curr Opin Cell Biol*, **13**, 146-152.
Irie, F., Okuno, M., Pasquale, E.B. and Yamaguchi, Y. (2005) EphrinB-EphB signalling regulates clathrin-mediated endocytosis through tyrosine phosphorylation of synaptojanin 1. *Nat Cell Biol*, **7**, 501-509.
Ito, H., Fukuda, Y., Murata, K. and Kimura, A. (1983) Transformation of intact yeast cells treated with alkali cations. *J Bacteriol*, **153**, 163-168.
Johnston, H.D., Foote, C., Santeford, A. and Nothwehr, S.F. (2005) Golgi-to-late endosome trafficking of the yeast pheromone processing enzyme Ste13p is regulated by a phosphorylation site in its cytosolic domain. *Mol Biol Cell*, **16**, 1456-1468.
Kaksonen, M., Sun, Y. and Drubin, D.G. (2003) A pathway for association of receptors, adaptors, and actin during endocytic internalization. *Cell*, **115**, 475-487.
Kaksonen, M., Toret, C.P. and Drubin, D.G. (2005) A modular design for the clathrin- and actin-mediated endocytosis machinery. *Cell*, **123**, 305-320.
Kaksonen, M., Toret, C.P. and Drubin, D.G. (2006) Harnessing actin dynamics for clathrin-mediated endocytosis. *Nat Rev Mol Cell Biol*, **7**, 404-414.
Kaminska, J., Gajewska, B., Hopper, A.K. and Zoladek, T. (2002) Rsp5p, a new link between the actin cytoskeleton and endocytosis in the yeast Saccharomyces cerevisiae. *Mol Cell Biol*, **22**, 6946-6948.
Kaminska, J., Wysocka-Kapcinska, M., Smaczynska-de Rooij, I., Rytka, J. and Zoladek, T. (2005) Pan1p, an actin cytoskeleton-associated protein, is required for growth of yeast on oleate medium. *Exp Cell Res*, **310**, 482-492.
Karpova, T.S., Tatchell, K. and Cooper, J.A. (1995) Actin filaments in yeast are unstable in the absence of capping protein or fimbrin. *J Cell Biol*, **131**, 1483-1493.
Katzmann, D.J., Odorizzi, G. and Emr, S.D. (2002) Receptor downregulation and multivesicular-body sorting. *Nat Rev Mol Cell Biol*, **3**, 893-905.
Katzmann, D.J., Stefan, C.J., Babst, M. and Emr, S.D. (2003) Vps27 recruits ESCRT machinery to endosomes during MVB sorting. *J Cell Biol*, **162**, 413-423.
Kim, W.T., Chang, S., Daniell, L., Cremona, O., Di Paolo, G. and De Camilli, P. (2002) Delayed reentry of recycling vesicles into the fusion-competent synaptic vesicle pool in synaptojanin 1 knockout mice. *Proc Natl Acad Sci U S A*, **99**, 17143-17148.

Kirchhausen, T. (1999) Adaptors for clathrin-mediated traffic. *Annu Rev Cell Dev Biol*, **15**, 705-732.
Kirchhausen, T. (2000) Clathrin. *Annu Rev Biochem*, **69**, 699-727.
Kirchhausen, T. and Harrison, S.C. (1981) Protein organization in clathrin trimers. *Cell*, **23**, 755-761.
Klionsky, D.J., Herman, P.K. and Emr, S.D. (1990) The fungal vacuole: composition, function, and biogenesis. *Microbiol Rev*, **54**, 266-292.
Kölling, R. and Hollenberg, C.P. (1994) The ABC-transporter Ste6 accumulates in the plasma membrane in a ubiquitinated form in endocytosis mutants. *Embo J*, **13**, 3261-3271.
Kolodziej, S.J., Penczek, P.A., Schroeter, J.P. and Stoops, J.K. (1996) Structure-function relationships of the Saccharomyces cerevisiae fatty acid synthase. Three-dimensional structure. *J Biol Chem*, **271**, 28422-28429.
Kübler, E. and Riezman, H. (1993) Actin and fimbrin are required for the internalization step of endocytosis in yeast. *Embo J*, **12**, 2855-2862.
Laemmli, U.K. (1970) Cleavage of structural proteins during the assembly of the head of bacteriophage T4. *Nature*, **227**, 680-685.
Lafourcade, C., Galan, J.M., Gloor, Y., Haguenauer-Tsapis, R. and Peter, M. (2004) The GTPase-activating enzyme Gyp1p is required for recycling of internalized membrane material by inactivation of the Rab/Ypt GTPase Ypt1p. *Mol Cell Biol*, **24**, 3815-3826.
Lappalainen, P. and Drubin, D.G. (1997) Cofilin promotes rapid actin filament turnover in vivo. *Nature*, **388**, 78-82.
Lee, S.Y., Wenk, M.R., Kim, Y., Nairn, A.C. and De Camilli, P. (2004) Regulation of synaptojanin 1 by cyclin-dependent kinase 5 at synapses. *Proc Natl Acad Sci U S A*, **101**, 546-551.
Lemmon, M.A. (2003) Phosphoinositide recognition domains. *Traffic*, **4**, 201-213.
Lemmon, S.K. and Jones, E.W. (1987) Clathrin requirement for normal growth of yeast. *Science*, **238**, 504-509.
Li, R. (1997) Bee1, a yeast protein with homology to Wiscott-Aldrich syndrome protein, is critical for the assembly of cortical actin cytoskeleton. *J Cell Biol*, **136**, 649-658.
Liu, J., Kaksonen, M., Drubin, D.G. and Oster, G. (2006) Endocytic vesicle scission by lipid phase boundary forces. *Proc Natl Acad Sci U S A*, **103**, 10277-10282.
Longtine, M.S., McKenzie III, A., Demarini, D.J., Shah, N.G., Wach, A., Brachat, A., Philippsen, P. and Pringle, J.R. (1998) Additional modules for versatile and economical PCR-based gene deletion and modification in Saccharomyces cerevisiae. *Yeast*, **14**, 953-961.
Maldonado-Baez, L. and Wendland, B. (2006) Endocytic adaptors: recruiters, coordinators and regulators. *Trends Cell Biol*, **16**, 505-513.
Marsh, M. (2001) *Clathrin-coated vesicles and receptor-mediated endocytosis.* Nature Publishing group.
Martin, T.F. (2001) PI(4,5)P(2) regulation of surface membrane traffic. *Curr Opin Cell Biol*, **13**, 493-499.
Maudsley, S., Pierce, K.L., Zamah, A.M., Miller, W.E., Ahn, S., Daaka, Y., Lefkowitz, R.J. and Luttrell, L.M. (2000) The beta(2)-adrenergic receptor mediates extracellular signal-regulated kinase activation via assembly of a multi-receptor complex with the epidermal growth factor receptor. *J Biol Chem*, **275**, 9572-9580.
McNiven, M.A. and Thompson, H.M. (2006) Vesicle formation at the plasma membrane and trans-Golgi network: the same but different. *Science*, **313**, 1591-1594.
McPherson, P.S., Garcia, E.P., Slepnev, V.I., David, C., Zhang, X., Grabs, D., Sossin, W.S., Bauerfeind, R., Nemoto, Y. and De Camilli, P. (1996) A presynaptic inositol-5-phosphatase. *Nature*, **379**, 353-357.

Mell, J.C. and Burgess, S.M. (2002) *Yeast as a model genetic organism*. Macmillan Publishers Ltd.

Merrifield, C.J., Perrais, D. and Zenisek, D. (2005) Coupling between clathrin-coated-pit invagination, cortactin recruitment, and membrane scission observed in live cells. *Cell*, **121**, 593-606.

Morales-Johansson, H., Jenoe, P., Cooke, F.T. and Hall, M.N. (2004) Negative regulation of phosphatidylinositol 4,5-bisphosphate levels by the INP51-associated proteins TAX4 and IRS4. *J Biol Chem*, **279**, 39604-39610.

Mueller, S.C. and Branton, D. (1984) Identification of coated vesicles in Saccharomyces cerevisiae. *J Cell Biol*, **98**, 341-346.

Mulholland, J., Preuss, D., Moon, A., Wong, A., Drubin, D. and Botstein, D. (1994) Ultrastructure of the yeast actin cytoskeleton and its association with the plasma membrane. *J Cell Biol*, **125**, 381-391.

Munn, A.L., Heese-Peck, A., Stevenson, B.J., Pichler, H. and Riezman, H. (1999) Specific sterols required for the internalization step of endocytosis in yeast. *Mol Biol Cell*, **10**, 3943-3957.

Naqvi, S.N., Zahn, R., Mitchell, D.A., Stevenson, B.J. and Munn, A.L. (1998) The WASp homologue Las17p functions with the WIP homologue End5p/verprolin and is essential for endocytosis in yeast. *Curr Biol*, **8**, 959-962.

Newpher, T.M. and Lemmon, S.K. (2006) Clathrin is important for normal actin dynamics and progression of Sla2p-containing patches during endocytosis in yeast. *Traffic*, **7**, 574-588.

Newpher, T.M., Smith, R.P., Lemmon, V. and Lemmon, S.K. (2005) In vivo dynamics of clathrin and its adaptor-dependent recruitment to the actin-based endocytic machinery in yeast. *Dev Cell*, **9**, 87-98.

Novick, P., Field, C. and Schekman, R. (1980) Identification of 23 complementation groups required for post-translational events in the yeast secretory pathway. *Cell*, **21**, 205-215.

Odorizzi, G., Babst, M. and Emr, S.D. (2000) Phosphoinositide signaling and the regulation of membrane trafficking in yeast. *Trends Biochem Sci*, **25**, 229-235.

Ohno, H., Stewart, J., Fournier, M.C., Bosshart, H., Rhee, I., Miyatake, S., Saito, T., Gallusser, A., Kirchhausen, T. and Bonifacino, J.S. (1995) Interaction of tyrosine-based sorting signals with clathrin-associated proteins. *Science*, **269**, 1872-1875.

Ooms, L.M., McColl, B.K., Wiradjaja, F., Wijayaratnam, A.P., Gleeson, P., Gething, M.J., Sambrook, J. and Mitchell, C.A. (2000) The yeast inositol polyphosphate 5-phosphatases inp52p and inp53p translocate to actin patches following hyperosmotic stress: mechanism for regulating phosphatidylinositol 4,5-bisphosphate at plasma membrane invaginations. *Mol Cell Biol*, **20**, 9376-9390.

Opekarova, M., Malinska, K., Novakova, L. and Tanner, W. (2005) Differential effect of phosphatidylethanolamine depletion on raft proteins: further evidence for diversity of rafts in Saccharomyces cerevisiae. *Biochim Biophys Acta*, **1711**, 87-95.

Pang, D.T., Wang, J.K., Valtorta, F., Benfenati, F. and Greengard, P. (1988) Protein tyrosine phosphorylation in synaptic vesicles. *Proc Natl Acad Sci U S A*, **85**, 762-766.

Payne, G.S., Baker, D., van Tuinen, E. and Schekman, R. (1988) Protein transport to the vacuole and receptor-mediated endocytosis by clathrin heavy chain-deficient yeast. *J Cell Biol*, **106**, 1453-1461.

Payne, G.S., Hasson, T.B., Hasson, M.S. and Schekman, R. (1987) Genetic and biochemical characterization of clathrin-deficient Saccharomyces cerevisiae. *Mol Cell Biol*, **7**, 3888-3898.

Pearse, B.M. (1975) Coated vesicles from pig brain: purification and biochemical characterization. *J Mol Biol*, **97**, 93-98.

Peter, B.J., Kent, H.M., Mills, I.G., Vallis, Y., Butler, P.J., Evans, P.R. and McMahon, H.T. (2004) BAR domains as sensors of membrane curvature: the amphiphysin BAR structure. *Science*, **303**, 495-499.

Pichler, H. and Riezman, H. (2004) Where sterols are required for endocytosis. *Biochim Biophys Acta*, **1666**, 51-61.

Polo, S., Confalonieri, S., Salcini, A.E. and Di Fiore, P.P. (2003) EH and UIM: endocytosis and more. *Sci STKE*, **2003**, re17.

Prescianotto-Baschong, C. and Riezman, H. (2002) Ordering of compartments in the yeast endocytic pathway. *Traffic*, **3**, 37-49.

Ptacek, J., Devgan, G., Michaud, G., Zhu, H., Zhu, X., Fasolo, J., Guo, H., Jona, G., Breitkreutz, A., Sopko, R., McCartney, R.R., Schmidt, M.C., Rachidi, N., Lee, S.J., Mah, A.S., Meng, L., Stark, M.J., Stern, D.F., De Virgilio, C., Tyers, M., Andrews, B., Gerstein, M., Schweitzer, B., Predki, P.F. and Snyder, M. (2005) Global analysis of protein phosphorylation in yeast. *Nature*, **438**, 679-684.

Quintero-Monzon, O., Rodal, A.A., Strokopytov, B., Almo, S.C. and Goode, B.L. (2005) Structural and functional dissection of the Abp1 ADFH actin-binding domain reveals versatile in vivo adapter functions. *Mol Biol Cell*, **16**, 3128-3139.

Regelmann, J., Schule, T., Josupeit, F.S., Horak, J., Rose, M., Entian, K.D., Thumm, M. and Wolf, D.H. (2003) Catabolite degradation of fructose-1,6-bisphosphatase in the yeast Saccharomyces cerevisiae: a genome-wide screen identifies eight novel GID genes and indicates the existence of two degradation pathways. *Mol Biol Cell*, **14**, 1652-1663.

Riezman, H. (1985) Endocytosis in yeast: several of the yeast secretory mutants are defective in endocytosis. *Cell*, **40**, 1001-1009.

Robinson, M.S. (2004) Adaptable adaptors for coated vesicles. *Trends Cell Biol*, **14**, 167-174.

Rodal, A.A., Manning, A.L., Goode, B.L. and Drubin, D.G. (2003) Negative regulation of yeast WASp by two SH3 domain-containing proteins. *Curr Biol*, **13**, 1000-1008.

Roth, M.G. (2004) Phosphoinositides in constitutive membrane traffic. *Physiol Rev*, **84**, 699-730.

Roth, T.F. and Porter, K.R. (1964) Yolk Protein Uptake in the Oocyte of the Mosquito Aedes Aegypti. L. *J Cell Biol*, **20**, 313-332.

Rotin, D., Staub, O. and Haguenauer-Tsapis, R. (2000) Ubiquitination and endocytosis of plasma membrane proteins: role of Nedd4/Rsp5p family of ubiquitin-protein ligases. *J Membr Biol*, **176**, 1-17.

Rubino, M., Miaczynska, M., Lippe, R. and Zerial, M. (2000) Selective membrane recruitment of EEA1 suggests a role in directional transport of clathrin-coated vesicles to early endosomes. *J Biol Chem*, **275**, 3745-3748.

Sambrook, J., Fritsch, E.F. and Manniatis, T. (1989) *Molecular Cloning-A laboratory Manual.* Cold Spring Harbor Laboratory Press.

Schekman, R. and Novick, P. (2004) 23 genes, 23 years later. *Cell*, **116**, S13-15, 11 p following S19.

Schmid, S.L. and Carter, L.L. (1990) ATP is required for receptor-mediated endocytosis in intact cells. *J Cell Biol*, **111**, 2307-2318.

Scott, P.M., Bilodeau, P.S., Zhdankina, O., Winistorfer, S.C., Hauglund, M.J., Allaman, M.M., Kearney, W.R., Robertson, A.D., Boman, A.L. and Piper, R.C. (2004) GGA proteins bind ubiquitin to facilitate sorting at the trans-Golgi network. *Nat Cell Biol*, **6**, 252-259.

Seeger, M. and Payne, G.S. (1992) A role for clathrin in the sorting of vacuolar proteins in the Golgi complex of yeast. *Embo J*, **11**, 2811-2818.

Seet, B.T., Dikic, I., Zhou, M.M. and Pawson, T. (2006) Reading protein modifications with interaction domains. *Nat Rev Mol Cell Biol*, **7**, 473-483.

Sekiya-Kawasaki, M., Groen, A.C., Cope, M.J., Kaksonen, M., Watson, H.A., Zhang, C., Shokat, K.M., Wendland, B., McDonald, K.L., McCaffery, J.M. and Drubin, D.G. (2003) Dynamic phosphoregulation of the cortical actin cytoskeleton and endocytic machinery revealed by real-time chemical genetic analysis. *J Cell Biol*, **162**, 765-772.

Shih, S.C., Katzmann, D.J., Schnell, J.D., Sutanto, M., Emr, S.D. and Hicke, L. (2002) Epsins and Vps27p/Hrs contain ubiquitin-binding domains that function in receptor endocytosis. *Nat Cell Biol*, **4**, 389-393.

Sigismund, S., Polo, S. and Di Fiore, P.P. (2004) Signaling through monoubiquitination. *Curr Top Microbiol Immunol*, **286**, 149-185.

Simons, K. and Ikonen, E. (1997) Functional rafts in cell membranes. *Nature*, **387**, 569-572.

Simonsen, A., Wurmser, A.E., Emr, S.D. and Stenmark, H. (2001) The role of phosphoinositides in membrane transport. *Curr Opin Cell Biol*, **13**, 485-492.

Singer, B. and Riezman, H. (1990) Detection of an intermediate compartment involved in transport of alpha-factor from the plasma membrane to the vacuole in yeast. *J Cell Biol*, **110**, 1911-1922.

Singer-Krüger, B., Frank, R., Crausaz, F. and Riezman, H. (1993) Partial purification and characterization of early and late endosomes from yeast. Identification of four novel proteins. *J Biol Chem*, **268**, 14376-14386.

Singer-Krüger, B., Nemoto, Y., Daniell, L., Ferro-Novick, S. and De Camilli, P. (1998) Synaptojanin family members are implicated in endocytic membrane traffic in yeast. *J Cell Sci*, **111 (Pt 22)**, 3347-3356.

Slepnev, V.I., Ochoa, G.C., Butler, M.H., Grabs, D. and De Camilli, P. (1998) Role of phosphorylation in regulation of the assembly of endocytic coat complexes. *Science*, **281**, 821-824.

Souza, C.M. and Pichler, H. (2006) Lipid requirements for endocytosis in yeast. *Biochim Biophys Acta*.

Srinivasan, S., Seaman, M., Nemoto, Y., Daniell, L., Suchy, S.F., Emr, S., De Camilli, P. and Nussbaum, R. (1997) Disruption of three phosphatidylinositol-polyphosphate 5-phosphatase genes from Saccharomyces cerevisiae results in pleiotropic abnormalities of vacuole morphology, cell shape, and osmohomeostasis. *Eur J Cell Biol*, **74**, 350-360.

Stamenova, S.D., Dunn, R., Adler, A.S. and Hicke, L. (2004) The Rsp5 ubiquitin ligase binds to and ubiquitinates members of the yeast CIN85-endophilin complex, Sla1-Rvs167. *J Biol Chem*, **279**, 16017-16025.

Staub, O. and Rotin, D. (2006) Role of ubiquitylation in cellular membrane transport. *Physiol Rev*, **86**, 669-707.

Stefan, C.J., Audhya, A. and Emr, S.D. (2002) The yeast synaptojanin-like proteins control the cellular distribution of phosphatidylinositol (4,5)-bisphosphate. *Mol Biol Cell*, **13**, 542-557.

Stefan, C.J., Padilla, S.M., Audhya, A. and Emr, S.D. (2005) The phosphoinositide phosphatase Sjl2 is recruited to cortical actin patches in the control of vesicle formation and fission during endocytosis. *Mol Cell Biol*, **25**, 2910-2923.

Stolz, L.E., Huynh, C.V., Thorner, J. and York, J.D. (1998) Identification and characterization of an essential family of inositol polyphosphate 5-phosphatases (INP51, INP52 and INP53 gene products) in the yeast Saccharomyces cerevisiae. *Genetics*, **148**, 1715-1729.

Sudol, M., Chen, H.I., Bougeret, C., Einbond, A. and Bork, P. (1995) Characterization of a novel protein-binding module--the WW domain. *FEBS Lett*, **369**, 67-71.

Sweeney, D.A., Siddhanta, A. and Shields, D. (2002) Fragmentation and re-assembly of the Golgi apparatus in vitro. A requirement for phosphatidic acid and phosphatidylinositol 4,5-bisphosphate synthesis. *J Biol Chem*, **277**, 3030-3039.

Swerdlow, P.S., Finley, D. and Varshavsky, A. (1986) Enhancement of immunoblot sensitivity by heating of hydrated filters. *Anal Biochem*, **156**, 147-153.
Takei, K., Slepnev, V.I., Haucke, V. and De Camilli, P. (1999) Functional partnership between amphiphysin and dynamin in clathrin-mediated endocytosis. *Nat Cell Biol*, **1**, 33-39.
Tan, P.K., Davis, N.G., Sprague, G.F. and Payne, G.S. (1993) Clathrin facilitates the internalization of seven transmembrane segment receptors for mating pheromones in yeast. *J Cell Biol*, **123**, 1707-1716.
Tang, H.Y., Xu, J. and Cai, M. (2000) Pan1p, End3p, and S1a1p, three yeast proteins required for normal cortical actin cytoskeleton organization, associate with each other and play essential roles in cell wall morphogenesis. *Mol Cell Biol*, **20**, 12-25.
ter Haar, E., Musacchio, A., Harrison, S.C. and Kirchhausen, T. (1998) Atomic structure of clathrin: a beta propeller terminal domain joins an alpha zigzag linker. *Cell*, **95**, 563-573.
Terui, T., Kahn, R.A. and Randazzo, P.A. (1994) Effects of acid phospholipids on nucleotide exchange properties of ADP-ribosylation factor 1. Evidence for specific interaction with phosphatidylinositol 4,5-bisphosphate. *J Biol Chem*, **269**, 28130-28135.
Toshima, J., Toshima, J.Y., Martin, A.C. and Drubin, D.G. (2005) Phosphoregulation of Arp2/3-dependent actin assembly during receptor-mediated endocytosis. *Nat Cell Biol*, **7**, 246-254.
Toshima, J.Y., Toshima, J., Kaksonen, M., Martin, A.C., King, D.S. and Drubin, D.G. (2006) Spatial dynamics of receptor-mediated endocytic trafficking in budding yeast revealed by using fluorescent alpha-factor derivatives. *Proc Natl Acad Sci U S A*, **103**, 5793-5798.
Towbin, H., Staehelin, T. and Gordon, J. (1979) Electrophoretic transfer of proteins from polyacrylamide gels to nitrocellulose sheets: procedure and some applications. *Proc Natl Acad Sci U S A*, **76**, 4350-4354.
Traub, L.M. (2003) Sorting it out: AP-2 and alternate clathrin adaptors in endocytic cargo selection. *J Cell Biol*, **163**, 203-208.
Turner, K.M., Burgoyne, R.D. and Morgan, A. (1999) Protein phosphorylation and the regulation of synaptic membrane traffic. *Trends Neurosci*, **22**, 459-464.
Ungewickell, E. and Branton, D. (1981) Assembly units of clathrin coats. *Nature*, **289**, 420-422.
Verstreken, P., Koh, T.W., Schulze, K.L., Zhai, R.G., Hiesinger, P.R., Zhou, Y., Mehta, S.Q., Cao, Y., Roos, J. and Bellen, H.J. (2003) Synaptojanin is recruited by endophilin to promote synaptic vesicle uncoating. *Neuron*, **40**, 733-748.
Vida, T.A., Huyer, G. and Emr, S.D. (1993) Yeast vacuolar proenzymes are sorted in the late Golgi complex and transported to the vacuole via a prevacuolar endosome-like compartment. *J Cell Biol*, **121**, 1245-1256.
Walch-Solimena, C. and Novick, P. (1999) The yeast phosphatidylinositol-4-OH kinase pik1 regulates secretion at the Golgi. *Nat Cell Biol*, **1**, 523-525.
Wang, G., Yang, J. and Huibregtse, J.M. (1999) Functional domains of the Rsp5 ubiquitin-protein ligase. *Mol Cell Biol*, **19**, 342-352.
Wang, Y.J., Wang, J., Sun, H.Q., Martinez, M., Sun, Y.X., Macia, E., Kirchhausen, T., Albanesi, J.P., Roth, M.G. and Yin, H.L. (2003) Phosphatidylinositol 4 phosphate regulates targeting of clathrin adaptor AP-1 complexes to the Golgi. *Cell*, **114**, 299-310.
Warren, D.T., Andrews, P.D., Gourlay, C.W. and Ayscough, K.R. (2002) Sla1p couples the yeast endocytic machinery to proteins regulating actin dynamics. *J Cell Sci*, **115**, 1703-1715.

Watson, H.A., Cope, M.J., Groen, A.C., Drubin, D.G. and Wendland, B. (2001) In vivo role for actin-regulating kinases in endocytosis and yeast epsin phosphorylation. *Mol Biol Cell*, **12**, 3668-3679.

Welch, M.D. and Mullins, R.D. (2002) Cellular control of actin nucleation. *Annu Rev Cell Dev Biol*, **18**, 247-288.

Wendland, B. and Emr, S.D. (1998) Pan1p, yeast eps15, functions as a multivalent adaptor that coordinates protein-protein interactions essential for endocytosis. *J Cell Biol*, **141**, 71-84.

Wendland, B., Emr, S.D. and Riezman, H. (1998) Protein traffic in the yeast endocytic and vacuolar protein sorting pathways. *Curr Opin Cell Biol*, **10**, 513-522.

Wendland, B., Steece, K.E. and Emr, S.D. (1999) Yeast epsins contain an essential N-terminal ENTH domain, bind clathrin and are required for endocytosis. *Embo J*, **18**, 4383-4393.

Wicky, S., Frischmuth, S. and Singer-Kruger, B. (2003) Bsp1p/Ypr171p is an adapter that directly links some synaptojanin family members to the cortical actin cytoskeleton in yeast. *FEBS Lett*, **537**, 35-41.

Winter, D., Lechler, T. and Li, R. (1999) Activation of the yeast Arp2/3 complex by Bee1p, a WASP-family protein. *Curr Biol*, **9**, 501-504.

Woelk, T., Oldrini, B., Maspero, E., Confalonieri, S., Cavallaro, E., Di Fiore, P.P. and Polo, S. (2006) Molecular mechanisms of coupled monoubiquitination. *Nat Cell Biol*.

Yin, H.L. and Janmey, P.A. (2003) Phosphoinositide regulation of the actin cytoskeleton. *Annu Rev Physiol*, **65**, 761-789.

Young, M.E., Cooper, J.A. and Bridgman, P.C. (2004) Yeast actin patches are networks of branched actin filaments. *J Cell Biol*, **166**, 629-635.

Zeng, G. and Cai, M. (1999) Regulation of the actin cytoskeleton organization in yeast by a novel serine/threonine kinase Prk1p. *J Cell Biol*, **144**, 71-82.

Zeng, G., Yu, X. and Cai, M. (2001) Regulation of yeast actin cytoskeleton-regulatory complex Pan1p/Sla1p/End3p by serine/threonine kinase Prk1p. *Mol Biol Cell*, **12**, 3759-3772.

Acknowledgement

Als erstes möchte ich mich bei der Betreuerin meiner Doktorarbeit bedanken, PD Dr. Birgit Singer-Krüger. Ihr Engagement und umfassende wissenschaftliche Anleitung während der letzten drei Jahre waren lehrreich für mich und haben die Doktorarbeit bereichert. Vielen Dank für dieses spannende Projekt und die Hilfe bei der Fertigstellung dieser Arbeit.

Als nächstes möchte ich mich bei Prof. Dr. Dieter H. Wolf bedanken. Danke, dass ich die Möglichkeit hatte, meine Doktorarbeit am Institut für Biochemie durchführen zu können und für die Bereitschaft zu meinem Prüfungskomitee zu gehören.

Bei allen DoktorandInnen, DiplomandInnen und MitarbeiterInnen des Instituts für Biochemie der Universität Stuttgart möchte ich mich herzlich für die gute Zusammenarbeit und das großartige Arbeitsklima bedanken. Einen herzlichen Dank im Speziellen an Elisabeth und Dragica für die logistische Unterstützung.

Im speziellen möchte ich den Kollegen aus dem Südlabor danken, mit denen ich in den letzten Jahren zusammengearbeitet und viel Freizeit verbracht habe: Sidonie Wicky John, Maja Lasić, Sónia Barbosa, Anna Maria Bürger, Dagmar Siele, Alexandra Ziegler, Viola Günther und Svenja Kaden. Jeder hat auf seine unverwechselbare Weise zu einem entspannenden und kreativen Arbeitsklima beigetragen.

Ich danke ebenfalls Dr. Judit Kovać und Dipl-Biol. Jessica Rach für das geduldige Korrekturlesen dieser Arbeit. Ihr habt mir mit euerer Unterstützung und Kompetenz immer zur Seite gestanden, vielen Dank.

Mein ganz persönlicher Dank geht an meine gesamte Familie, die mir die wichtigen Dinge im Leben vorleben. Insbesondere gilt mein Dank meine Mutter, die mich durch ihren steten Zuspruch und ihrer Fürsorge immer unterstützt hat.

Dem allerwichtigsten Menschen möchte ich als letztes danken. Ich liebe dich, Jens.

Curriculum Vitae

PERSONAL DATA

Name: Claudia
Last name: Böttcher-Sehlmeyer
Title: German diploma in Biology
Nationality: German
Date of birth: June 25th 1976
Place of birth: in Halle (Saale), Germany

Current address:
Merzenstraße 13
70469 Stuttgart
Deutschland / Germany

Phone: +49-711-5779388
e-mail: boett23@web.de

EDUCATION

2003-today:	Ph.D. project at the Institute of Biochemistry at the Technical University of Stuttgart, Germany
2003:	Gratuated, Diploma title at the at the Hannover Medical School (MHH), Germany
1997-2002:	Studies of Biology at the University of Hannover, Major: human genetics, physiology, microbiology
1996:	Matthias-Claudiaus-Gymnasium of Gehrden, University entry diploma; German Type A

RESEARCH EXPERIENCE

2003-present:	Ph.D. student at the Institute of Biochemistry, University of Stuttgart, Germany (advisor: PD Dr. Birgit Singer-Krüger)
2002:	Diploma student at the Dept. of Human Genetics at the Hannover Medical School (MHH), Germany (advisor: Prof. Dr. med. Manfred Stuhmann-Spangenberg)
2001:	Undergraduate student at the Dept. of Human Genetics at the Hannover Medical School (MHH), Germany (advisor: Prof. Dr. med. Manfred Stuhmann-Spangenberg)
2000:	Undergraduate student at the Dept. of Pharmacology, Toxicology and Pharmacy at the School of Veterinary Medicine Hannover, Germany (advisor: PD Dr. Manuela Gernert)

TEACHING ACTIVITIES

Monitoring of undergraduate and diploma students at the Institute of Biochemistry at the University of Stuttgart

Teaching assistant at annual tutorials for second year students of Technical Biology and Chemistry at the University of Stuttgart, Germany

Teaching assistant at annual tutorials on the methods for molecular and embryological analysis at the Hannover Medical School (MHH), Germany

EXTRACURRICULAR COURSES

Internship in the company BIOBASE on the topic: elegans CYTOMER® û A database on anatomical/histological knowledge and gene expression extended to Caenorhabditis., Biobase, 2001, Germany

PUBLICATION

Böttcher, C., Wicky, S., Schwarz, H., Singer-Krüger, B. Sjl2p is specifically involved in early steps of endocytosis intimately linked to actin dynamics via Ark1p/Prk1p kinases. *FEBS Lett*. **580**, 633-641 (2006)

Böttcher, C., Wicky, S., Schwarz, H., Singer-Krüger, B. Sjl2p is associated with early endocytic structures, that clump upon interference with actin dynamics. Yeast Cell Biology meeting, 2005, CSHL, NY, USA

Böttcher, C., 2002, "Genetical analysis of patients with hemochromatosis", unpublished diploma Thesis, Hannover Medical School (MHH)